Naval Surface Warfare Center
Carderock Division
West Bethesda, MD 20817-5700

NSWCCD-70-TR–2004/115 August 2004

Signatures Directorate

Technical Report

Coated and Uncoated Models; What is the Difference? Part II: Cavity Resonances

by

G. Maidanik

K. J. Becker

L. J. Maga

[Work supported by ONR and In-House Fundings.]

NSWCCD-70-TR—2004/115 August 2004 Coated and Uncoated Models; What is the Difference? Part II: Cavity Resonances

REPORT DOCUMENTATION PAGE

Form Approved OMB No. 0704-0188

1. REPORT DATE *(DD-MM-YYYY)*	2. REPORT TYPE	3. DATES COVERED *(From - To)*
1-Aug-2004	Final	-

4. TITLE AND SUBTITLE

Coated and Uncoated Models; What is the Difference? Part II: Cavity Resonances

5a. CONTRACT NUMBER

5b. GRANT NUMBER

5c. PROGRAM ELEMENT NUMBER

6. AUTHOR(S)

G. Maidanik, K. J. Becker, L. J. Maga

5d. PROJECT NUMBER

5e. TASK NUMBER

5f. WORK UNIT NUMBER

7. PERFORMING ORGANIZATION NAME(S) AND ADDRESS(ES) AND ADDRESS(ES)

Naval Surface Warfare Center
Carderock Division
9500 Macarthur Boulevard
West Bethesda, MD 20817-5700

8. PERFORMING ORGANIZATION REPORT NUMBER

NSWCCD-70-TR-2003/115 AUG 2004

9. SPONSORING / MONITORING AGENCY NAME(S) AND ADDRESS(ES)

Attn ONR 334
Chief of Naval Research
Ballston Centre Tower One
800 North Quincy Street
Arlington, VA 22217-5660

10. SPONSOR/MONITOR'S ACRONYM(S)

11. SPONSOR/MONITOR'S REPORT NUMBER(S)

12. DISTRIBUTION / AVAILABILITY STATEMENT

Approved for public release; distribution is unlimited.

13. SUPPLEMENTARY NOTES

14. ABSTRACT

The rudimentary model of Part I is elaborated by introducing a baffle below the equivalent plate. In the cavity that forms, between the equivalent plate and the baffle, fluid is introduced. The cavity induces resonances and anti-resonances in the response of the equivalent plate. In turn, these resonances and anti-resonances imprint their presence on the regular transfer functions. These imprints are modulated by the resonance between the surface mass impedance of the equivalent plate and the surface stiffness (compliance) impedance of the coating when the coating is present. In the absence of coating, this modulation is also absent, although the imprints of the resonances and anti-resonances in the transfer functions persist. The influence of the coating, on the imprints of the cavity resonances and anti-resonances, is isolated by presenting the ratio of the transfer function in the presence of coating to that in absence of coating. The transfer functions and their ratios are computed as functions of the normalized frequency. Variations on the theme, in which parameters are changed from standard values, are examined and displayed. In particular, the major hump and minor dump emerge in these displays. Since resonances (and anti-resonances) are sensitive to damping, a number of types and degrees of damping are examined and assessed for effectiveness as noise control agents.

15. SUBJECT TERMS

16. SECURITY CLASSIFICATION OF:			17. LIMITATION OF ABSTRACT	18. NUMBER OF PAGES	19a. NAME OF RESPONSIBLE PERSON
a. REPORT	b. ABSTRACT	c. THIS PAGE			G. Maidanik
UNCLASSIFIED	UNCLASSIFIED	UNCLASSIFIED	UL	68	19b. TELEPHONE NUMBER *(include area code)* 301-227-1292

Table of Contents to Part II

ABSTRACT TO PART II

The rudimentary model of Part I is elaborated by introducing a baffle below the equivalent plate. In the cavity that forms, between the equivalent plate and the baffle, fluid is introduced. The cavity induces resonances and anti-resonances in the response of the equivalent plate. In turn, these resonances and anti-resonances imprint their presence on the regular transfer functions. These imprints are modulated by the resonance between the surface mass impedance of the equivalent plate and the surface stiffness (compliance) impedance of the coating when the coating is present. In the absence of coating, this modulation is also absent, although the imprints of the resonances and anti-resonances in the transfer functions persist. The influence of the coating, on the imprints of the cavity resonances and anti-resonances, is isolated by presenting the ratio of the transfer function in the presence of coating to that in absence of coating. The transfer functions and their ratios are computed as functions of the normalized frequency. Variations on the theme, in which parameters are changed from standard values, are examined and displayed. In particular, the *major hump* and *minor dump* emerge in these displays. Since resonances (and anti-resonances) are sensitive to damping, a number of types and degrees of damping are examined and assessed for effectiveness as noise control agents.

II1. Introduction.

The dynamic system that the model, depicted in Figure I1, tries to simulate is sketched in Figure I2. In Figure I1, one recalls, the fluids possess essentially equal properties, the fluids occupy the semi-infinite spaces above and below the surfaces that they interface, and the surfaces of the mechanical components are uniform and of infinite spatial extent. The attraction for utilizing this model is that it generates an analysis that can be readily manipulated and the quantities issued are easy to interpret. A glance at Figures I1 and I2 can tell that the analysis developed from Figure I1 may not incorporate some of the features in the transfer functions that a more authentic model, of the dynamic system sketched in Figure I2, may. For example, Figure I2 indicates that the fluid interfacing the inner wall is, in fact, partially enclosed thereby forming a cavity. Another example, Figure I2 suggests that the plates and the cavity are spatially finite. Indeed, the transfer functions derived of a dynamic system resembling that sketched in Figure I2 are beset by multitude of resonances (and by multitude of anti-resonances). Clearly no such resonances are exhibited in the transfer functions issued by the analysis based on the model depicted in Figure I1. At best, a single fairly broad resonance was squeezed out from this model. Moreover, even then, a definition for mechanisms that would mollify the surface impedance of the bottom fluid (fluid no. 2) had to be invented. Among these mechanisms are

the reduced characteristic impedance of that fluid, the defaulting of the plate-syntactic foam-plate system to introduce compliance into this combination and, not the least, the introduction of a special form for the transfer function. Each of these mechanisms was required in order to squeeze out this resonance. Is the absence of resonances, in the transfer functions of the model depicted in Figure I1, related directly to the absence of a cavity and/or finiteness in this model? (Nothwithstanding that the cavity is a result of some finiteness in the dynamic system under investigation and that a resonance in the structure may render the fluid in the cavity (fluid no. 2) to lose much of its high modulus, thereby, rendering its speed of sound low and, therefore, its characteristic impedance low. As the wiser man said: "A resonance is a vibrational state that is associated with a vanishing impedance and, therefore, a resonance is a resonance *to all intents and purposes.*" [cf. Figure I2.]) The answer to the question just posed is obvious; no cavity and no finiteness and, therefore, no resonances. A second question thus follows: Can one then devise a modeling scheme that simulates resonances in the transfer functions and yet largely retains the infinite stance of the model depicted in Figure I1? It is anticipated that if such a modeling scheme can be devised it will furnish an analysis that remains physically viable and computationally tractable. In such an analysis the interpretations of the results issued remain reasonable and the influence of the finiteness as such, if significant, may either be included in a later

effort or be judicially guessed at. There are a number of analytical schemes that will introduce resonances (and anti-resonances) to the transfer functions. In this report two are considered. In the first only cavity resonances are introduced. In the second only structural resonances are introduced. Finally, the presence of both, cavity and structural resonances are introduced. In this introduction the interactions among the resonances of each can be investigated. As just stated, the cavity resonances are dealt with first in this part of the report; namely, Part II.

In this vein, the resonances are simulated by the model presented in Figure II1. Figure II1 differs from Figure I1 in that a baffle is placed below the bottom plate (plate no. 2). The space (cavity) between this bottom plate and the baffle is filled with a fluid of the kind previously assigned and remains assigned as fluid no. 2. [cf. Figures I1 and II1.] Clearly, the baffle will generate resonances in the transfer functions relating to the radiation from an external drive that is placed on a plane that lies between the bottom plate and the baffle. These resonances, once again, are generated by obviations of the fluid surface impedance when cavity resonances occur. The cavity resonances, of course, are dependent on the choice of the gap between the surfaces of the bottom plate (plate no. 2) and the baffle; the gap can be set or adjusted as may be dictated. A third question may then be in order: Do such resonances in the transfer functions simulate some of the resonances that are

found in the dynamic system sketched in Figure I2 and, conversely, do some of the properties of such resonances match with those resonances that they simulate. It is taken for granted, but is not essential to this report that the resonance frequencies in both cases overlap. Again, if need be, the overlap may be achieved by merely and artificially adjusting the gap. Yet a fourth question arises: Do these resonances modulate the resonance between the surface (mass) impedance of the top plate and the surface compliance of the coating when this coating is in situ, thus exhibiting a major hump when the coated transfer functions are compared with the corresponding transfer functions in the absence of coating? In part the answer to this question is the subject matter under consideration. Consideration in this and subsequent parts incorporates a plate-syntactic foam-plate dynamic system that is merged into *an equivalent plate*. The merging procedure was previously described in the transition from Figures I1a and I3a to Figures I1b and I3b.

The formalism accounting for the cavity resonances, for the model shown in Figure II1, is depicted in Figure II2 by an equivalent electrical circuit diagram. [cf. Figures I1 and I3.] The quantities defined in this electrical circuit diagram are also defined in Figure II2.

The task of defining the various quantities and parameters that define the dynamical system under investigation are being introduced in the various parts of this report. The first introduction in this effort is the definition of the normalized surface stiffness of the coating and its dependence on depth. [The surface stiffness of the coating is inversely proportional to the surface compliance of the coating.] The properties of the coating are briefly presented in Section II2. The effects of depth on the regular transfer functions is of paramount interest and, therefore, these effects need to be investigated. The next section, Section II2, is presented in order to facilitate such investigations.

II2. Depth Dependent Coating.

The surface stiffness of the coating usually changes with depth. [In the definition of the properties of the coating the surface stiffness is inversely proportional to the surface compliance.] At shallow depth, with a normalized depth of unity, a typical coating has a reasonable surface stiffness. The surface stiffness decreases with increase in the normalized depth reaching a minimum value when the normalized depth (h_0) assumes a value between four (4) and five (5). With further increase of the normalized depth, the surface stiffness recovers and reaches the value in shallow depth. The recovery is complete at a normalized depth of about eight (8). Further increases in the normalized depth results in further increase in the surface stiffness of the coating. The normalized surface stiffness, as a function of the normalized frequency (ω), is depicted in Figure II3a; the normalized stiffness $S(\omega, h_2, t_2)$ with h_0 = 4.3, h_2 = 4 and t_2 = 20^oC is plotted in this figure. [Note that in this figure $S(\omega, 4, 20^\circ C) \equiv S1(\omega)$.] On the other hand, the normalized surface stiffness $S(\omega, h_2, t_2)$ with h_0 = 4.3, ω = 1 and t_2 = 20^oC, as a function of the normalized depth (h_2), is depicted in Figure II3b. [Note that in the figure $S(1, x, 20^\circ C) \equiv S2(x)$.] Finally, the normalized surface stiffness $S(\omega, h_2, t_2)$ with h_0 = 4.3, h_2 = 4 and

ω = 1, as a function of the temperature (t_2), is depicted in Figure II3c. [Note that in the figure $S(1,4,t_2) \equiv S3(y)$.] All three figures, Figures II3a, II3b and II3c are representative of the properties of the coating. These representations are, however, hypothetical. The analytical expression for the normalized surface stiffness $S(\omega, h_2, t_2)$ used to generate these figures is, for the records, of the form

$$S(\omega, h_2, t_2) = 2[X(h_2)]^{-1} \nu_1(\omega, t_2) \quad , (II1)$$

with

$$X(x) := [3 + (\varsigma) \cdot |x - h_0| \cdot \exp(|x - h_0|)]^{-1} \cdot [3 + \exp(|x - h_0|)] \quad , (II2a)$$

and

$$\nu_1(\omega, t) = [1 + \nu_3(t)(\omega/\omega_h)][(1 + a_1)\{\nu_3(t)/\pi\}]$$
$$[1 + a_1\{\nu_3(t)/\pi\}(\omega/\omega_h)]^{-1} \quad , (II2b)$$

where

$$a_1 = \pi - [(\omega_h + 1) / \omega_h] \;\; ; \;\; \omega_h = 2\pi \;\; ; \;\; \varsigma = (2/7) \quad , (II3a)$$

and

$$\nu_3(t) = [1 + (t/t_h)]^{-1}[1 + (t_0/t_h)] \quad ; \quad t_0 = 4 \quad ; \quad t_h = 20 \qquad \text{.(II3b)}$$

The expression for $S(\omega, h_2, t_2)$ presented in Equations (II1) - (II3) are rough empirical attempt to capture the salient properties of a coating in general, not in detail. When computations involving the transfer function are performed these are the properties of the coating to be employed. When the properties are known more precisely, provisions may be made for their incorporation in the computations. In this part; Part II, the standard coating is that for which $h_2 = 4$ and $t_2 = 20$. Moreover, in this part; Part II, effects associated with depth dependence only are computed and shown. The subject of the properties of the coating will be revisited when scaling laws in reference to scaled models are discussed in subsequent parts; Parts V and VI. In this part; Part II and in the next couple of parts; Parts III and IV, the properties just stated are adequate for the tasks on hand.

II3. Parametric Modifications in Lieu of the Cavity.

To accommodate the cavity, a number of modifications to the formalism stated in Part I must be instituted. These modifications consist of changing the surface impedance $Z_{f2}(k,\omega)$ of the fluid in the absence of a cavity (fluid no. 2) to the surface impedance $Z^b_{f2}(k,\omega)$ in the presence of the cavity and changing the external force-drive $P_e(k,\omega)$ in the absence of the cavity to $P^b_e(k,\omega)$ in the presence of the cavity. Once $Z_{f2}(k,\omega)$ and $P_e(k,\omega)$ are simply replaced by $Z^b_{f2}(k,\omega)$ and $P^b_e(k,\omega)$ in the previously stated formalism, the formalism is adapted to deal with the presence of the cavity. The modified surface impedance $Z^b_{f2}(k,\omega)$ of the fluid in the cavity (fluid no. 2) may be expressed in the form

$$Z^b_{f2}(k,\omega) \Rightarrow Z_{f2}(k,\omega)\left[1+R\exp\left\{-(2i\omega)(bk_o)(c_1/c_2)\bar{k}_{32}\right\}\right]$$
$$\left[1-R\exp\left\{-(2i\omega)(bk_o)(c_1/c_2)\bar{k}_{32}\right\}\right]^{-1} \quad , \text{(II1a)}$$

where (R) is the reflection coefficient at the baffle's surface, $(\bar{k}_{32})$ is defined in Equation (I6b), $k_o = (\omega_o/c_1)$ and the appropriate normalizations of (ω) and (k) are implied; namely, (ω) is normalized

(ω_o) and (k) is normalized by (k_o). Similarly, the modified blocked external force-drive $P_e^b(k,\omega)$ may be expressed in the form

$$P_e^b(k,\omega) \Rightarrow P_e(k,\omega)[1+(-1)^n R\exp\{-(2i\omega)(b_2 k_o)(c_1/c_2)\bar{k}_{32}\}]$$
$$[1-R\exp\{-(2i\omega)(b\,k_o)(c_1/c_2)\bar{k}_{32}\}]^{-1} \quad , (II1b)$$

where n = o represents a monopole-like external source, n = 1 represents a dipole-like external source, etc. Thus, if one states that the regular transfer function with coating is a functional of $\{Z_{f1},\ Z_c,\ Z_p,\ Z_{f2}\}$ so that

$$Tc(k,\omega) = Tc\{Z_{f1},\ Z_c,\ Z_p,\ Z_{f2}\} \quad , (II2a)$$

and without coating is

$$T(k,\omega) = Tc\{Z_{f1},\ |Z_c| \to \infty,\ Z_p,\ Z_{f2}\} \quad , (II2b)$$

then the modified regular transfer function with coating; designated (Tbc), may be stated simply as

$$Tbc(k,\omega) \Rightarrow (B_e)T\{Z_{f1},\ Z_c,\ Z_p,\ Z_{f2}^b\} \quad ;$$
$$B_e(k,\omega) = [P_e^b(k,\omega)/P_e(k,\omega)] \quad , (II2c)$$

and without coating as

$$Tb(k,\omega) \Rightarrow (B_e)\,T_c\left\{Z_{f1},\ |Z_c| \to \infty,\ Z_p,\ Z_{f2}^b\right\} \qquad \text{, (II2d)}$$

where Z_{f2}^b and (P_e^b / P_e) are explicitly stated in Equations (II1a) and (II1b). Clearly, in any computational procedure involving the cavity it is necessary to provide, above and beyond the values previously quoted in Part I, the values of $(b k_o)$, $(b_2 k_o)$ and (R). In this connection, the standard values of these parameters are:

$$(b k_o) = \pi \quad ; \quad (b_2 k_o) = S_k (b k_o),\ S_k = 1 \qquad \text{, (II3a)}$$

$$R(k,\omega) \Rightarrow R(\omega) = \exp\left\{-(10^{-7})\right\} \Rightarrow 1 \qquad \text{. (II3b)}$$

With this addendum to the formalism developed in Part I, computational tasks involving the presence of a cavity may now be undertaken.

II4. Typical Transfer Functions in the Presence of Cavity Resonances.

Typical computations that illustrate the role played by the presence of the cavity resonances (and anti-resonances) are exemplified in Figure II4. The computations are of the transfer functions as function of the normalized frequency. In Figure II4 the gap between the bottom of the equivalent plate and the baffle is (π). This gap is now designated the standard gap. In Figure II4a the standard conditions with the standard coating and standard gap stand in place. Figure II4b repeats Figure II4a except that the coating is absent. The ratio of the transfer function $Tbc(k,\omega)$ in Figure II4a to the transfer function $Tb(k,\omega)$ in Figure II4b is presented in Figure II4c; this ratio is designated $Tbc\_Tb(k,\omega)$. The influence of the coating is, therefore, made bare in Figure II4c. Figures II4a, II4b and II4c are repeated in Figures II4d, II4e and II4f except that the normalized depth is changed from four (4) to one (1); i.e., from $h_2 = 4$ to $h_2 = 1$. Similarly, Figures II4g, II4h and II4i repeat Figures II4a, II4b and II4c, respectively, except that the normalized depth is changed from that of four (4) in the latter set to that of eight (8) in the former; i.e., from $h_2 = 4$ to $h_2 = 8$. The differences in the three sets of figures are, clearly, due to the depth dependence of the coating. To accentuate these differences, Figure II4j, which superposes the three figures; Figures II4c, II4f

and II4i, is shown. With the aid of Section II2, the differences can be readily interpreted; the differences are due to the quoted changes in depth.

Variations on the theme are presented largely in the format of Figures II4a, II4b and II4c; e.g., Figures II5a, II5b and II5c repeat these figures, respectively, except that the gap between the baffle and the bottom of the equivalent plate is changed from the standard value of (π) to $(2\pi)(\omega)^{-1/2}$. The change in the modal density, in the higher normalized frequency domain, is of special interest in comparing Figures II4a-II4c to Figures II5a-II5c, respectively; in Figure II5 the modal density (number of resonances per unit frequency) is higher in the lower frequency range, where $\omega \leq 1$, and is lower in the higher frequency range, where $\omega \geq 1$, than is the case in Figure II4.

Another example, Figures II6a-II6c repeat Figures II4a-II4c, respectively, except that the standard beam-directed radiation in the latter set is replaced by a $(\pi/3)$-directed radiation. The transition in the equivalent plate surface impedance from surface mass control to surface stiffness control, where $\omega^2 = [4\omega_c^2/3]$, is distinguishable in Figure II6. This statement is made clearer when this figure; Figure II6, is held in comparison with Figure II4; the transition is clearly absent in the latter figure.

The major hump in the transfer function due to the coating is amply exhibited in Figures II4 - II6; especially in Figures II4c, II4f, II4i, II5c and II6c. One is confronted, once again, by a question: Can the major hump, which represents higher levels for the regular transfer functions, be subdued? For example, can increase in damping bring relief? If yes, what type of dampings would do better and by how much? One is reminded in this connection that the standard loss factors are all equal to one-thousandth (10^{-3}). The standard loss factors are applicable to all of Figures II4 - II6. That a change in the loss factor may cause a major change in the transfer function is depicted in Figure II7; in this figure Figures II4a, II4b and II4c are repeated except that the loss factor (η) in the cavity is changed from the standard value of (10^{-3}) to (10^{-1}). The resonances and anti-resonances are subdued by this change as the comparison between Figures II4a-II4c and Figures II7a-II7c, respectively, clearly show. The influence of changes in the loss factors on the regular transfer functions is, therefore, an essential topic to be investigated. However, before embarking on this investigation there is a need to determine base-levels that the transfer functions may attain when the maximum noise control is implemented. Only then may one decide whether the noise control procedures are adequately achieving their ultimate goals.

II5. Base Levels.

The major hump and the accompanied minor dump are direct consequences of the resonances and the accompanied anti-resonances in the dynamic system. As such they possess bottoming levels that conform to Skudrzyk mean-values. One recalls that the major hump is constituted by resonances in the dynamic system and the minor dump is correspondingly constituted by anti-resonances. When considering ways to subdue the major hump, these bottoming levels represent the *best* that can be accomplished; trying to do better is an idle attempt. It is, therefore, imperative that the bottoming levels be well defined. One need be cognizant that whatever means subdues the major hump, in turn, subdues the accompanied minor dump. [Were one relying for some tactical purpose on the minor dump for salvation, eliminating the major hump may not be the appropriate noise control procedure; no major hump, no minor dump.]

To well nigh subdue the major hump and the minor dump, it suffices to render negligible the reflection coefficient at the baffle. Introducing a negligible reflection coefficient into the conditions that yielded the transfer functions depicted in Figures II4a-II4c, II5a-II5c and II6a-II6c, now yields Figures II4k-II4m, II5d-II5f, and II6d-II6f, respectively. [It is noted that Figures II4k-II4m and the corresponding Figures II5d-II5f are identical. On the other hand, Figures II6d-II6f stand alone.] The latter three

sets of figures then depict the bottom levels of the transfer functions. In particular, in these latter three sets of figures the major hump merges with the minor dump to yield smooth curves in which neither resonances nor anti-resonances rear their signatures heads. In Figures II4k-II4m, II5d-II5f and II6d-II6f dotted curves are superposed on the line curves. The bold dotted curves, so obtained, are hereafter, superposed on all subsequent curves in order to indicate the bottom levels of the transfer functions. Of course, one realizes that the values of the transfer functions depicted in Figures II4k-II4m, II5d-II5f and II6d-II6f are commensurate with Skudrzyk mean-values. Again, it is emphasized that these figures represent transfer functions that are the best that could be done by whatever means noise control may be implemented. [It is also to be understood that the bold dotted curves are calculated under the same conditions assigned to the curves on which they are superposed. These dotted curves, superposed on Figures II4a-II4c, II5a-II5c and II6a-II6c, are shown in Figures II4n-II4p, II5g-II5i and II6g-II6i, respectively.] One series of noise control means, in this connection, is the various types and increases of dampings. This was already and singularly demonstrated in Figures II7a-II7c when compared with Figures II4a-II4c. The various measures and identifications of damping are defined in terms of loss factors and are investigated starting with the next section. To end this section, however, it may be in order to cursorily consider the influence of variations in the external source character and

location. For this purpose Figures II4q-II4s, II5j-II5l and II6i-II6l are presented. These figures are derived by changing the conditions imposed on Figures II4n-II4p, II5g-II5i and II6g-II6i in the index (n) is changed from unity to zero. This change replaces a dipole external source by a monopole. Similarly, these figures are derived in Figures II4n-II4p, II5g-II5i and II6g-II6i, Figures II4t-II4v, II5m-II5o are presented, respectively. In these sets of figures the external source remains a dipole; i.e., $n = 1$, but the location of the plane on which the external sources are placed is moved from the bottom surface of the equivalent plate, for which $S_k = 1$ to $S_k = 0.8$. Both, these changes cause variations in the details of the resonances and anti-resonances, but not in the gross properties of the major hump and minor dump. Moreover, there are hardly any changes from Figures II4p, II5i and II6i and Figures II4s and II4v, II5l and II5o and II6l and II6o, respectively. In these figures the influence of the coating alone is emphasized; it is concluded that a coating is a coating is a coating!

II6. Influence of Damping on Cavity Resonances.

There is no intention to comprehensively explore detail of the influence of damping on the cavity resonances. Rather, merely a number of examples are used to explore the influence of changes in the loss factors on the transfer functions; in particular on the major hump. In this vein, the transfer functions and ratios thereof in Figures II4n-II4p, II5g-II5i and II6g-II6i are subjected to various changes in the loss factors. The table; Table II1, reflects the changes instituted in the loss factors and the assigned figures that carry the specific changes; the figures in this table are designated II8, II9 and II10, respectively. A few salient observations are in order:

1. Comparing Figures II4n-II4p, II5g-II5i and II6g-II6i with Figures II8a-II8c, II9a-II9c and II10a-II10c, respectively, indicates, that increasing the loss factor of the cavities from (10^{-3}) to (10^{-1}) effectively subdues the cavity resonances and anti-resonances. Indeed, the change nearly renders unity the modal overlap parameter in the upper normalized frequency range of the major hump; $1 \leq \omega \leq 3$. The modal overlap parameter (op) is the ratio of the normalized width of a typical resonance; i.e., $(\eta\omega)$ to the normalized frequency separation between resonances; $(\delta(\omega))$,

thus op $\cong [(\eta\omega)/\delta\omega]$. When (op) exceeds unity, resonances and anti-resonances are suppressed in the response quantities of the relevant dynamic system. This process is manifested in that the individual resonances in this range are smoothed-out. It follows that Figures II8a-II8c, II9a-II9c and II10a-II10c become more akin to Figures II4k-II4m, II5d-II5f and II6d-II6f, than to Figures II4a-II4c, II5a-II5c and II6a-II6c, respectively. Again, proving that the increase in the loss factors are most effective in the normalized frequency range where resonances and anti-resonances rein supreme. [cf. Figures II7a-II7c.]

2. Again, comparing Figures II4a-II4c, II5a-II5c and II6a-II6c with Figures II8d-II8f, II9d-II9f and II10d-II10f, respectively, one learns that increasing the loss factor of the coating only, does little to subdue the cavity resonances and, therefore, does not afford an effective mechanism to control the cavity resonances and anti-resonances in the transfer functions. [The damping in the coating largely helps to keep the integrity of the coating rather than provide a major role in subduing cavity resonances. This is similar to the role of damping in machinery mounts. The damping in the machinery mounts is used for the integrity of the mounts not as devices that

contribute to the control of resonances on the machinery platforms.]

3. Comparison is conducted between Figures II8g-II8i, II9g-II9i and II10g-II10i, and Figures II4n-II4p, II5g-II5i and II6g-II6i, respectively. This comparison reveals that the first two pairs; {II8g-II8i, II4n-II4p} and {II9g-II9i, II5g-II5i}, are hardly influenced by the change in the standard loss factor $\eta_p = 10^{-3}$ to $\eta_p = 10^{-1}$. However, the comparison of Figure II10g-II10i with Figure II6g-II6i shows that the change is effective in reducing the resonances and anti-resonances. The loss factor (η_p) is a surface stiffness control. In the employed model, for a beam-directed radiation, the surface stiffness, in the surface impedance of the equivalent plate, does not participate in the determination of the response of the dynamic system. The surface impedance is, in this case, controlled by the surface mass only. Since (η_p) is a surface stiffness control loss factor the conclusion is covered. The surface stiffness of the equivalent plate, however, does participate in the off beam-directed radiation and hence (η_p) influences the so directed transfer functions. This influence is discernible in the comparison of Figures II6g-II6i with Figures II10g-II10i, respectively. Nonetheless,

even in this case the influence of rendering $\eta_p = 10^{-1}$ is not nearly as dramatic as is the rendering of $\eta = 10^{-1}$; i.e., examine Figures II8g-II8i with Figures II10a-II10c and II10g-II10i.

4. Comparing Figures II8j-II8l, II9j-II9l and II10j-II10l with II4n-II4p, II5g-II5i and II6g-II6i, respectively, show that now that an essential component in the equivalent plate damping is associated with the surface mass term, in the absence of the surface stiffness term, damping in the equivalent plate is not absent. The surface mass controlled damping is measured by (η_m). In this case whether the radiation is on beam or off beam is not crucial with respect to providing damping in the equivalent plate.

5. A full press changes in the damping from the standard in which all loss factors are (10^{-3}) to all loss factors assuming the value of (10^{-1}), is depicted in Figures II8m-II8o, II9m-II9o and II10m-II10o. Again, in the transfer functions that are governed by the cavity, it is emphasized that most of the reduction in the peaks and valleys are caused by increases in the loss factor that is associated with the cavity; i.e., the loss factor (η), the other loss factors assume only a minor role in this reduction.

II7. Parametric Variations on the Theme.

Whereas, in the preceding section the influence of damping on the cavity resonances is investigated, in this section the influence of other variations in the parametric values are briefly investigated, computed and displayed. Largely, both cases, in which the beam-directed and off beam-directed radiations, are examined. In these cases, the first is a standard condition, the second is a change from that standard. Again, it is emphasized that in this part; Part II, only a cavity is introduced, giving rise to cavity resonances and anti-resonances in the transfer functions. The influence on the transfer functions of variations in the reflection coefficient (R) is computed and displayed in Figures II11a - II11c for $R = \exp\left[-\left(10^{-1}\right)\right]$ and in Figures II11d - II11f for $R = \exp\left[-\left(1\right)\right]$. These two sets of figures are to be compared with the corresponding basic figures; Figures II4n - II4p, respectively. Expectedly, as the reflection coefficient is reduced, the figures tend toward Figures II4k - II4m, respectively. This reduction, caused by the reduction in the reflection coefficient (R), is, as already intimated, commensurate with the increase in the damping of the cavity. [cf. Figures II8a - II8c.] Figures II11a - II11f are repeated, respectively, in Figures II11g - II11l except that, in the latter set of figures, the value of (k) is changed from the standard value of (0) to $(\omega\sqrt{3}/2)$; a change from beam-directed to off beam-directed

radiation. The latter set of figures are to be compared with the corresponding basic figures; Figures II6g - II6i, respectively. Again and expectedly, as the reflection coefficient is reduced, the figures tend toward Figures II6d - II6f, respectively. [cf. Figures II10a - II10c.] Another parametric variation to be investigated is that of replacing the pole index (n) of the external sources from (1) to (0), thereby, introducing an external drive that is monopole-like rather than dipole-like. The changes in the transfer functions due to a change in the pole index (n), from the standard value of one (1) to zero (0), are depicted in Figures II12a - II12c for the beam-directed radiation; $\theta = 0$, and in Figures II12d - II12f for the off beam-directed radiation; $\theta = (\pi/3)$. There are significant differences, mostly in the details, between these figures and the corresponding basic figures depicted in Figures II4n and II4o and Figures II6g and II6h, respectively. However, there are no differences between Figures II4p and II6i and Figures II12c and II12f, respectively; again, a coating is a coating is a coating. The coating in Figures II4n, II12a, II6g and II12d is the same and, after all, Figures II4p, II12c, II6i and II2f merely isolate the influence of the coating. To further emphasize this isolation, Figures II12g - II12i are displayed. These figures repeat Figures II6g - II6i except that the plane on which the external sources are places lies a distance $b_2 = 0.8b$ above the baffle. [cf. Figure II1.] In the standard condition $b_2 = b$. Again, one finds significant differences,

mostly in details, between these figures and the corresponding basic Figures II6g and II6h, as well as with Figures II12d and II12e. By now not surprising, since the coating remains unchanged, Figure II12i matches Figures II6i and II12f. Finally, two variations in the off beam-directed radiation are examined. Figures II4n - II4p are repeated twice, in Figures II13a - II13c and in Figures II13d - II13f. In the first set $\theta = (\pi/9.2)$ and in the second $\theta = (\pi/6)$. The changes induced in the transfer functions by these variations are well nigh predictable when compared with the corresponding Figures II4n - II4o and Figures II6g - II6i which are, respectively, for the beam-directed radiation with $\theta = 0$ and for the off beam-directed radiation with $\theta = (\pi/3)$. Eventually, a waterfall representation in the $\{k, \omega\}$-domain will provide a more comprehensive representation than is here offered by all these figures; e.g., by Figures II4n - II4p, II6g - II6i, II13a - II13c and II13d - II13f.

Type of Loss Factors / Figure designations	η	η_c	η_p	η_m	Remarks
0. II4n-II4p, II5g-II5i, II6g-II6i	10^{-3}	10^{-3}	10^{-3}	10^{-3}	Lightly damped
1. II8a-II8c, II9a-II9c, II10a-II110c	10^{-1}	10^{-3}	10^{-3}	10^{-3}	Cavity damped
2. II8d-II8f, II9d-II9f, II10d-II10f	10^{-3}	10^{-1}	10^{-3}	10^{-3}	Coating damped
3. II8g-II8i, II9g-II9i, II10g-II10i	10^{-3}	10^{-3}	10^{-1}	10^{-3}	Stiffness control plate damping
4. II8j-II8l, II9j-II9l, II10j-II10l	10^{-3}	10^{-3}	10^{-1}	10^{-1}	Stiffness and mass control plate damping
5. II8m-II8o, II9m-II9o, II10m-II10o	10^{-1}	10^{-1}	10^{-1}	10^{-1}	All components damped

Table II1. [In Figures II4 and II8, $k = 0$ and $b_2 = b = \pi$; in Figures II5 and II9, $k = 0$ and $b_2 = b = (2\pi/\sqrt{\omega})$; in Figures II6 and II10, $k = (\omega\sqrt{3}/2)$ and $b_2 = b = \pi$.]

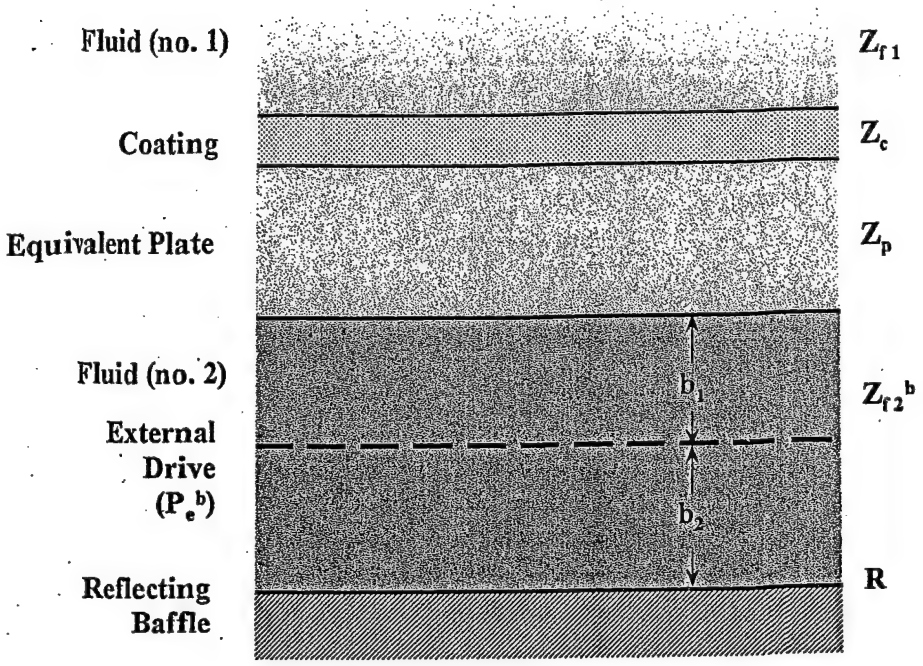

$$P_e^b = B_e P_e$$

$$Z_{f2}^b = I^b Z_{f2}$$

$$B_e = \left[1+(-1)^n R \exp\left\{-(2i\omega)(b_2 k_o)(c_1/c_2)\bar{k}_{32}\right\}\right] \left[1-R\exp\left\{-(2i\omega)(bk_o)(c_1/c_2)\bar{k}_{32}\right\}\right]^{-1}$$

$$I^b = \left[1+R \exp\left\{-(2i\omega)(b_2 k_o)(c_1/c_2)\bar{k}_{32}\right\}\right] \left[1-R\exp\left\{-(2i\omega)(bk_o)(c_1/c_2)\bar{k}_{32}\right\}\right]^{-1}$$

(n) is the multipole index; $n = 0$ (monopole), $n = 1$ (dipole), etc.

(b) is the gap length; $b = b_1 + b_2$.

(R) is the reflection coefficient at the baffle.

Here it is assumed that (R) is independent of the normalized wave vector (k), but may be a function of the normalized frequency (ω). The parameters and qualities; e.g., $(b), (c_1), (c_2), (\bar{k}_{32}), (P_e)$ and (Z_{f2}) are defined in Part I.

Figure II1. A baffled plane dynamic system yielding cavity resonances and anti-resonances. [cf. Figure I1.]

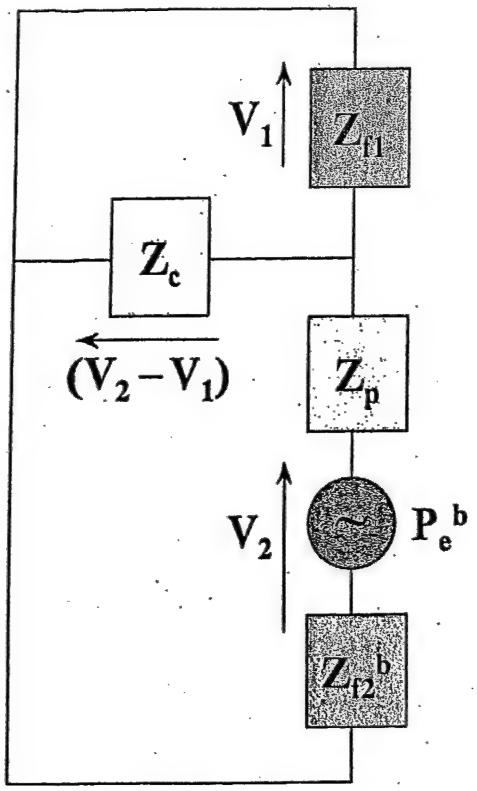

$$\boldsymbol{Z}^b \boldsymbol{V} = \boldsymbol{P}_e^b \quad ; \quad \boldsymbol{V} = \boldsymbol{Y}\, \boldsymbol{P}_e^b$$

$$\boldsymbol{V} = \left\{ V_{f1}, V_2 \right\} \quad ; \quad \boldsymbol{P}_e^b = \left\{ 0, P_e^b \right\}$$

$$\boldsymbol{Z}^b = \begin{matrix} (Z_c + Z_{f1}) & -Z_c \\ -Z_c & (Z_{f2}^b + Z_p + Z_c) \end{matrix}$$

$$\boldsymbol{Y} = \begin{matrix} Y_{f1f1} & Y_{f12} \\ Y_{f2f1} & Y_{22} \end{matrix} = (\boldsymbol{Z}^b)^{-1}$$

$$\boldsymbol{P}_e^b = \boldsymbol{P}_e \boldsymbol{B}_e$$

$$Y_{f1f1} = \left| \boldsymbol{Z}^b \right|^{-1} (Z_{f2}^b + Z_p + Z_c) \quad ; \quad Y_{22} = \left| \boldsymbol{Z}^b \right|^{-1} (Z_c + Z_{f1})$$

$$Y_{2f1} = Y_{f12} = \left| \boldsymbol{Z}^b \right|^{-1} Z_c \quad ; \quad \left| \boldsymbol{Z}^b \right| = (Z_c + Z_{f1})(Z_{f2}^b + Z_p + \overline{Z_{f1} Z_c})$$

where

$$\overline{Z_{f1} Z_c} = Z_{f1}\, Z_c\, (Z_c + Z_{f1})^{-1}$$

Figure II2. The equivalent electrical circuit diagram representing the model depicted in Figure II1. [cf. Figures I1 and I3.]

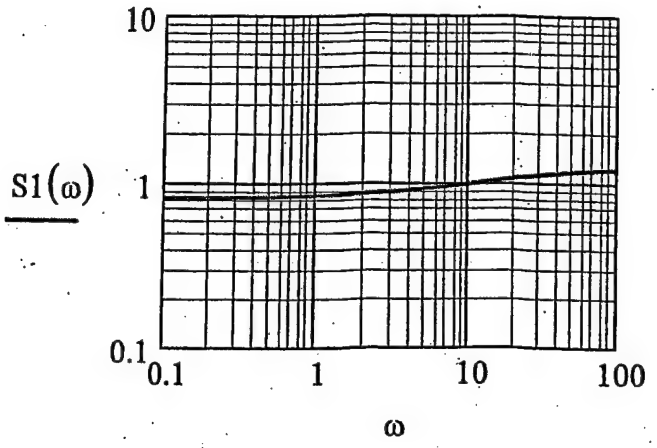

a.

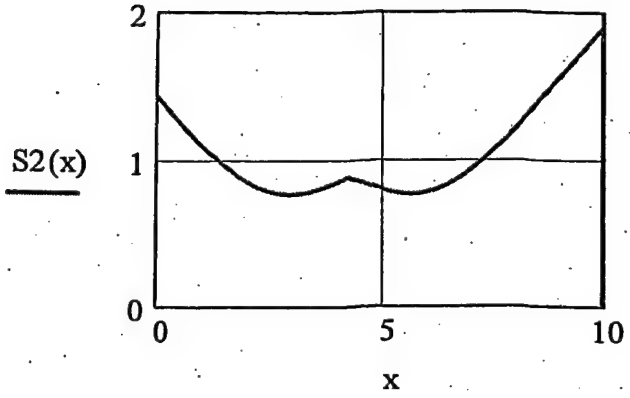

b.

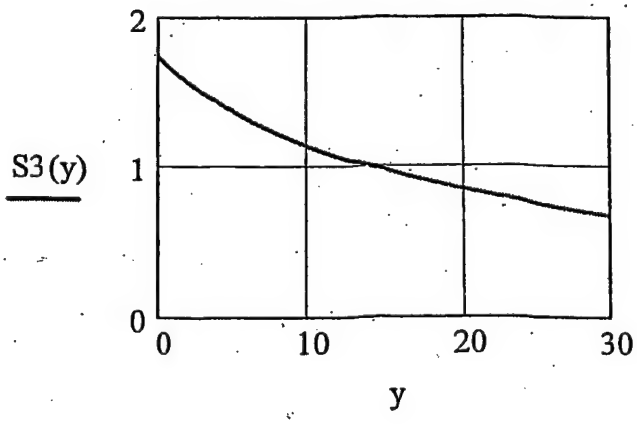

c.

Figure II3. The assumed dependence of the surface stiffness of the coating on the normalized frequency (ω), on the normalized depth (x) and on the temperature (y) in degrees centigrade.

Figure II4a. The coated transfer function, as a function of the normalized frequency, under standard conditions and in the presence of a cavity.

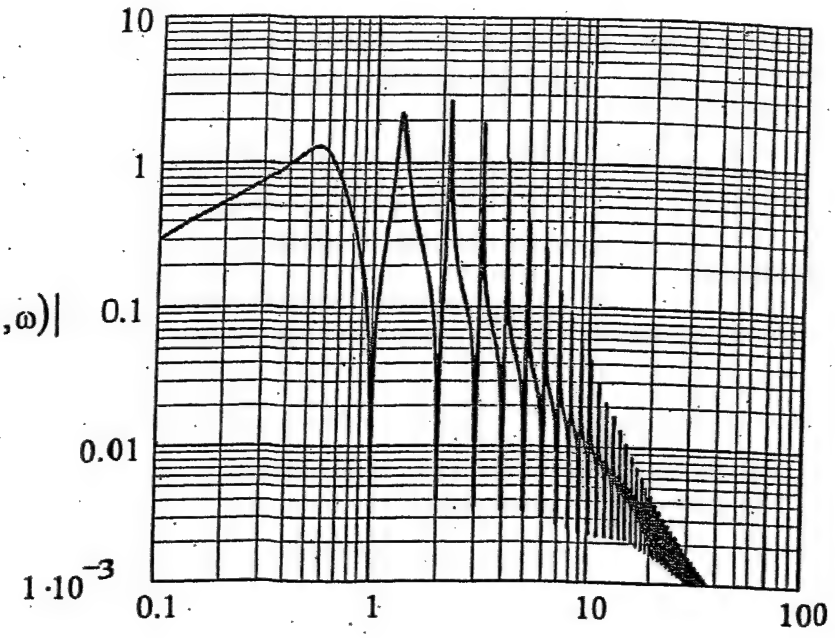

Figure II4b. The uncoated transfer function, as a function of the normalized frequency, under standard conditions and in the presence of a cavity.

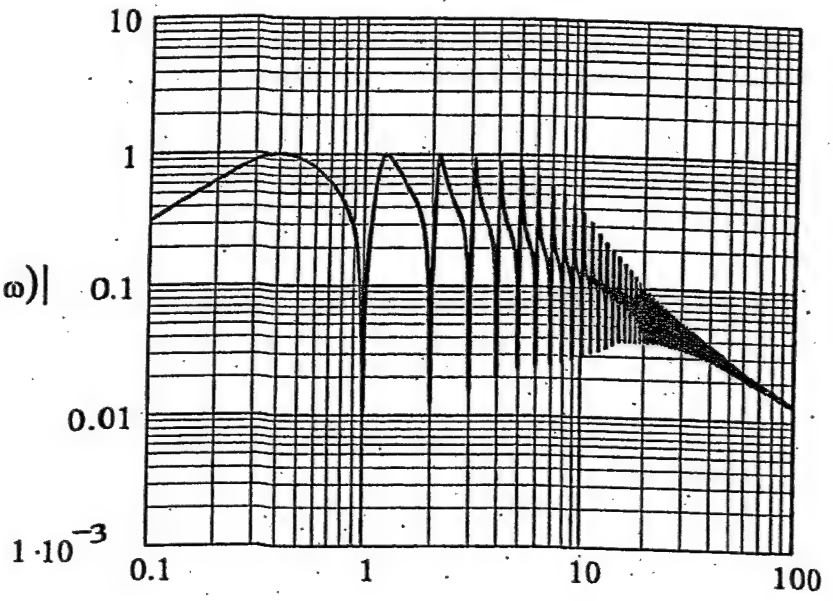

Figure II4c. The ratio of the transfer functions, as a function of the normalized frequency. The ratio is of the transfer function depicted in Figure II4a to that depicted in Figure II4b, thereby, revealing the influence of the coating on the transfer function in the presence of a cavity.

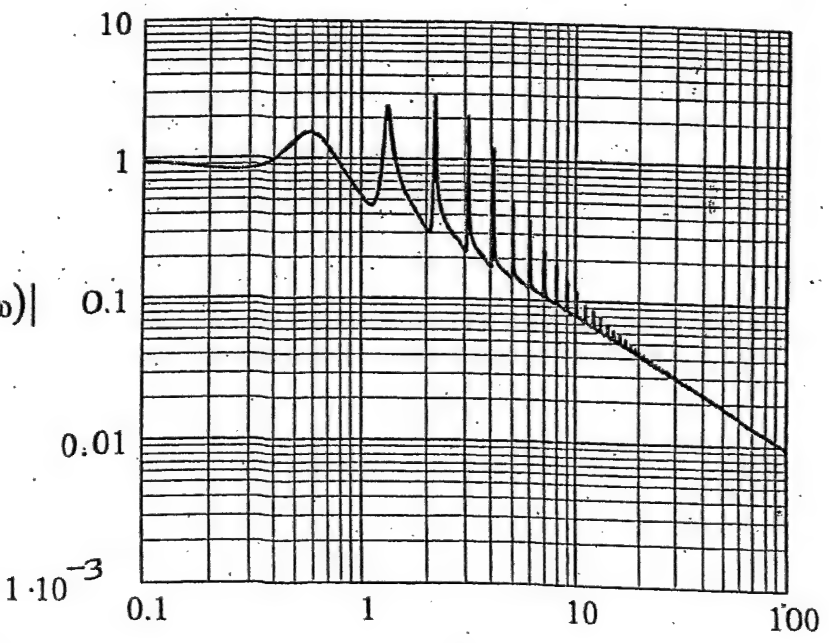

Figure II4d. Figure II4a is repeated except that the normalized depth is changed from the standard value of (4) to (1).

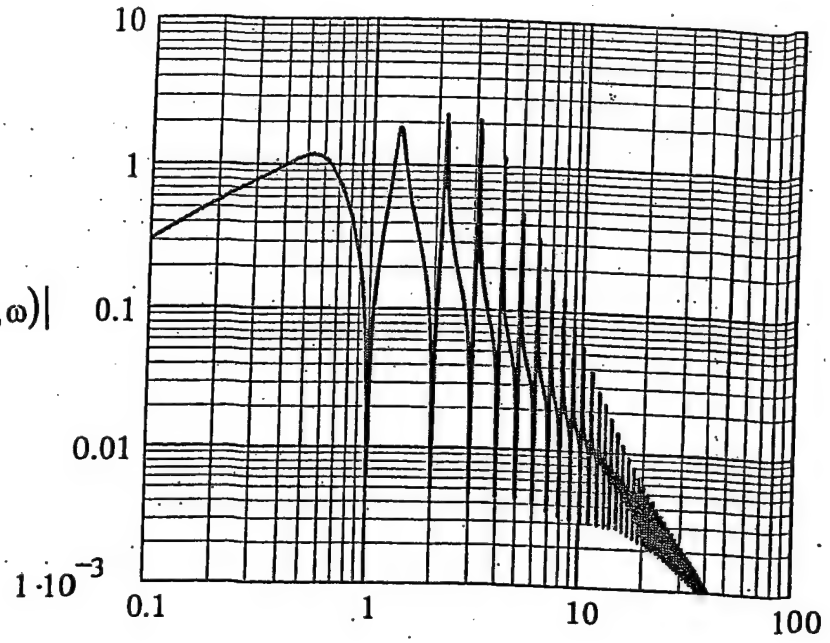

Figure II4e. Figure II4b is repeated except that the normalized depth is changed from the standard value of (4) to (1).

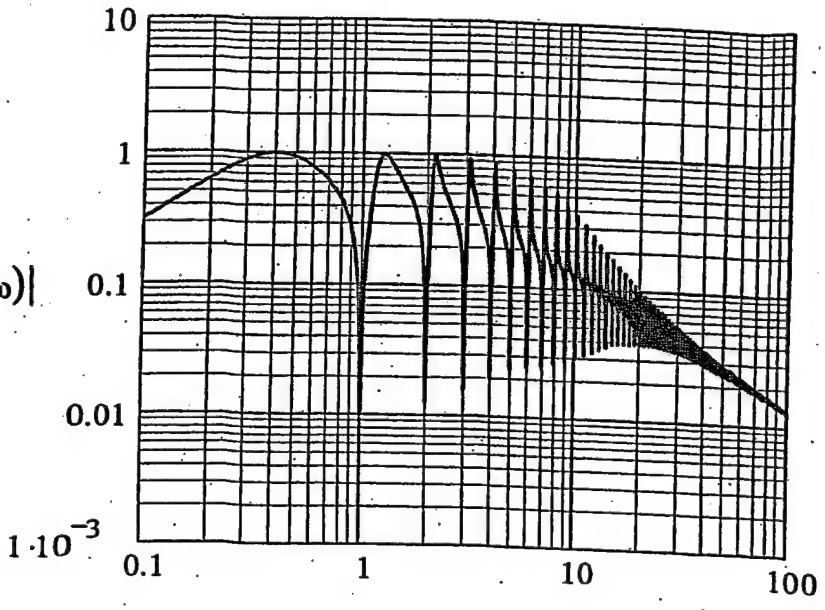

Figure II4f. Figure II4c is repeated except that the normalized depth is changed from the standard value of (4) to (1).

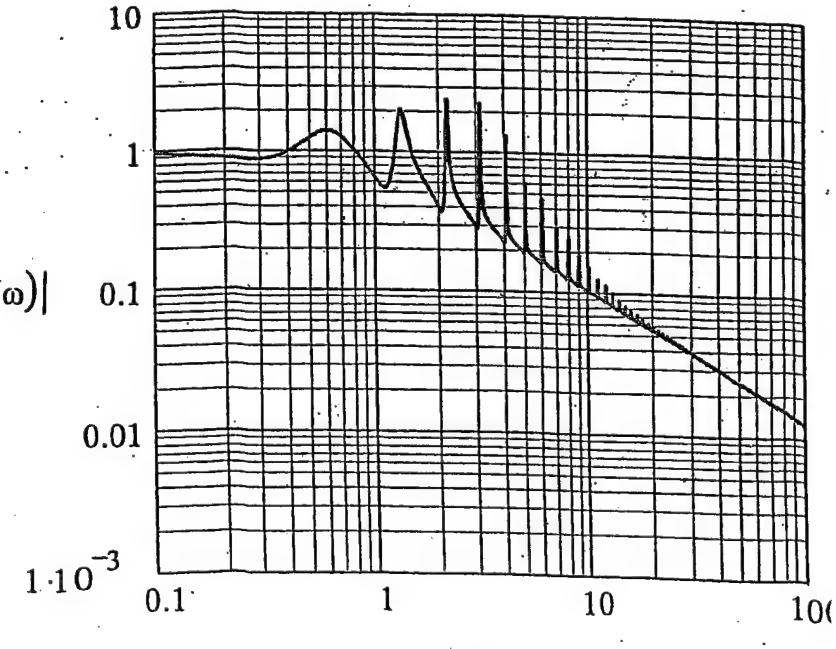

Figure II4g. Figure II4a is repeated except that the normalized depth is changed from the standard value of (4) to (8).

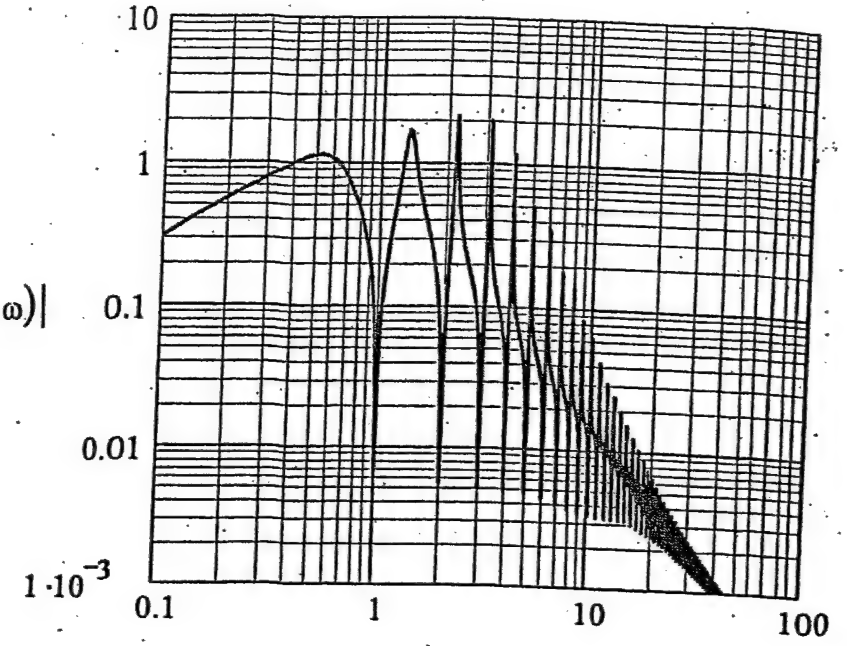

Figure II4h. Figure II4b is repeated except that the normalized depth is changed from the standard value of (4) to (8).

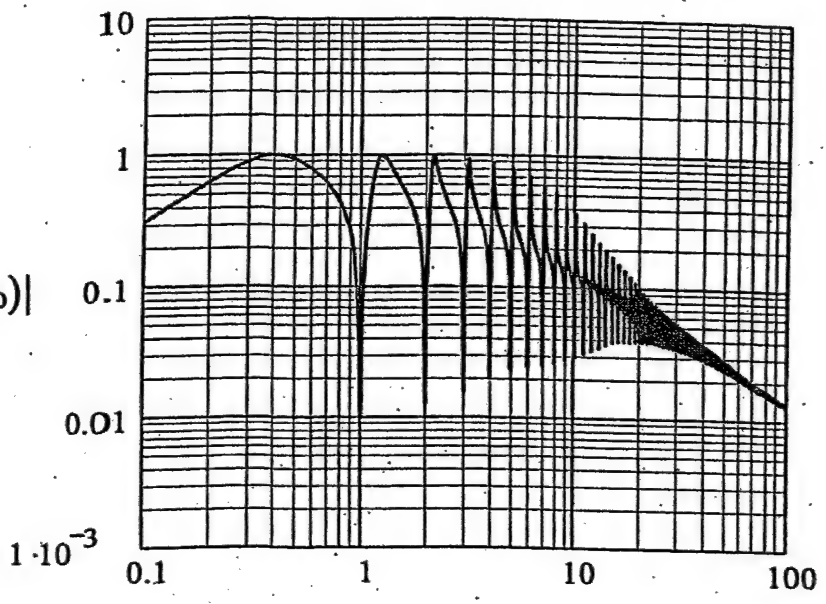

Figure II4i. Figure II4c is repeated except that the normalized depth is changed from the standard value of (4) to (8).

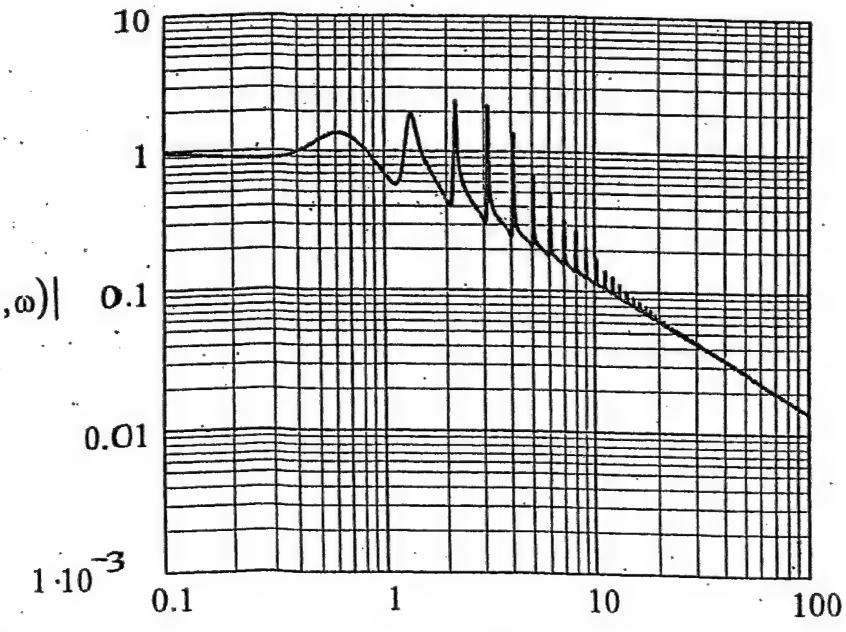

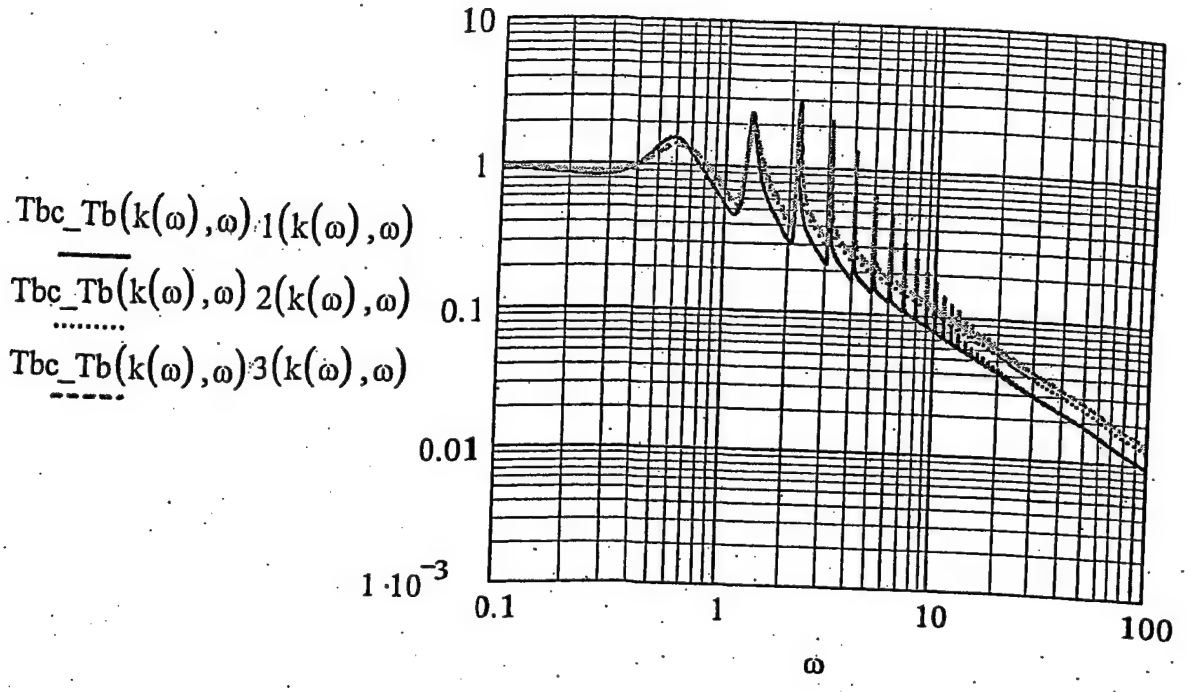

Figure II4j. The superposition of Figures II4c, II4f and II4i, designated 1, 2 and 3, respectively. The differences are due to the depth dependence of the surface stiffness impedance of the coating.

Figure II4k. Figure II4a is repeated except that the reflection coefficient (R) of the baffle is rendered negligible, thereby, removing the cavity. Hence |Tbc| = |Tc|.

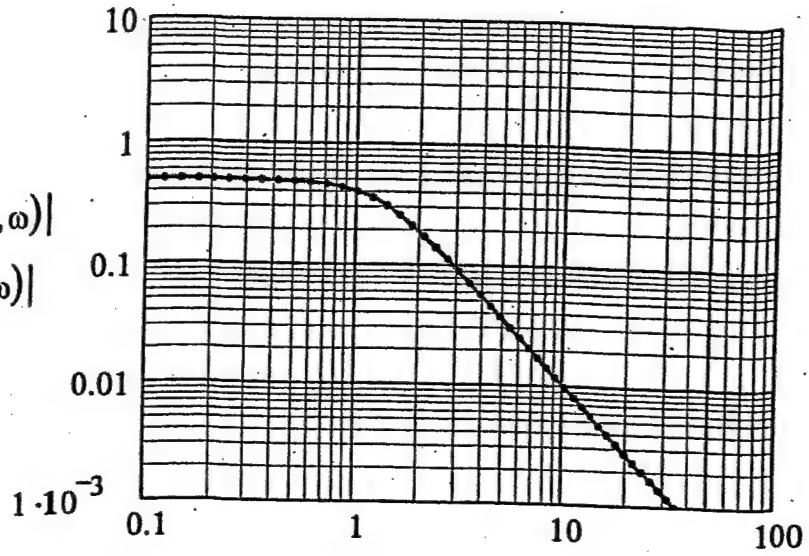

Figure II4l. Figure II4b is repeated except that the reflection coefficient (R) of the baffle is rendered negligible, thereby, removing the cavity. Hence |Tb| = |T|.

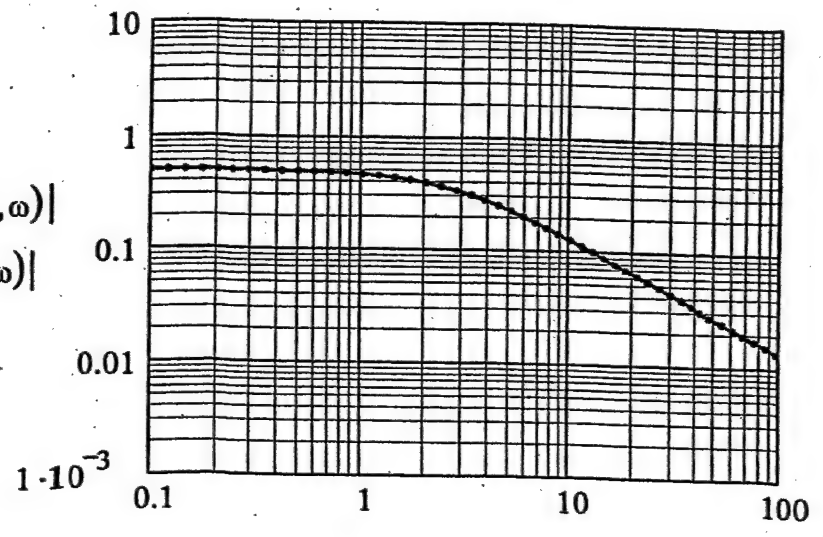

Figure II4m. Figure II4c is repeated except that the reflection coefficient (R) of the baffle is rendered negligible, thereby removing the cavity. Hence |Tbc_Tb| = |Tc_T|.

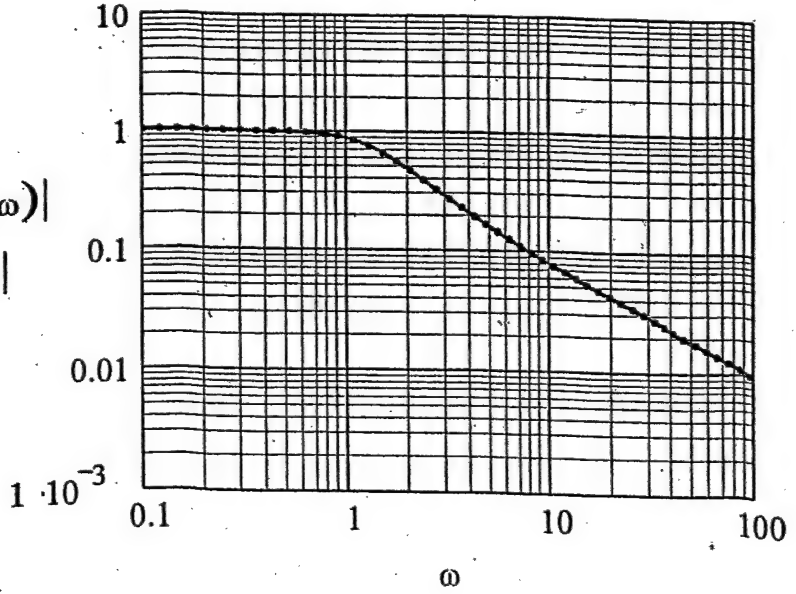

Figure II4n. Figure II4a is repeated (solid curve) and Figure II4k is superposed (dotted curve).

$$\frac{|Tbc(k(\omega),\omega)|}{|Tc(k(\omega),\omega)|}$$

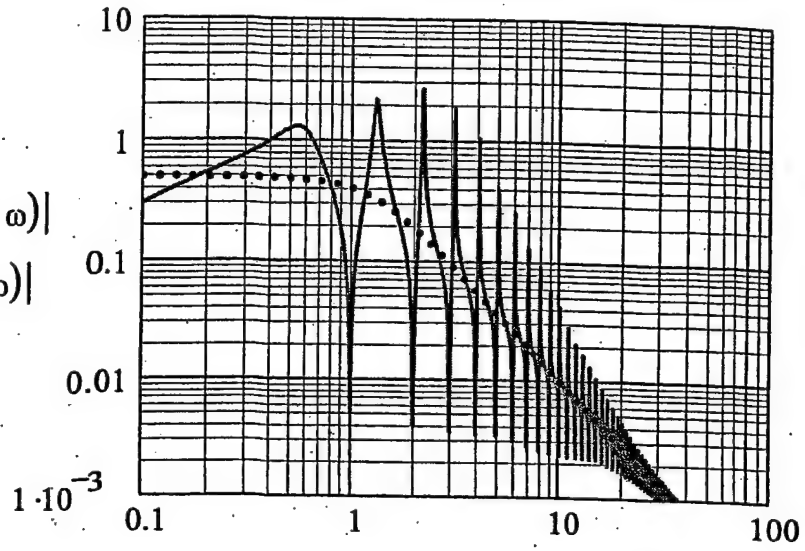

Figure II4o. Figure II4b is repeated (solid curve) and Figure II4l is superposed (dotted curve).

$$\frac{|Tb(k(\omega),\omega)|}{|T(k(\omega),\omega)|}$$

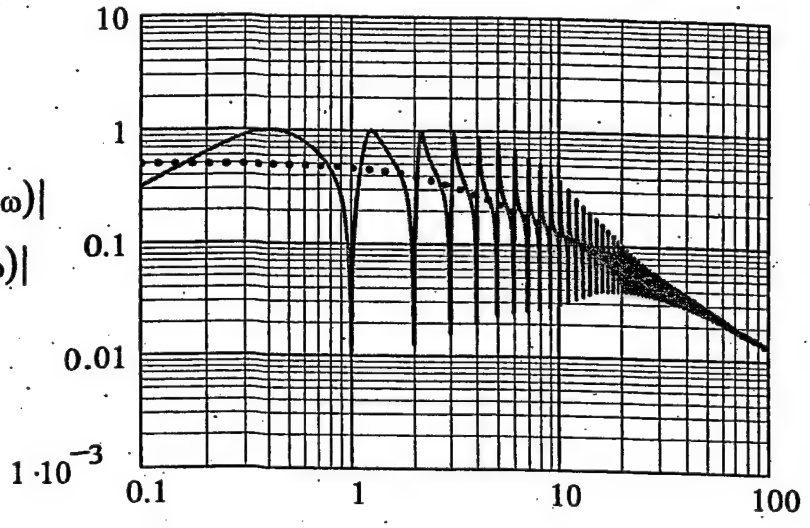

Figure II4p. Figure II4c is repeated (solid curve) and Figure II4m is superposed (dotted curve).

$$\frac{|Tbc\_Tb(k(\omega),\omega)|}{|Tc\_T(k(\omega),\omega)|}$$

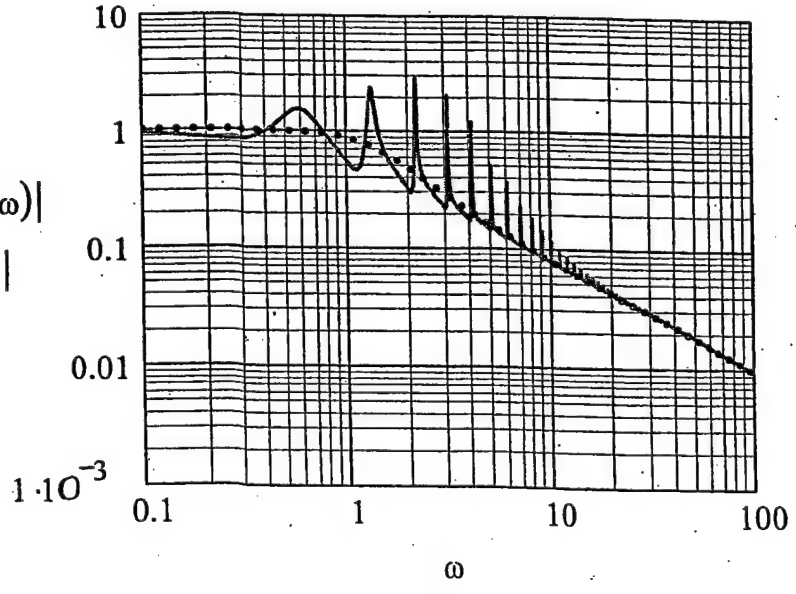

Figure II5a. Figure II4a is repeated except that the normalized gap (bk_o) is changed from the standard value of (π) to $(2\pi/\sqrt{\omega})$.

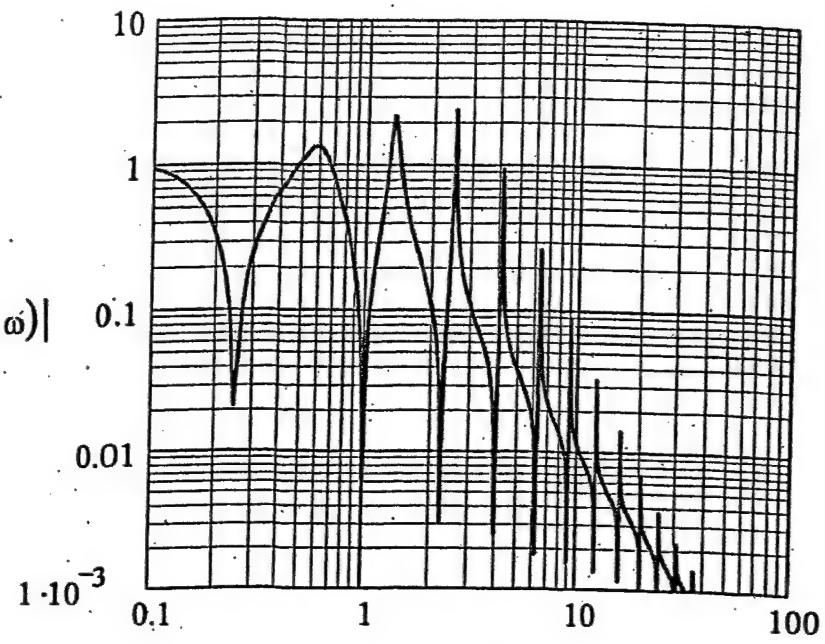

Figure II5b. Figure II4b is repeated except that the normalized gap (bk_o) is changed from the standard value of (π) to $(2\pi/\sqrt{\omega})$.

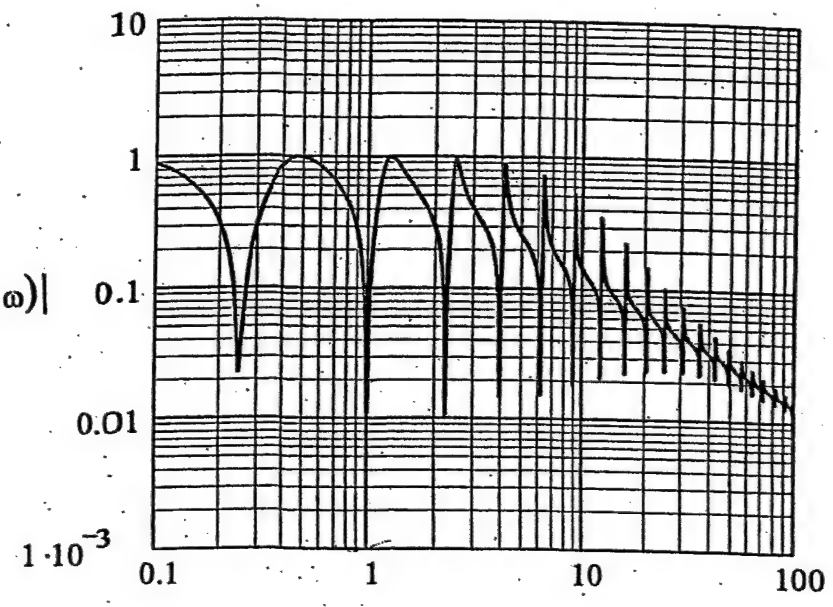

Figure II5c. Figure II4c is repeated except that the normalized gap (bk_o) is changed from the standard value of (π) to $(2\pi/\sqrt{\omega})$.

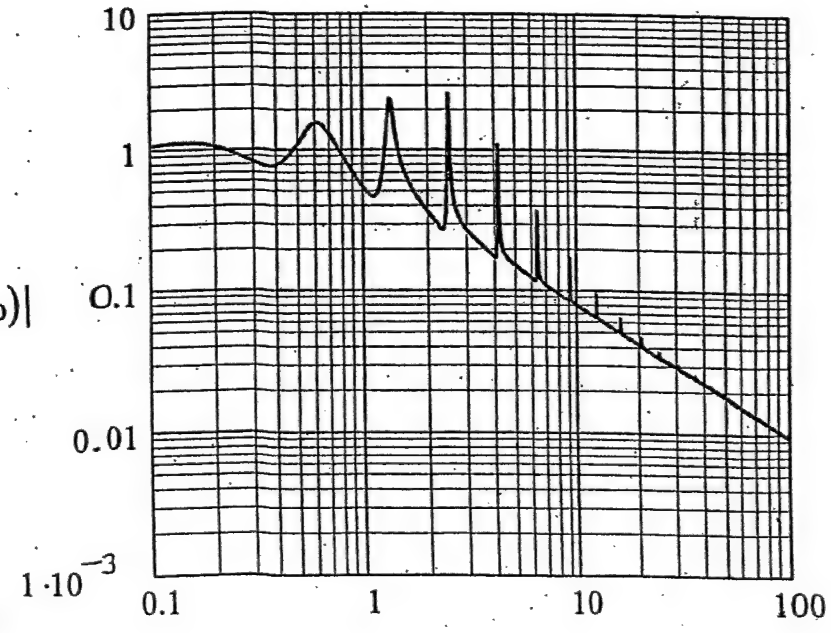

Figure II5d. Figure II5a is repeated except that the reflection coefficient (R) of the baffle is rendered negligible, thereby, removing the cavity. Hence |Tbc| = |Tc|. [cf. Figure II4k.]

$\frac{|Tbc(k(\omega),\omega)|}{|Tc(k(\omega),\omega)|}$

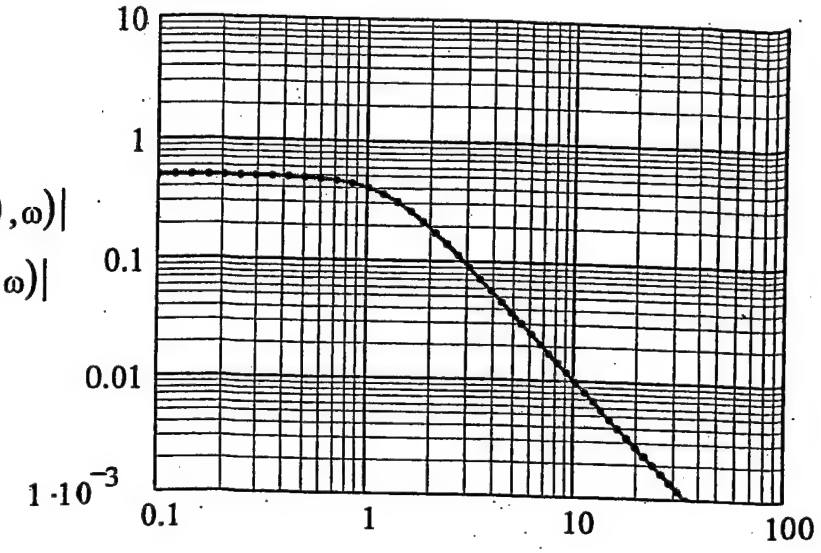

Figure II5e. Figure II5a is repeated except that the reflection coefficient (R) of the baffle is rendered negligible, thereby, removing the cavity. Hence |Tb| = |T|. [cf. Figure II4l.]

$\frac{|Tb(k(\omega),\omega)|}{|T(k(\omega),\omega)|}$

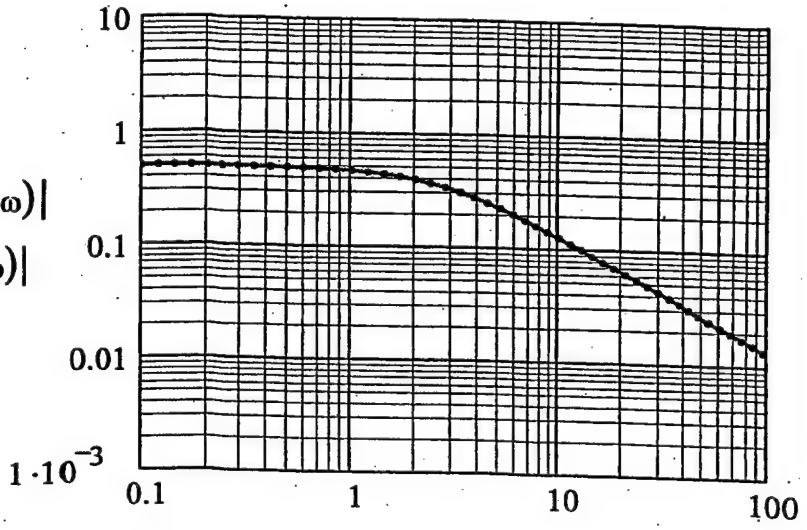

Figure II5f. Figure II5a is repeated except that the reflection coefficient (R) of the baffle is rendered negligible, thereby, removing the cavity. Hence |Tbc_Tb| = |Tc|_T|. [cf. Figure II4m.]

$\frac{|Tbc\_Tb(k(\omega),\omega)|}{|Tc\_T(k(\omega),\omega)|}$

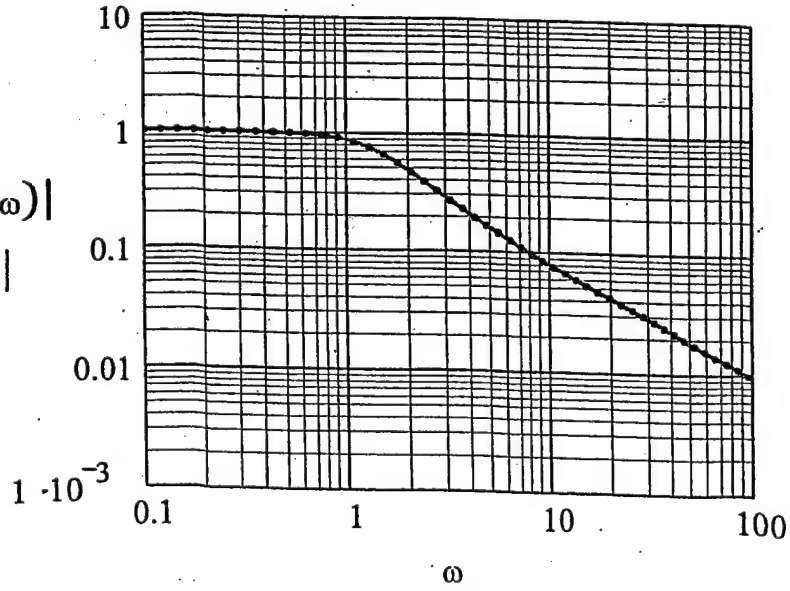

Figure II5g. Figure II5a is repeated (solid curve) and Figure II5d is superposed (dotted curve).

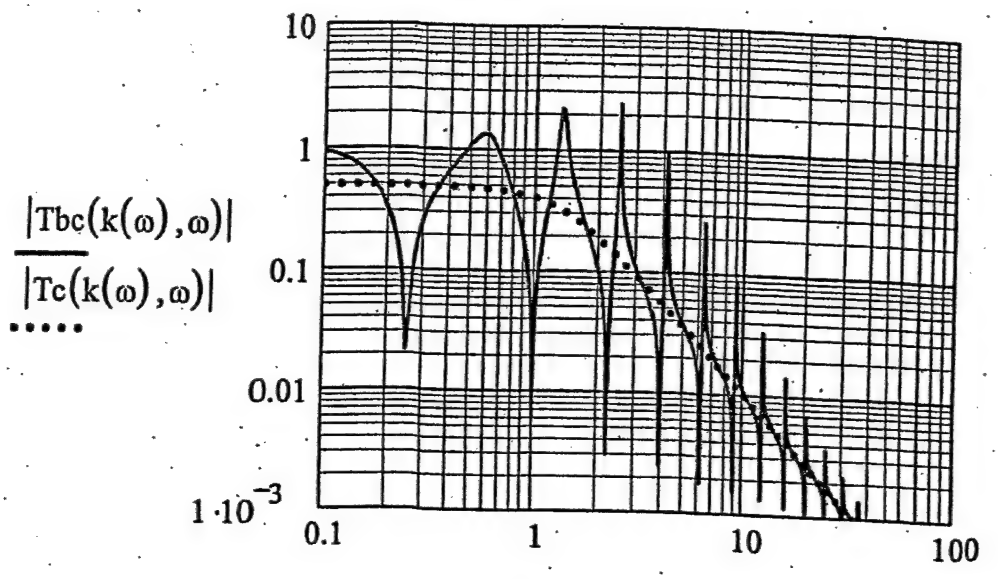

Figure II5h. Figure II5b is repeated (solid curve) and Figure II5e is superposed (dotted curve).

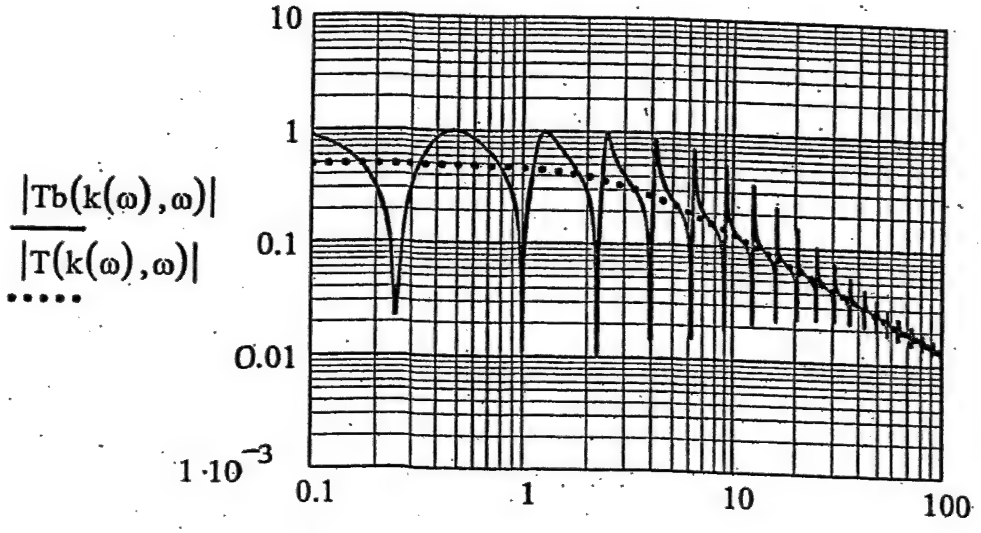

Figure II5i. Figure II5c is repeated (solid curve) and Figure II5f is superposed (dotted curve).

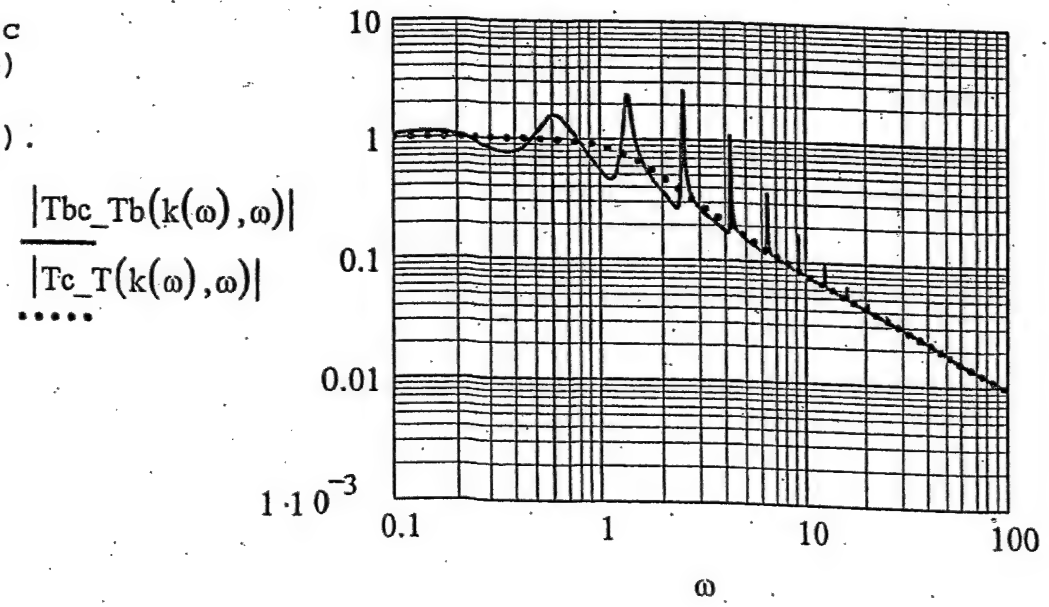

Figure II6a. Figure II4a is repeated except that the standard beam-directed radiation; $\theta = 0$, is changed to an off beam-directed radiation; $\theta = (\pi/3)$. The accompanied change from a surface mass control to a surface stiffness control in the surface impedance of the equivalent plate is observed at $\omega \cong 13$.

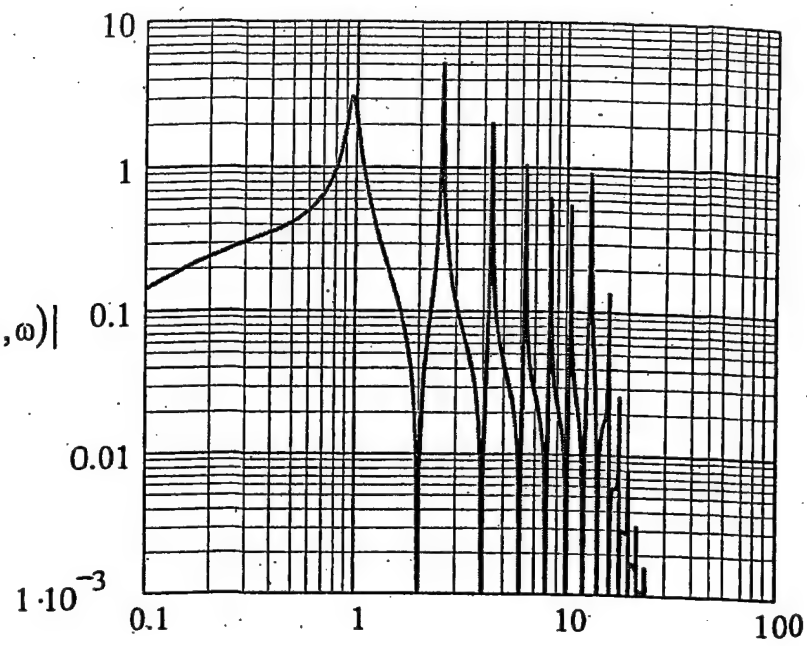

Figure II6b. Figure II4b is repeated except that the standard beam-directed radiation; $\theta = 0$, is changed to an off beam-directed radiation; $\theta = (\pi/3)$. The accompanied change from a surface mass control to a surface stiffness control in the surface impedance of the equivalent plate is observed at $\omega \cong 13$.

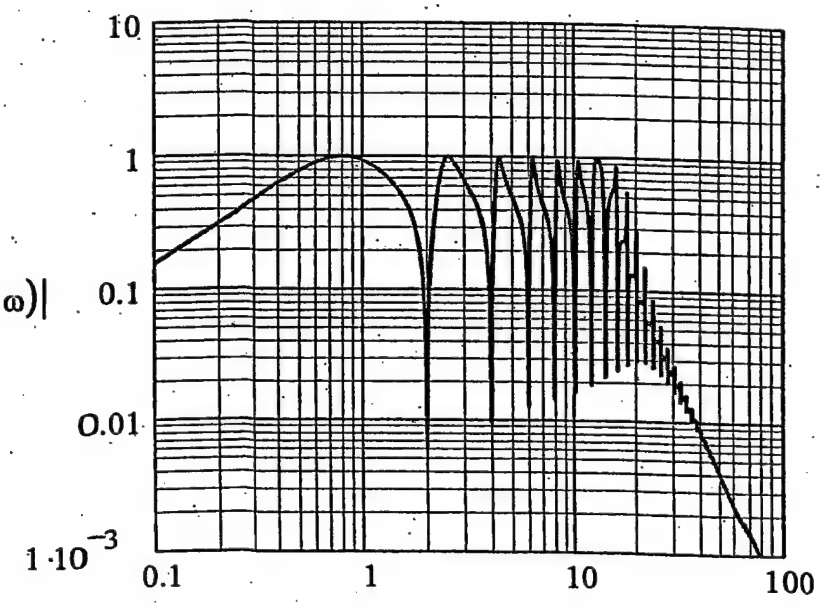

Figure II6c. Figure II4c is repeated except that the standard beam-directed radiation; $\theta = 0$, is changed to an off beam-directed radiation; $\theta = (\pi/3)$. The accompanied change from a surface mass control to a surface stiffness control in the surface impedance of the equivalent plate is observed at $\omega \cong 13$.

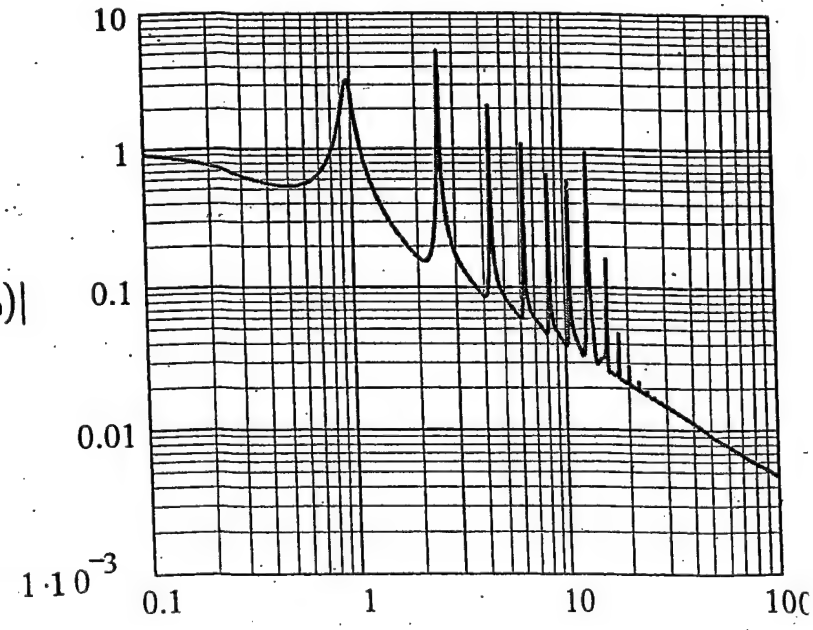

Figure II6d. Figure II4k is repeated except that the standard beam-directed radiation; $\theta = 0$, is changed to an off beam-directed radiation; $\theta = (\pi/3)$. The accompanied change from a surface mass control to a surface stiffness control in the surface impedance of the equivalent plate is observed at $\omega \cong 13$.

$\frac{|Tbc(k(\omega),\omega)|}{|Tc(k(\omega),\omega)|}$

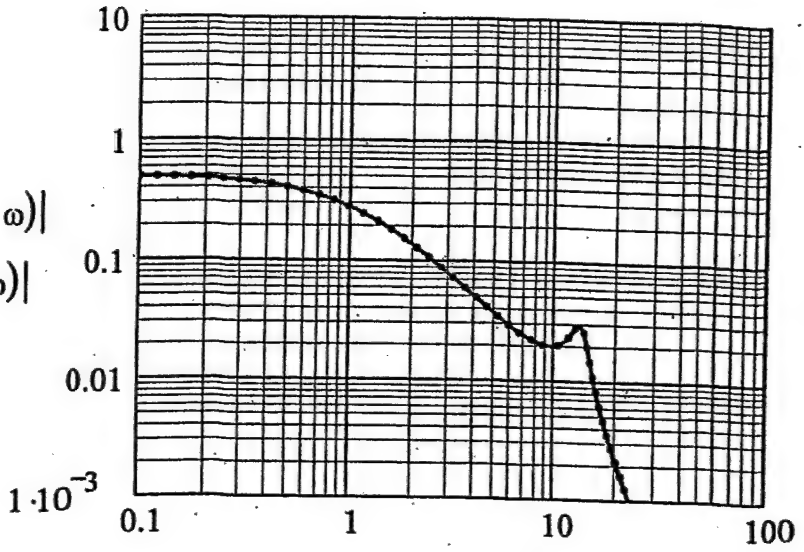

Figure II6e. Figure II4l is repeated except that the standard beam-directed radiation; $\theta = 0$, is changed to an off beam-directed radiation; $\theta = (\pi/3)$. The accompanied change from a surface mass control to a surface stiffness control in the surface impedance of the equivalent plate is observed at $\omega \cong 13$.

$\frac{|Tb(k(\omega),\omega)|}{|T(k(\omega),\omega)|}$

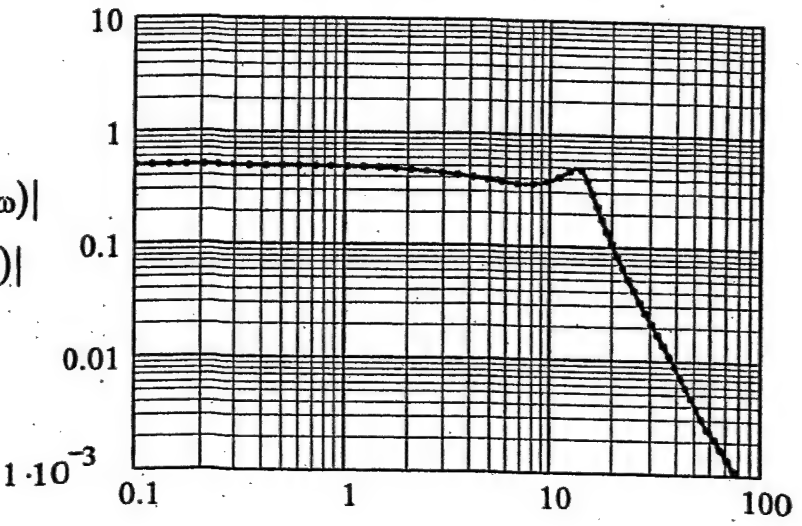

Figure II6f. Figure II4m is repeated except that the standard beam-directed radiation; $\theta = 0$, is changed to an off beam-directed radiation; $\theta = (\pi/3)$. The accompanied change from a surface mass control to a surface stiffness control in the surface impedance of the equivalent plate is observed at $\omega \cong 13$.

$\frac{|Tbc\_Tb(k(\omega),\omega)|}{|Tc\_T(k(\omega),\omega)|}$

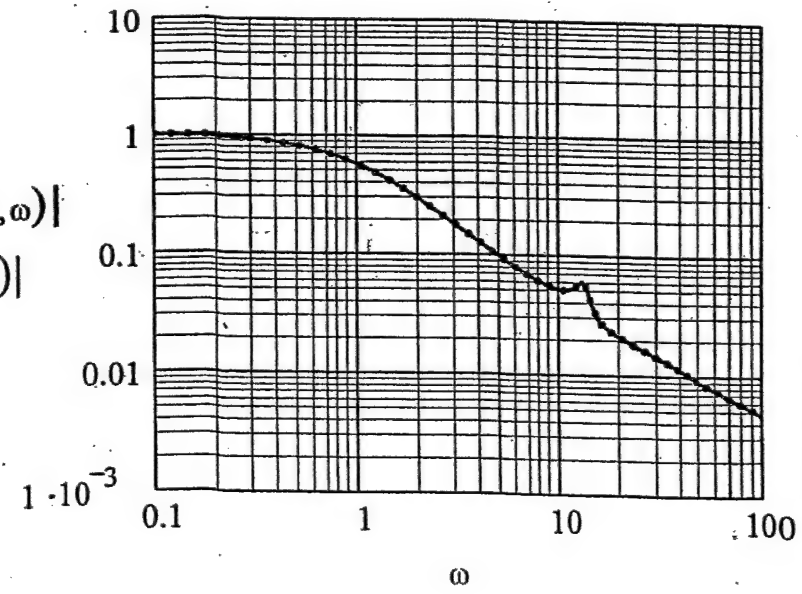

Figure II6g. Figure II6a is repeated (solid curve) and Figure II6d is superposed (dotted curve).

$$\frac{|Tbc(k(\omega),\omega)|}{|Tc(k(\omega),\omega)|}$$

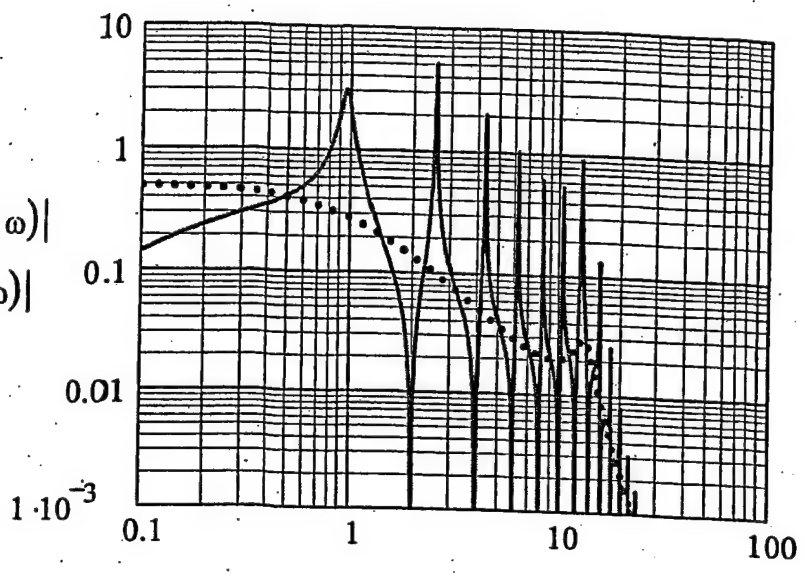

Figure II6h. Figure II6b is repeated (solid curve) and Figure II6e is superposed (dotted curve).

$$\frac{|Tb(k(\omega),\omega)|}{|T(k(\omega),\omega)|}$$

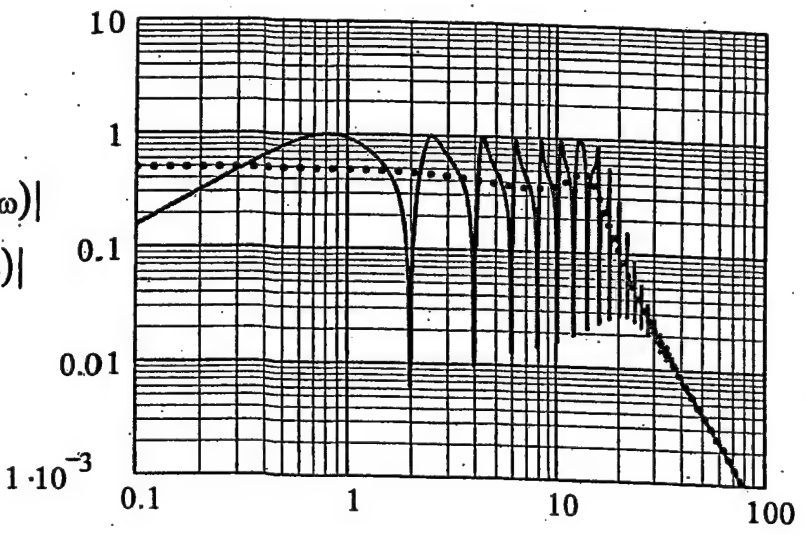

Figure II6i. Figure II6c is repeated (solid curve) and Figure II6f is superposed (dotted curve).

$$\frac{|Tbc\_Tb(k(\omega),\omega)|}{|Tc\_T(k(\omega),\omega)|}$$

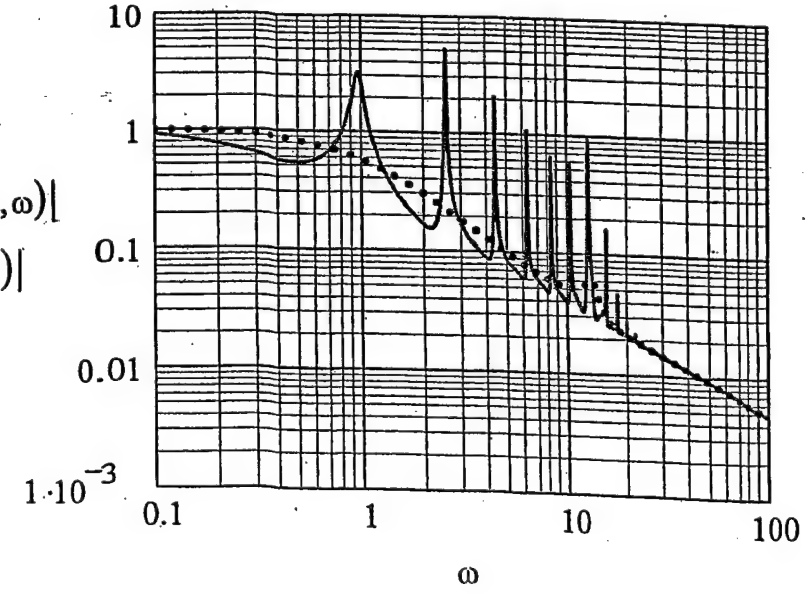

Figure II7a. Figure II4a is repeated except that the standard loss factor in the cavity is changed from the standard value of (10^{-3}) to (10^{-1}).

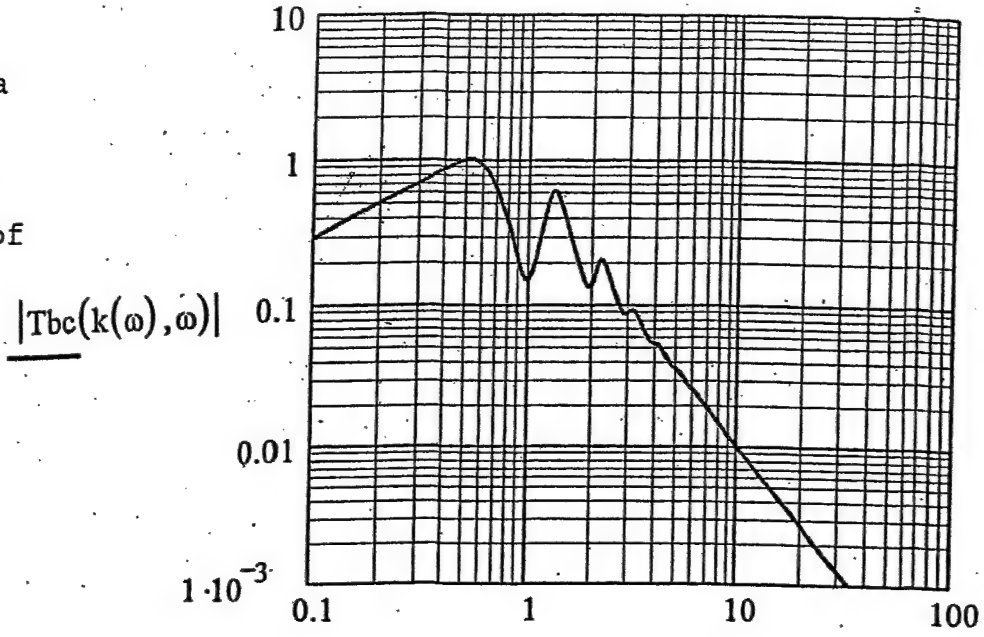

Figure II7b. Figure II4b is repeated except that the standard loss factor in the cavity is changed from the standard value of (10^{-3}) to (10^{-1}).

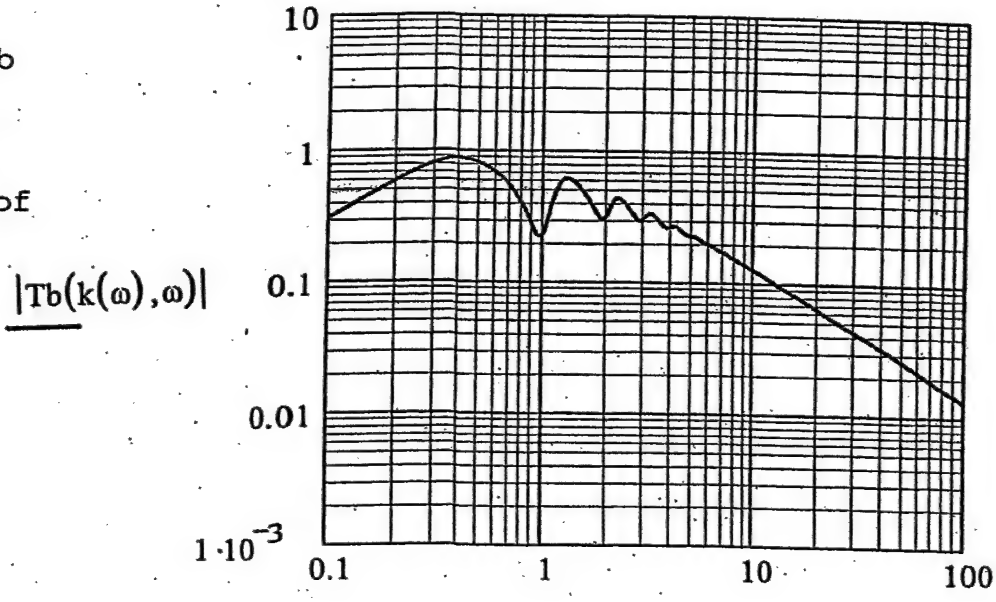

Figure II7c. Figure II4c is repeated except that the standard loss factor in the cavity is changed from the standard value of (10^{-3}) to (10^{-1}).

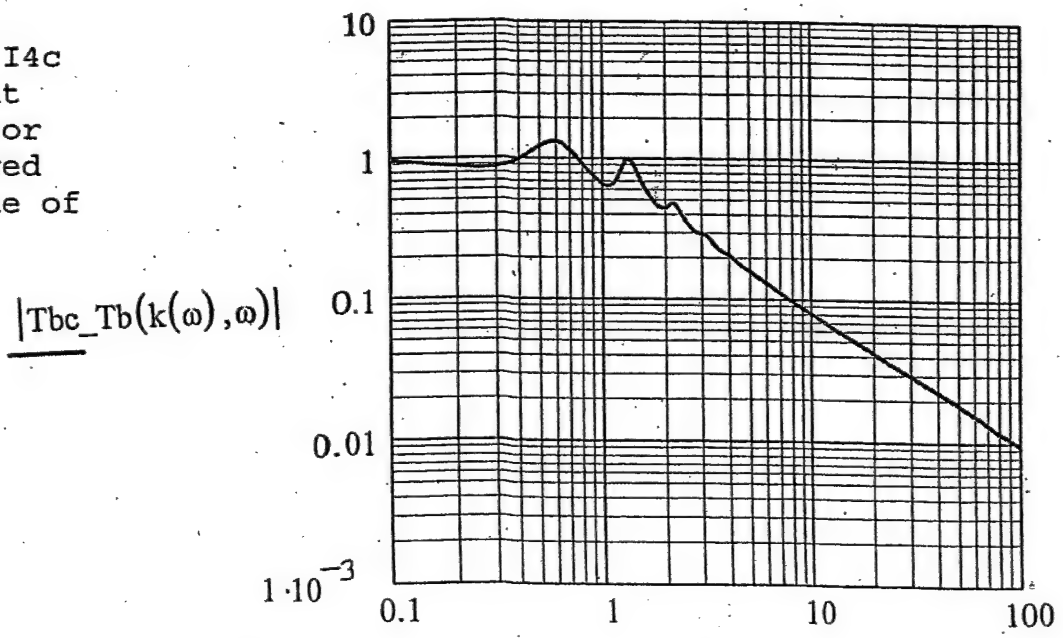

Figure II8a. Figure II4n is repeated except that the loss factor in the cavity (η) is changed from the standard value of (10^{-3}) to (10^{-1}). [cf. Table II1.]

$\frac{|Tbc(k(\omega),\omega)|}{|Tc(k(\omega),\omega)|}$ .....

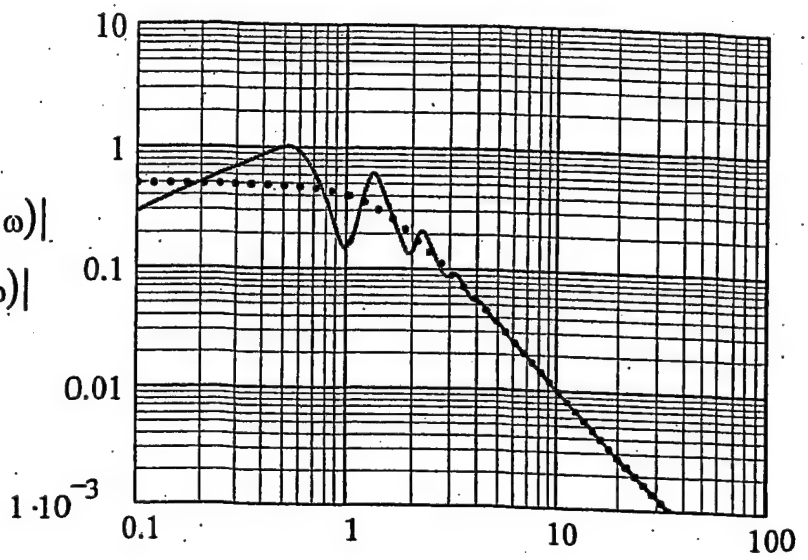

Figure II8b. Figure II4o is repeated except that the loss factor in the cavity (η) is changed from the standard value of (10^{-3}) to (10^{-1}). [cf. Table II1.]

$\frac{|Tb(k(\omega),\omega)|}{|T(k(\omega),\omega)|}$ .....

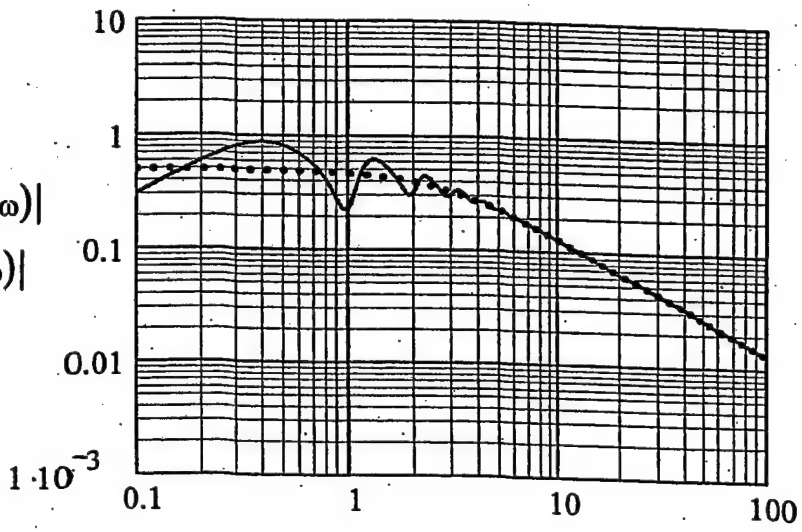

Figure II8c. Figure II4p is repeated except that the loss factor in the cavity (η) is changed from the standard value of (10^{-3}) to (10^{-1}). [cf. Table II1.]

$\frac{|Tbc\_Tb(k(\omega),\omega)|}{|Tc\_T(k(\omega),\omega)|}$ .....

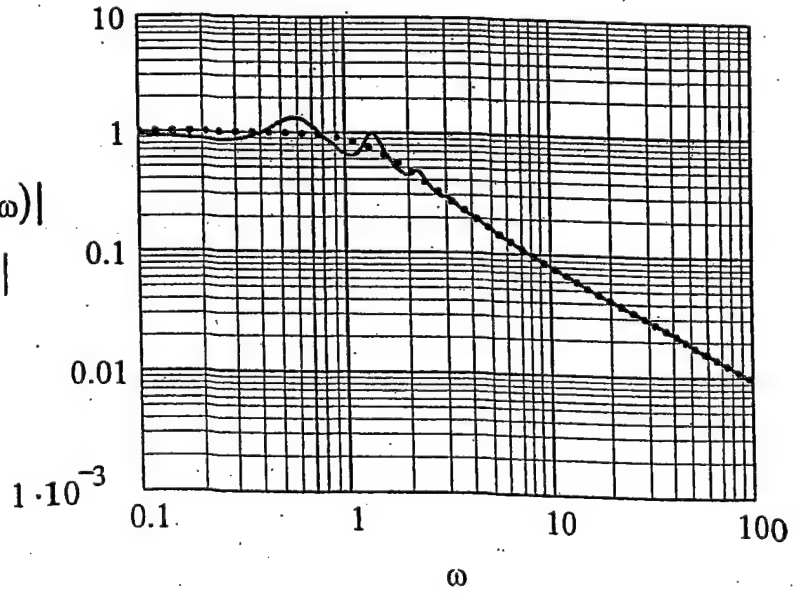

Figure II8d. Figure II4n is repeated except that the loss factor in the coating (η_c) is changed from the standard value of (10^{-3}) to (10^{-1}). [cf. Table II1.]

$\frac{|Tbc(k(\omega),\omega)|}{|Tc(k(\omega),\omega)|}$ .....

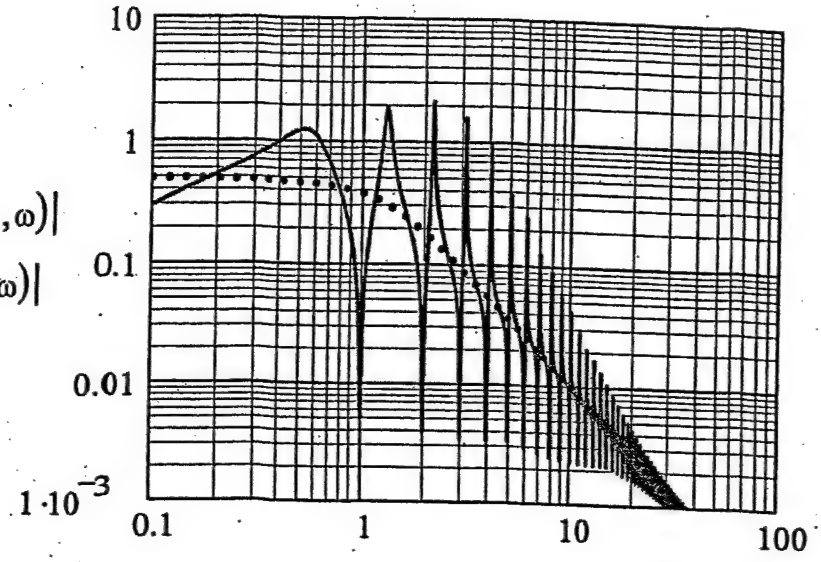

Figure II8e. Figure II4o is repeated except that the loss factor in the coating (η_c) is changed from the standard value of (10^{-3}) to (10^{-1}). [cf. Table II1.]

$\frac{|Tb(k(\omega),\omega)|}{|T(k(\omega),\omega)|}$ .....

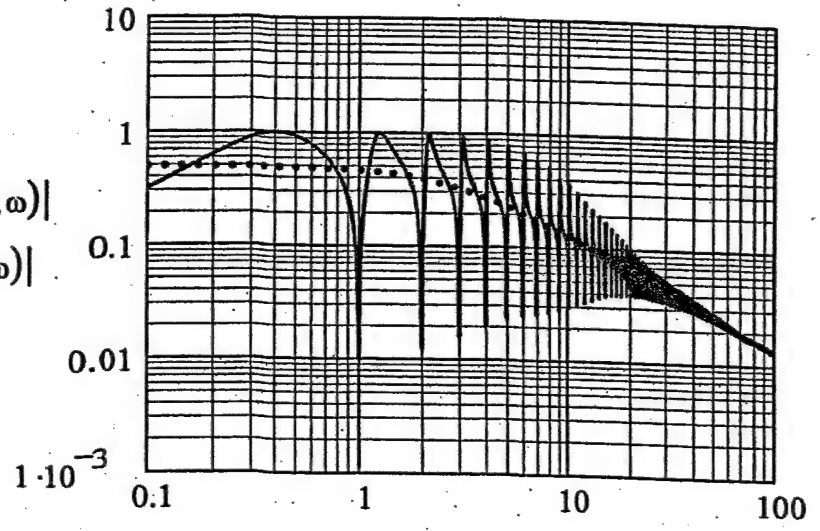

Figure II8f. Figure II4p is repeated except that the loss factor in the coating (η_c) is changed from the standard value of (10^{-3}) to (10^{-1}). [cf. Table II1.]

$\frac{|Tbc\_Tb(k(\omega),\omega)|}{|Tc\_T(k(\omega),\omega)|}$ .....

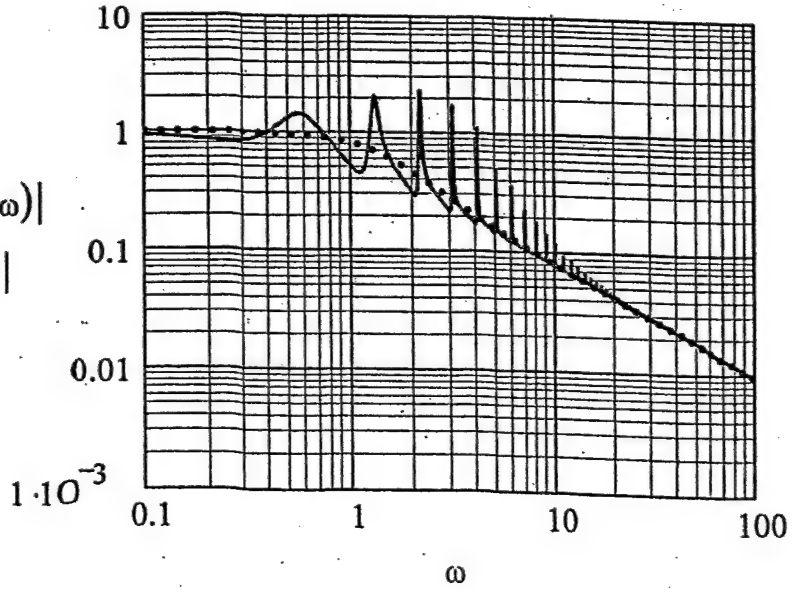

Figure II8g. Figure II4n is repeated except that the surface stiffness control loss factor in the equivalent plate (η_p) is changed from the standard value of (10^{-3}) to (10^{-1}). [cf. Table II1.]

$\frac{|Tbc(k(\omega),\omega)|}{|Tc(k(\omega),\omega)|}$ .....

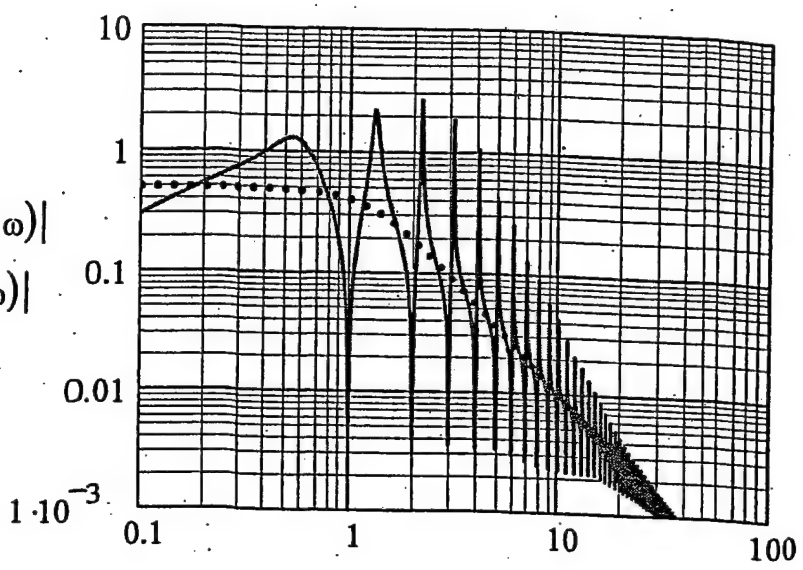

Figure II8h. Figure II4o is repeated except that the surface stiffness control loss factor in the equivalent plate (η_p) is changed from the standard value of (10^{-3}) to (10^{-1}). [cf. Table II1.]

$\frac{|Tb(k(\omega),\omega)|}{|T(k(\omega),\omega)|}$ .....

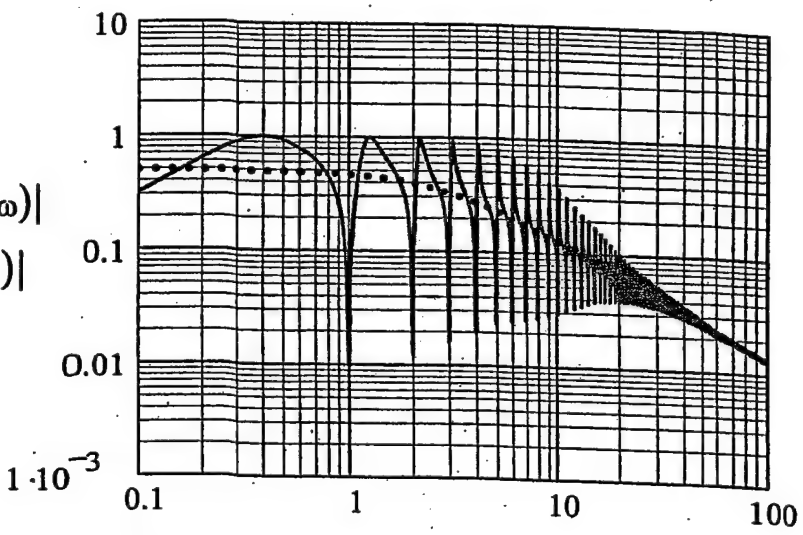

Figure II8i. Figure II4p is repeated except that the surface stiffness control loss factor in the equivalent plate (η_p) is changed from the standard value of (10^{-3}) to (10^{-1}). [cf. Table II1.]

$\frac{|Tbc\_Tb(k(\omega),\omega)|}{|Tc\_T(k(\omega),\omega)|}$ .....

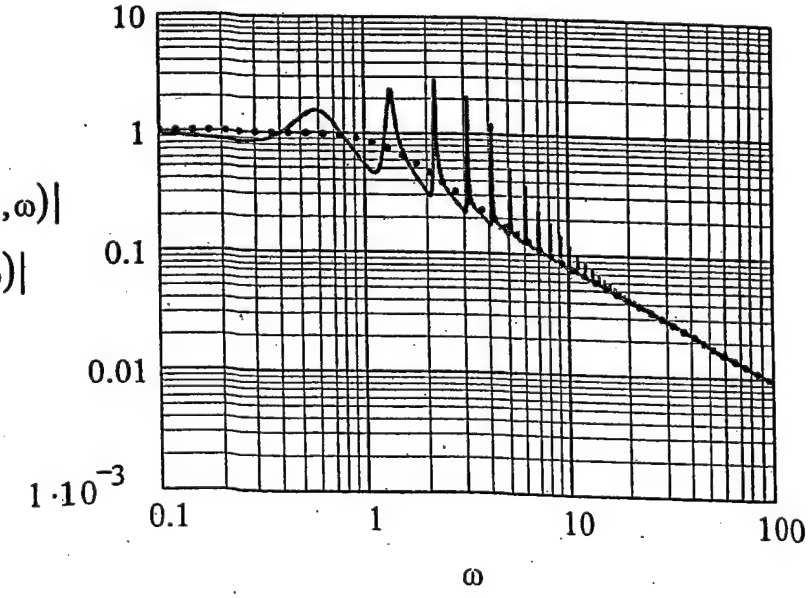

Figure II8j. Figure II4n is repeated except that the surface stiffness control and the surface mass control loss factors (η_p) and (η_m) are changed from the standard value of (10^{-3}) to (10^{-1}). [cf. Table II1.]

$\frac{|Tbc(k(\omega),\omega)|}{|Tc(k(\omega),\omega)|}$

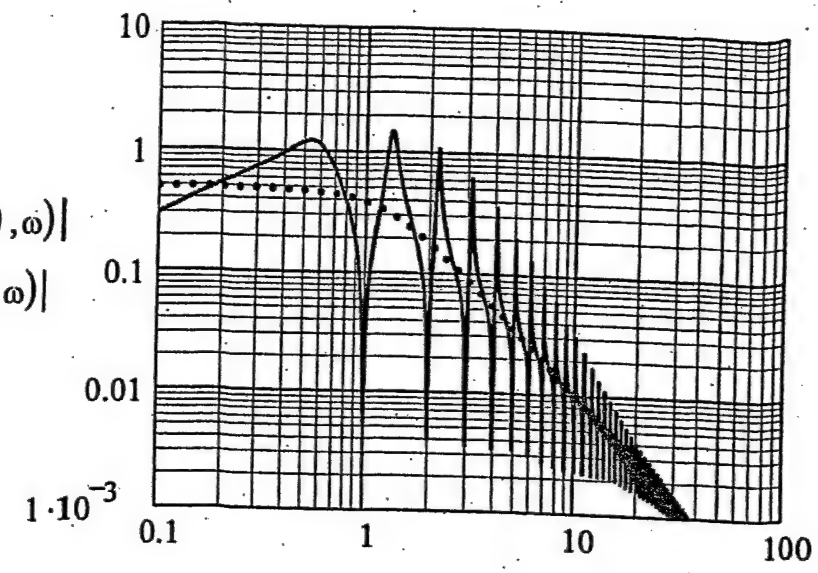

Figure II8k. Figure II4o is repeated except that the surface stiffness control and the surface mass control loss factors (η_p) and (η_m) are changed from the standard value of (10^{-3}) to (10^{-1}). [cf. Table II1.]

$\frac{|Tb(k(\omega),\omega)|}{|T(k(\omega),\omega)|}$

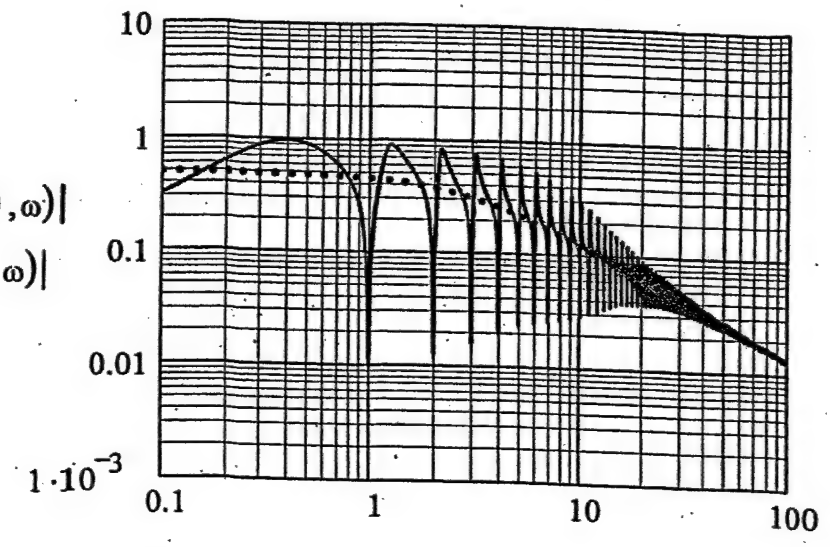

Figure II8l. Figure II4p is repeated except that the surface stiffness control and the surface mass control loss factors (η_p) and (η_m) are changed from the standard value of (10^{-3}) to (10^{-1}). [cf. Table II1.]

$\frac{|Tbc\_Tb(k(\omega),\omega)|}{|Tc\_T(k(\omega),\omega)|}$

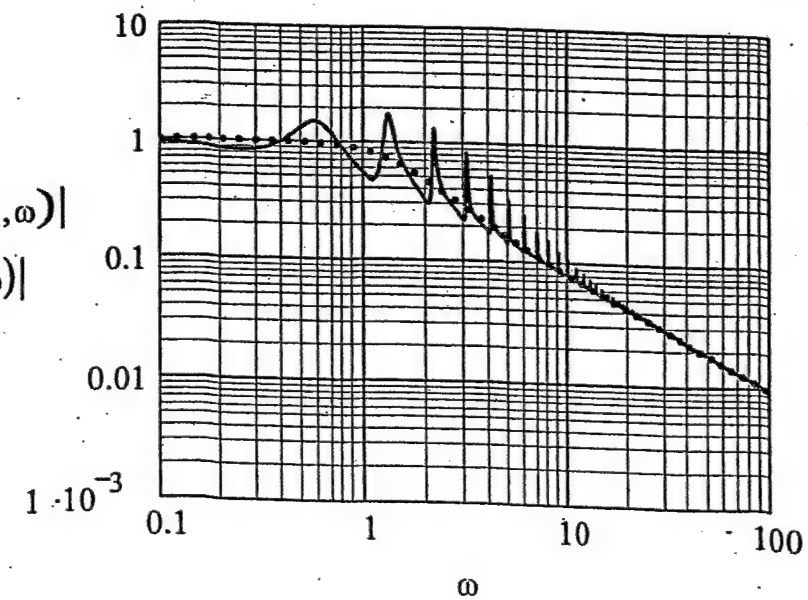

Figure II8m. Figure II4n is repeated except that all the loss factors; η, η_c, η_p, and η_m, are changed from the standard value of (10^{-3}) to (10^{-1}). [cf. Table II1.]

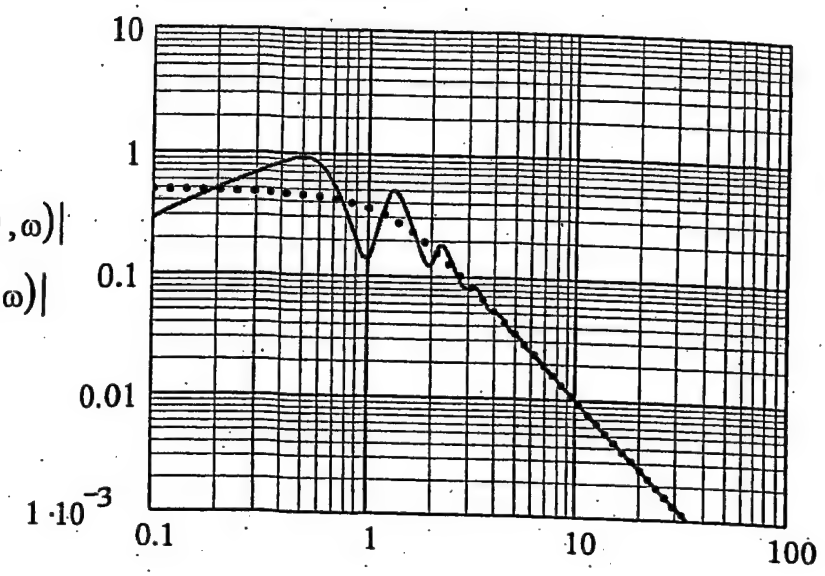

Figure II8n. Figure II4o is repeated except that all the loss factors; η, η_c, η_p, and η_m, are changed from the standard value of (10^{-3}) to (10^{-1}). [cf. Table II1.]

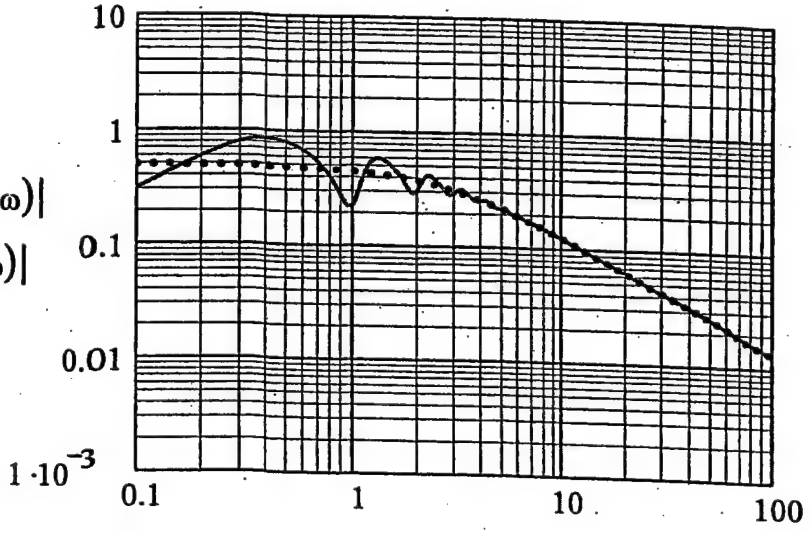

Figure II8o. Figure II4p is repeated except that all the loss factors; η, η_c, η_p, and η_m, are changed from the standard value of (10^{-3}) to (10^{-1}). [cf. Table II1.]

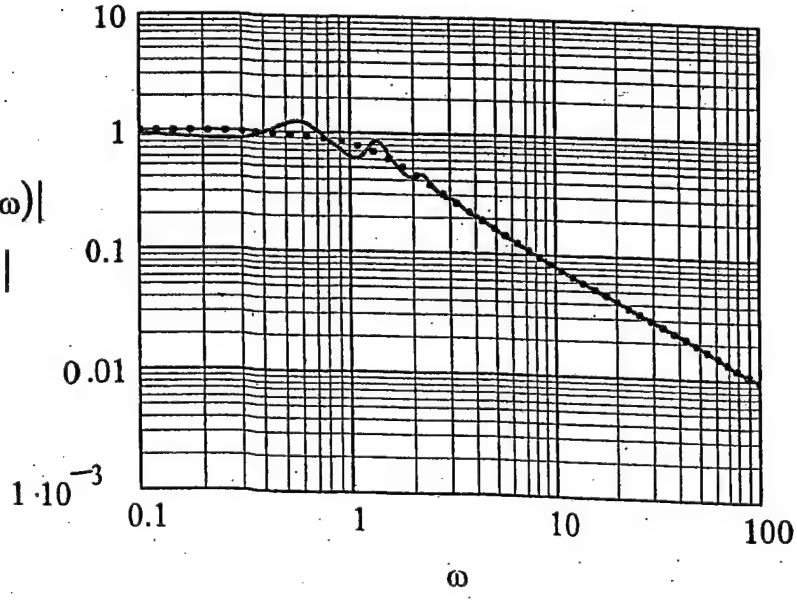

Figure II9a. Figure II5g is repeated except that the loss factor in the cavity (η) is changed from the standard value of (10^{-3}) to (10^{-1}). [cf. Table II1.]

$\frac{|Tbc(k(\omega),\omega)|}{|Tc(k(\omega),\omega)|}$

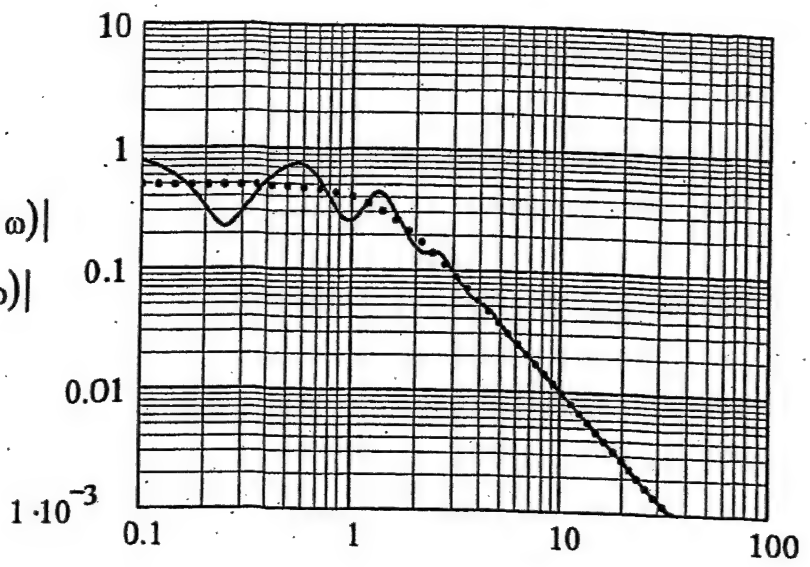

Figure II9b. Figure II5h is repeated except that the loss factor in the cavity (η) is changed from the standard value of (10^{-3}) to (10^{-1}). [cf. Table II1.]

$\frac{|Tb(k(\omega),\omega)|}{|T(k(\omega),\omega)|}$

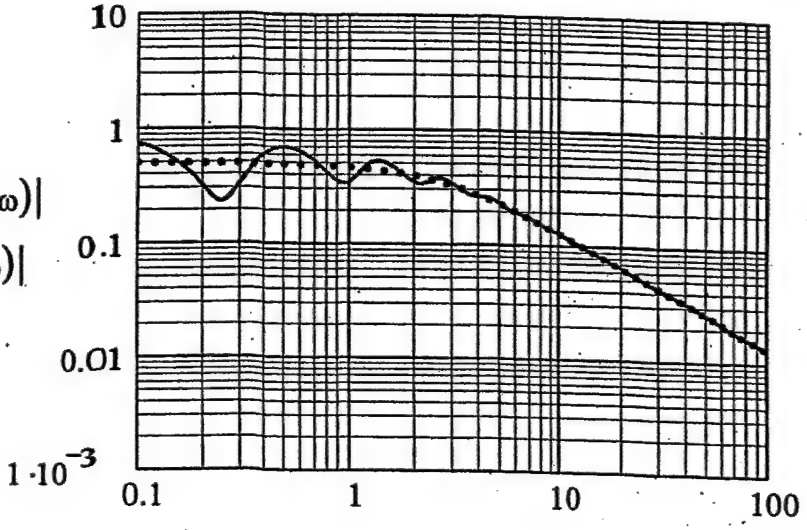

Figure II9c. Figure II5i is repeated except that the loss factor in the cavity (η) is changed from the standard value of (10^{-3}) to (10^{-1}). [cf. Table II1.]

$\frac{|Tbc\_Tb(k(\omega),\omega)|}{|Tc\_T(k(\omega),\omega)|}$

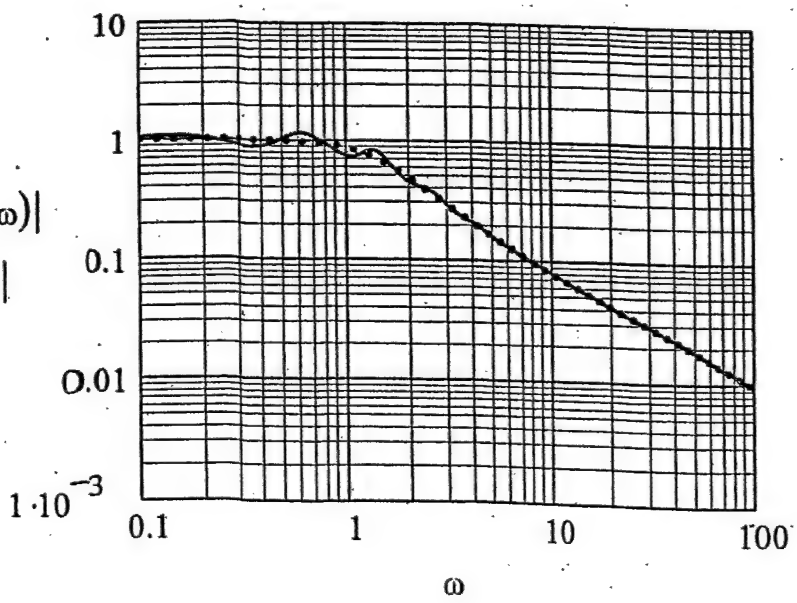

Figure II9d. Figure II5g is repeated except that the loss factor in the coating (η_c) is changed from the standard value of (10^{-3}) to (10^{-1}). [cf. Table II1.]

$\frac{|Tbc(k(\omega),\omega)|}{|Tc(k(\omega),\omega)|}$

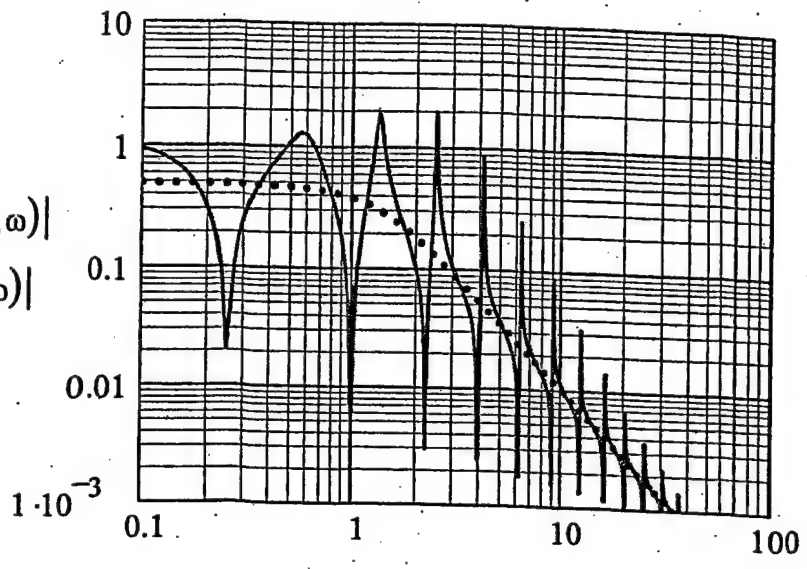

Figure II9e. Figure II5h is repeated except that the loss factor in the coating (η_c) is changed from the standard value of (10^{-3}) to (10^{-1}). [cf. Table II1.]

$\frac{|Tb(k(\omega),\omega)|}{|T(k(\omega),\omega)|}$

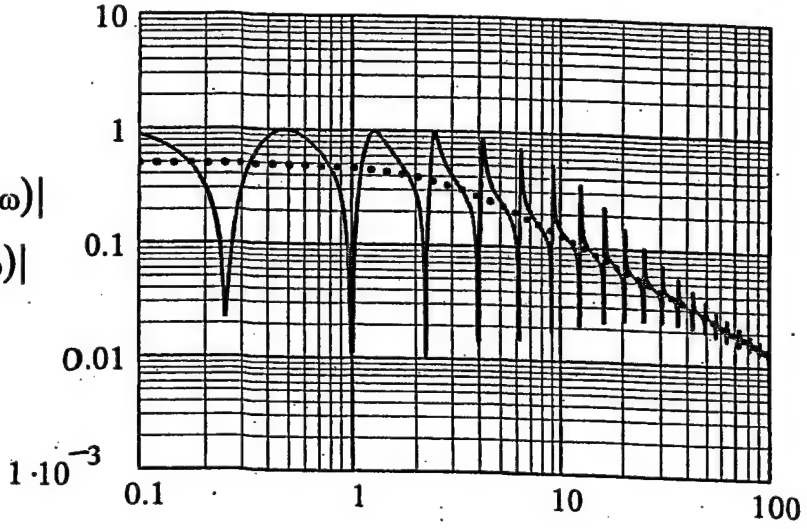

Figure II9f. Figure II5i is repeated except that the loss factor in the coating (η_c) is changed from the standard value of (10^{-3}) to (10^{-1}). [cf. Table II1.]

$\frac{|Tbc\_Tb(k(\omega),\omega)|}{|Tc\_T(k(\omega),\omega)|}$

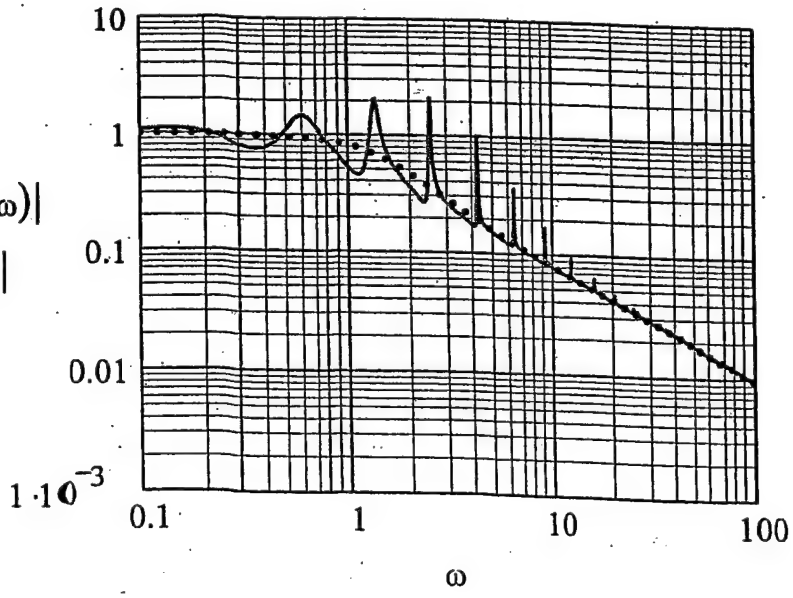

Figure II9g. Figure II5g is repeated except that the surface stiffness control loss factor in the equivalent plate (η_p) is changed from the standard value of (10^{-3}) to (10^{-1}). [cf. Table II1.]

$\frac{|Tbc(k(\omega),\omega)|}{|Tc(k(\omega),\omega)|}$ .....

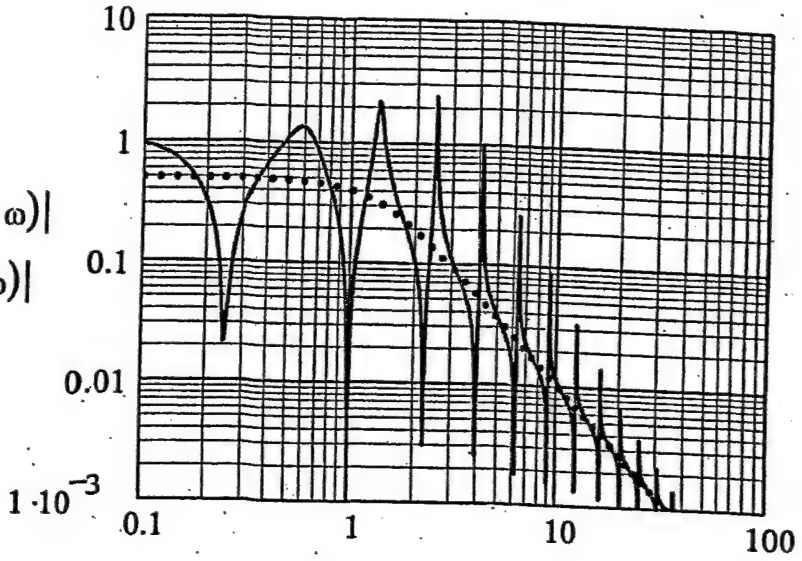

Figure II9h. Figure II5h is repeated except that the surface stiffness control loss factor in the equivalent plate (η_p) is changed from the standard value of (10^{-3}) to (10^{-1}). [cf. Table II1.]

$\frac{|Tb(k(\omega),\omega)|}{|T(k(\omega),\omega)|}$ .....

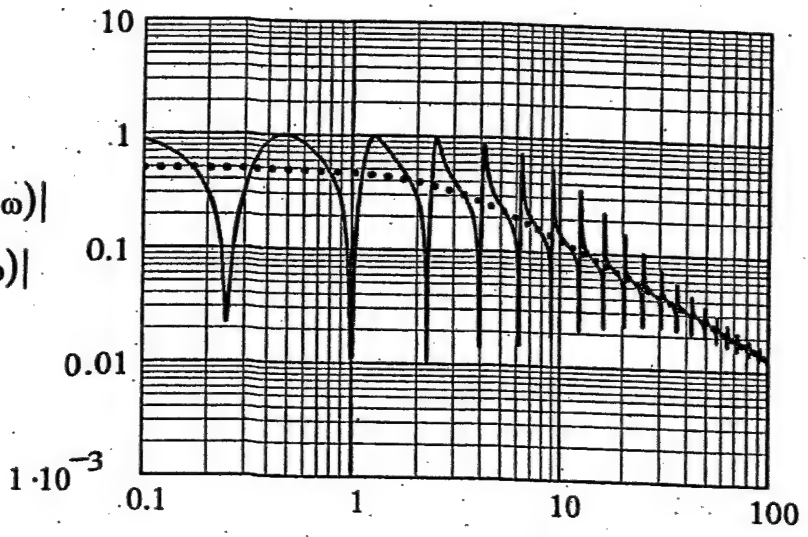

Figure II9i. Figure II5i is repeated except that the surface stiffness control loss factor in the equivalent plate (η_p) is changed from the standard value of (10^{-3}) to (10^{-1}). [cf. Table II1.]

$\frac{|Tbc\_Tb(k(\omega),\omega)|}{|Tc\_T(k(\omega),\omega)|}$ .....

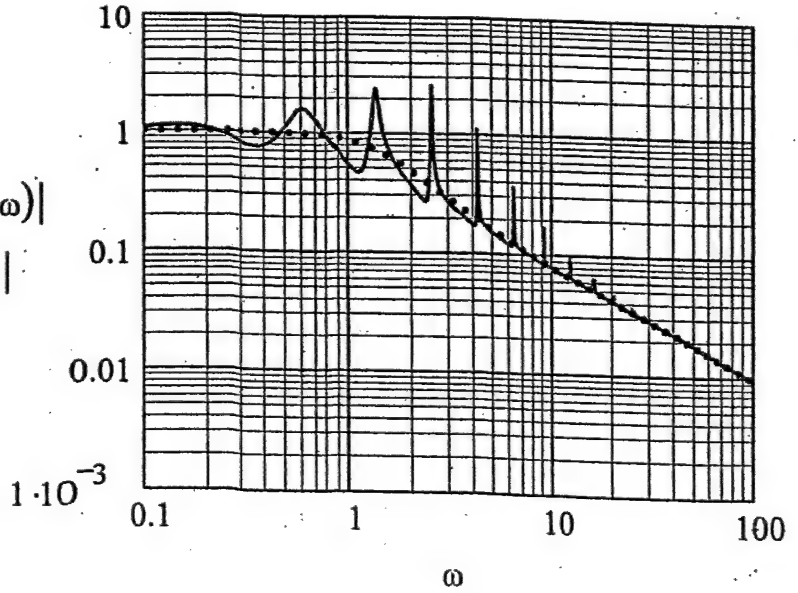

Figure II9j. Figure II5g is repeated except that the surface stiffness control and the surface mass control loss factors (η_p) and (η_m) are changed from the standard value of (10^{-3}) to (10^{-1}). [cf. Table II1.]

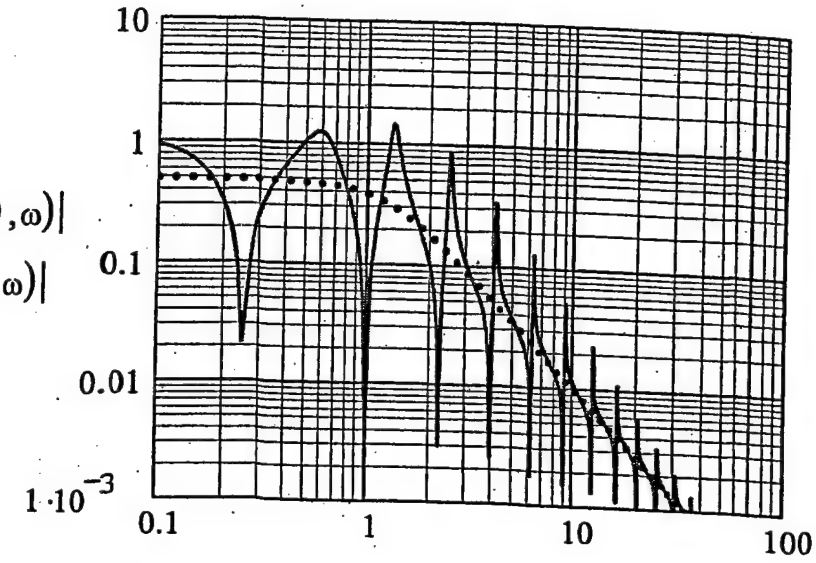

Figure II9k. Figure II5h is repeated except that the surface stiffness control and the surface mass control loss factors (η_p) and (η_m) are changed from the standard value of (10^{-3}) to (10^{-1}). [cf. Table II1.]

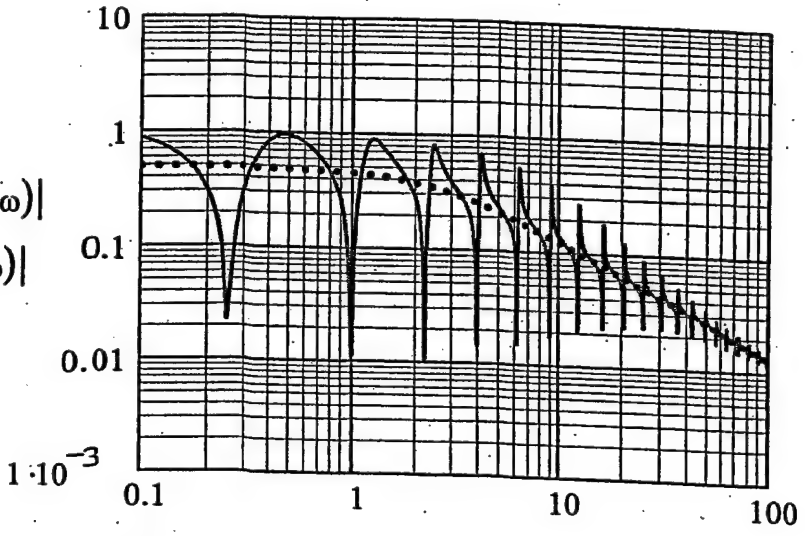

Figure II9l. Figure II5i is repeated except that the surface stiffness control and the surface mass control loss factors (η_p) and (η_m) are changed from the standard value of (10^{-3}) to (10^{-1}). [cf. Table II1.]

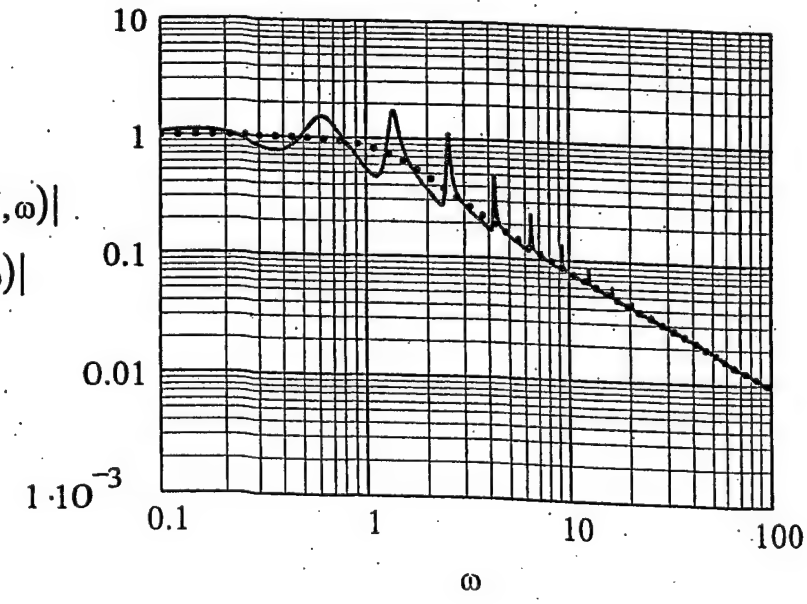

Figure II9m. Figure II5g is repeated except that all the loss factors; η, η_c, η_p, and η_m, are changed from the standard value of (10^{-3}) to (10^{-1}). [cf. Table II1.]

$\frac{|Tbc(k(\omega),\omega)|}{|Tc(k(\omega),\omega)|}$ .....

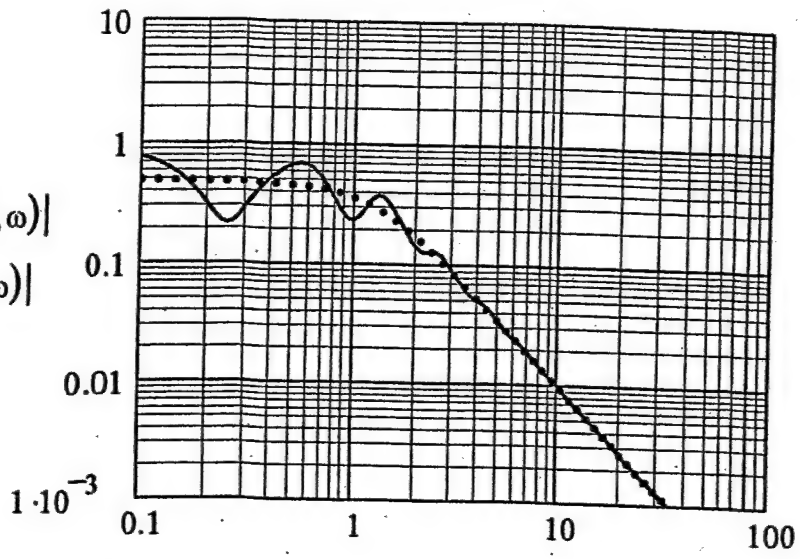

Figure II9n. Figure II5h is repeated except that all the loss factors; η, η_c, η_p, and η_m, are changed from the standard value of (10^{-3}) to (10^{-1}). [cf. Table II1.]

$\frac{|Tb(k(\omega),\omega)|}{|T(k(\omega),\omega)|}$ .....

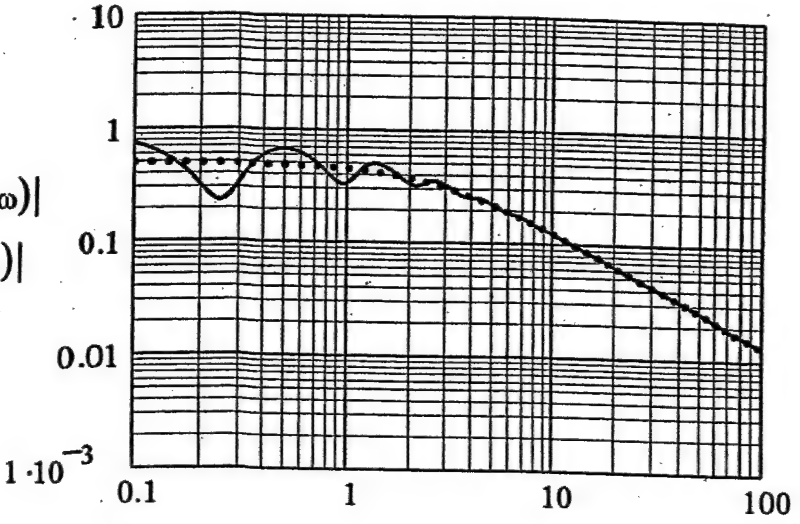

Figure II9o. Figure II5i is repeated except that all the loss factors; η, η_c, η_p, and η_m, are changed from the standard value of (10^{-3}) to (10^{-1}). [cf. Table II1.]

$\frac{|Tbc\_Tb(k(\omega),\omega)|}{|Tc\_T(k(\omega),\omega)|}$ .....

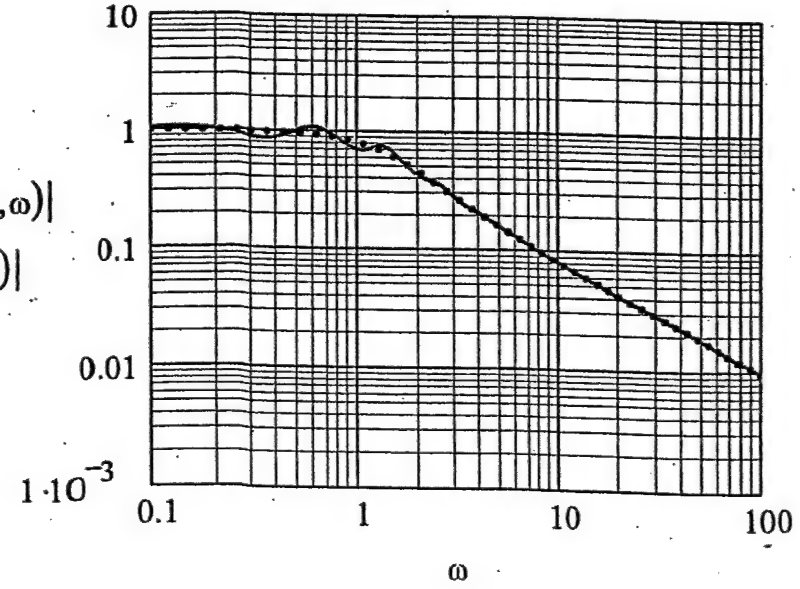

Figure II10a. Figure II6g is repeated except that the loss factor in the cavity (η) is changed from the standard value of (10^{-3}) to (10^{-1}). [cf. Table II1.]

$$\frac{|Tbc(k(\omega),\omega)|}{|Tc(k(\omega),\omega)|}$$

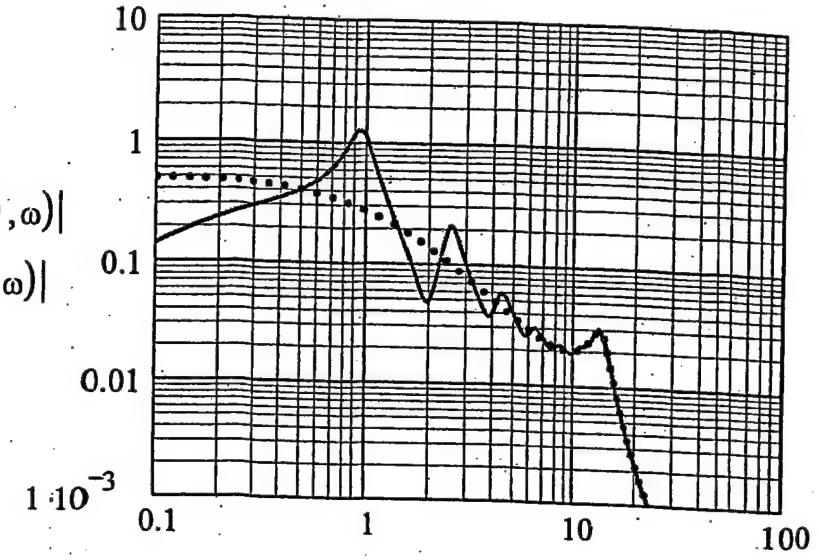

Figure II10b. Figure II6h is repeated except that the loss factor in the cavity (η) is changed from the standard value of (10^{-3}) to (10^{-1}). [cf. Table II1.]

$$\frac{|Tb(k(\omega),\omega)|}{|T(k(\omega),\omega)|}$$

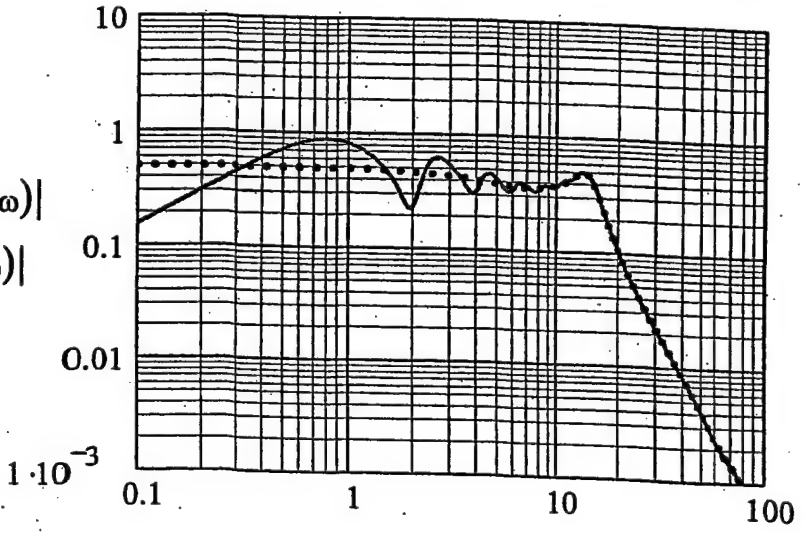

Figure II10c. Figure II6i is repeated except that the loss factor in the cavity (η) is changed from the standard value of (10^{-3}) to (10^{-1}). [cf. Table II1.]

$$\frac{|Tbc\_Tb(k(\omega),\omega)|}{|Tc\_T(k(\omega),\omega)|}$$

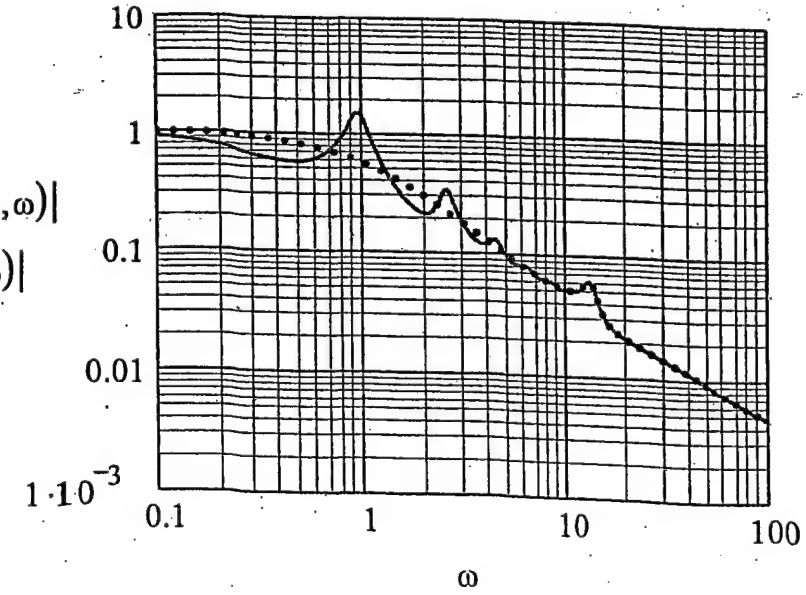

Figure II10d. Figure II6g is repeated except that the loss factor in the coating (η_c) is changed from the standard value of (10^{-3}) to (10^{-1}). [cf. Table II1.]

$\frac{|Tbc(k(\omega),\omega)|}{|Tc(k(\omega),\omega)|}$

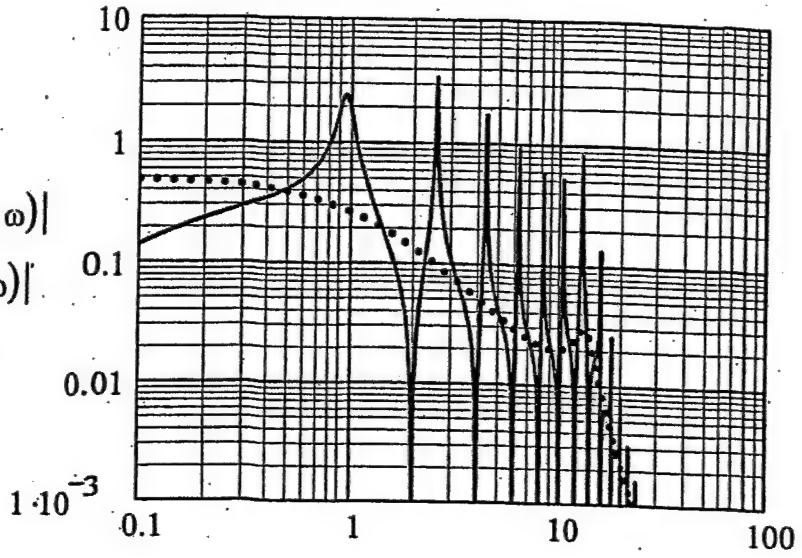

Figure II10e. Figure II6h is repeated except that the loss factor in the coating (η_c) is changed from the standard value of (10^{-3}) to (10^{-1}). [cf. Table II1.]

$\frac{|Tb(k(\omega),\omega)|}{|T(k(\omega),\omega)|}$

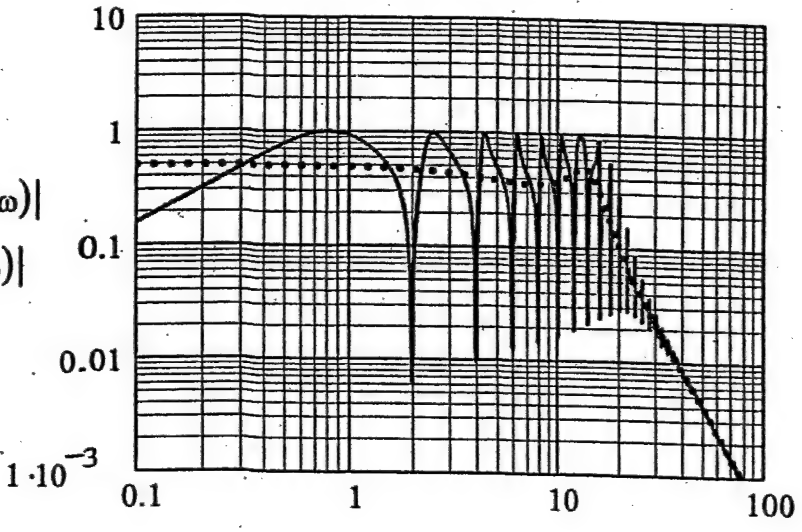

Figure II10f. Figure II6i is repeated except that the loss factor in the coating (η_c) is changed from the standard value of (10^{-3}) to (10^{-1}). [cf. Table II1.]

$\frac{|Tbc\_Tb(k(\omega),\omega)|}{|Tc\_T(k(\omega),\omega)|}$

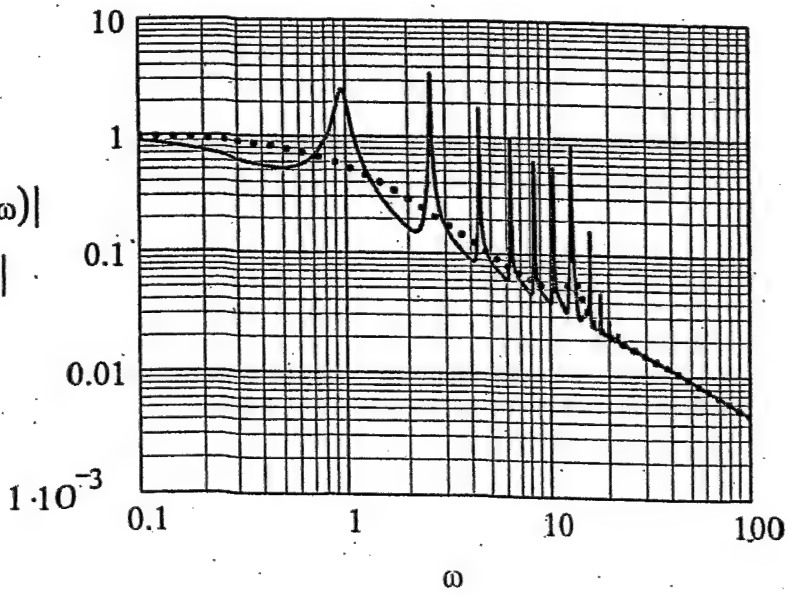

Figure II10g. Figure II6g is repeated except that the surface stiffness control loss factor in the equivalent plate (η_p) is changed from the standard value of (10^{-3}) to (10^{-1}). [cf. Table II1.]

$\frac{|Tbc(k(\omega),\omega)|}{|Tc(k(\omega),\omega)|}$ .....

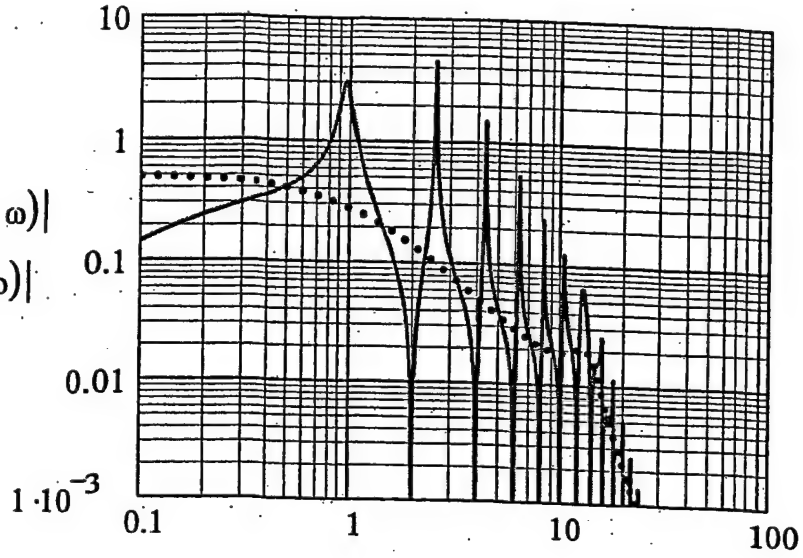

Figure II10h. Figure II6h is repeated except that the surface stiffness control loss factor in the equivalent plate (η_p) is changed from the standard value of (10^{-3}) to (10^{-1}). [cf. Table II1.]

$\frac{|Tb(k(\omega),\omega)|}{|T(k(\omega),\omega)|}$ .....

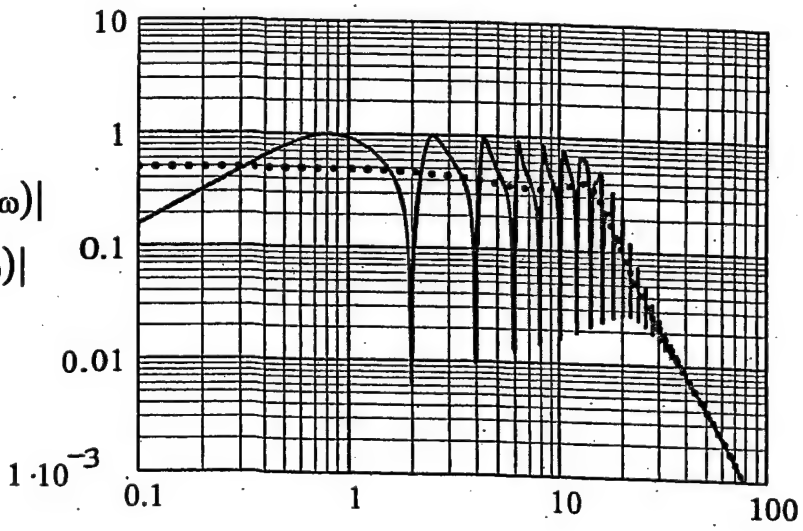

Figure II10i. Figure II6i is repeated except that the surface stiffness control loss factor in the equivalent plate (η_p) is changed from the standard value of (10^{-3}) to (10^{-1}). [cf. Table II1.]

$\frac{|Tbc\_Tb(k(\omega),\omega)|}{|Tc\_T(k(\omega),\omega)|}$ .....

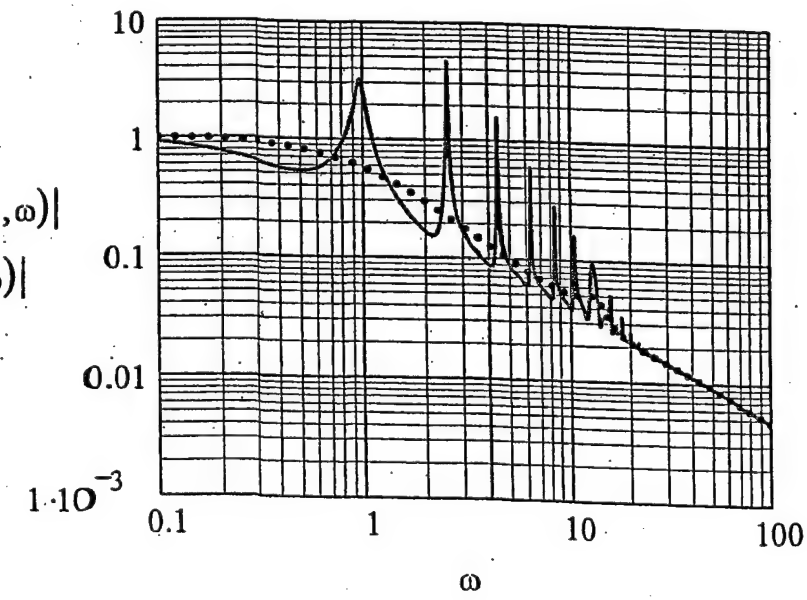

Figure II10j. Figure II6g is repeated except that the surface stiffness control and the surface mass control loss factors (η_p) and (η_m) are changed from the standard value of (10^{-3}) to (10^{-1}). [cf. Table II1.]

$\frac{|Tbc(k(\omega),\omega)|}{|Tc(k(\omega),\omega)|}$ .....

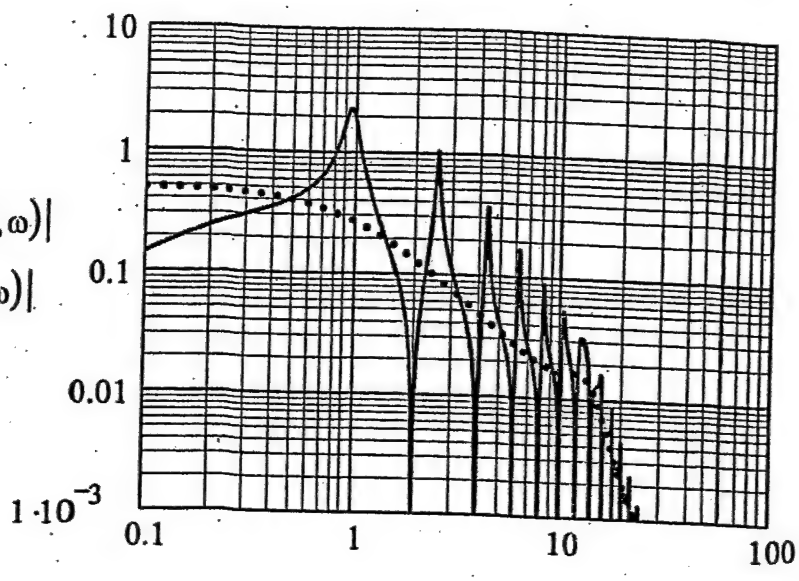

Figure II10k. Figure II6h is repeated except that the surface stiffness control and the surface mass control loss factors (η_p) and (η_m) are changed from the standard value of (10^{-3}) to (10^{-1}). [cf. Table II1.]

$\frac{|Tb(k(\omega),\omega)|}{|T(k(\omega),\omega)|}$ .....

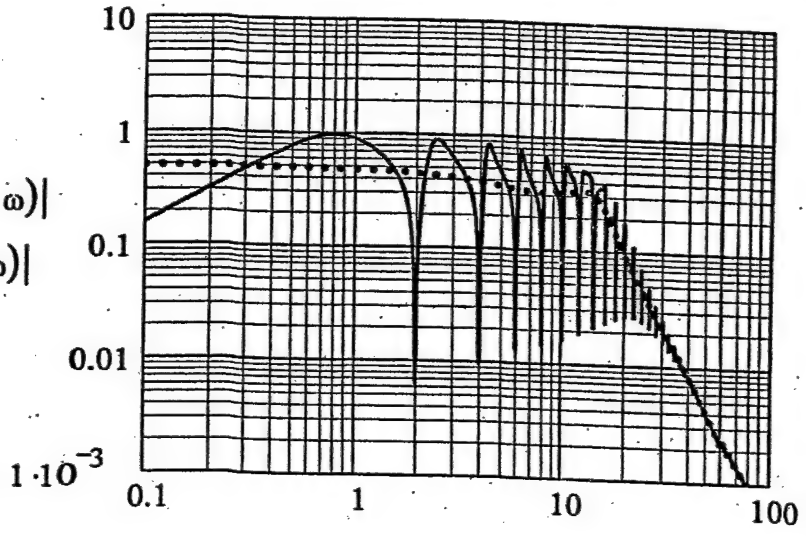

Figure II10l. Figure II6i is repeated except that the surface stiffness control and the surface mass control loss factors (η_p) and (η_m) are changed from the standard value of (10^{-3}) to (10^{-1}). [cf. Table II1.]

$\frac{|Tbc\_Tb(k(\omega),\omega)|}{|Tc\_T(k(\omega),\omega)|}$ .....

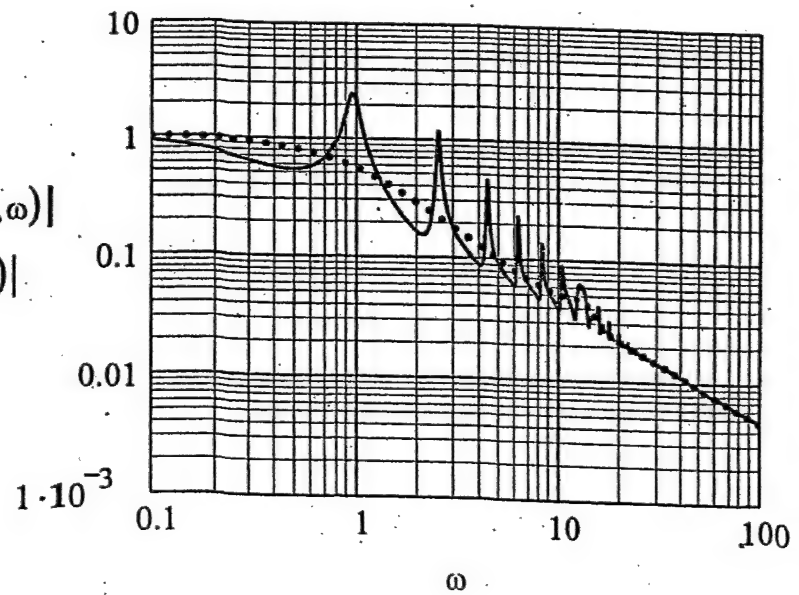

Figure II10m. Figure II6g is repeated except that all the loss factors; η, η_c, η_p, and η_m, are changed from the standard value of (10^{-3}) to (10^{-1}). [cf. Table II1.]

$\frac{|Tbc(k(\omega),\omega)|}{|Tc(k(\omega),\omega)|}$

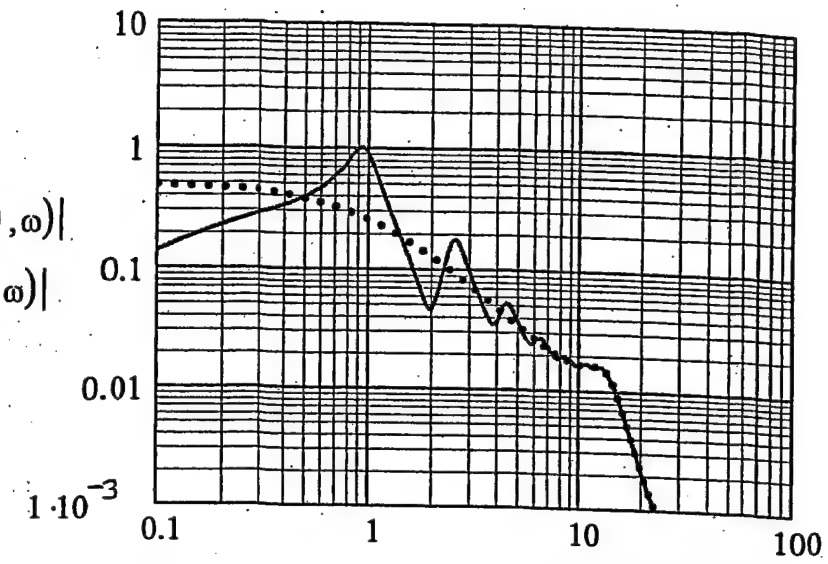

Figure II10n. Figure II6h is repeated except that all the loss factors; η, η_c, η_p, and η_m, are changed from the standard value of (10^{-3}) to (10^{-1}). [cf. Table II1.]

$\frac{|Tb(k(\omega),\omega)|}{|T(k(\omega),\omega)|}$

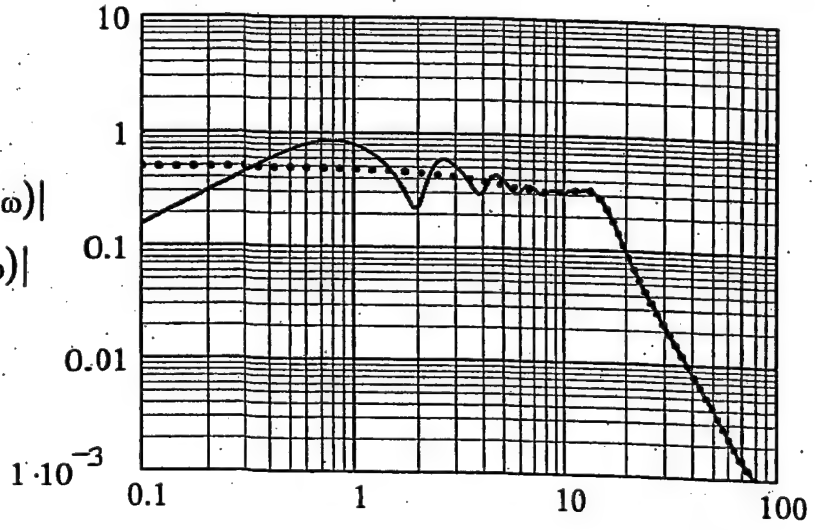

Figure II10o. Figure II6i is repeated except that all the loss factors; η, η_c, η_p, and η_m, are changed from the standard value of (10^{-3}) to (10^{-1}). [cf. Table II1.]

$\frac{|Tbc\_Tb(k(\omega),\omega)|}{|Tc\_T(k(\omega),\omega)|}$

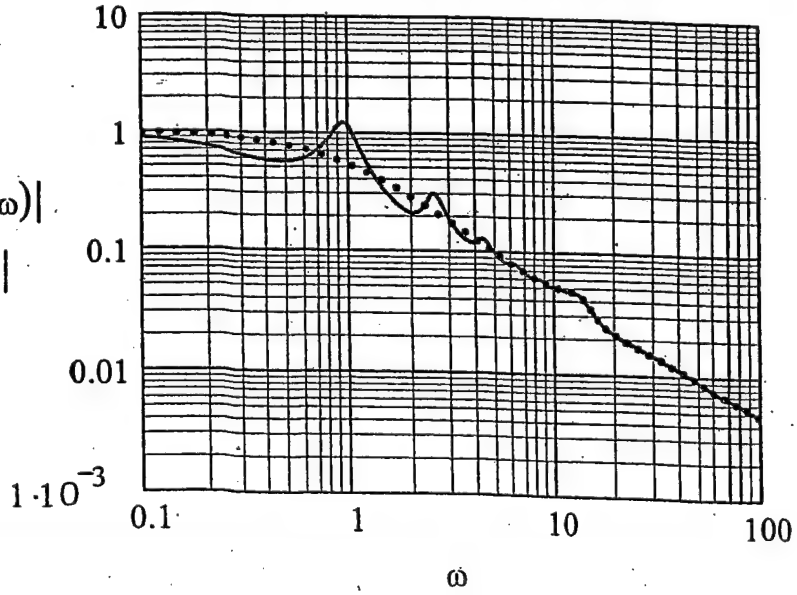

Figure II11a. Figure II4n is repeated except that the reflection coefficient (R) is changed from the standard value of $\exp(-10^{-7})$ to $\exp(-10^{-1})$. [cf. Table II1.]

$\frac{|Tbc(k(\omega),\omega)|}{|Tc(k(\omega),\omega)|}$

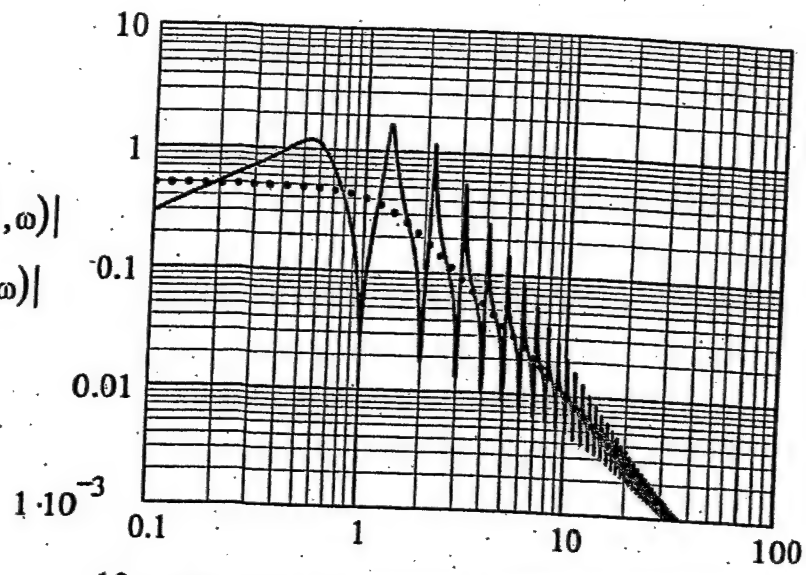

Figure II11b. Figure II4o is repeated except that the reflection coefficient (R) is changed from the standard value of $\exp(-10^{-7})$ to $\exp(-10^{-1})$. [cf. Table II1.]

$\frac{|Tb(k(\omega),\omega)|}{|T(k(\omega),\omega)|}$

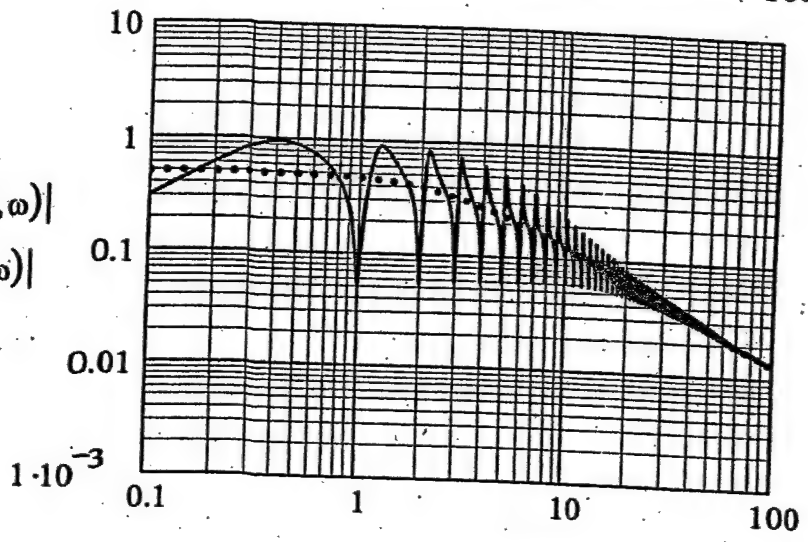

Figure II11c. Figure II4p is repeated except that the reflection coefficient (R) is changed from the standard value of $\exp(-10^{-7})$ to $\exp(-10^{-1})$. [cf. Table II1.]

$\frac{|Tbc\_Tb(k(\omega),\omega)|}{|Tc\_T(k(\omega),\omega)|}$

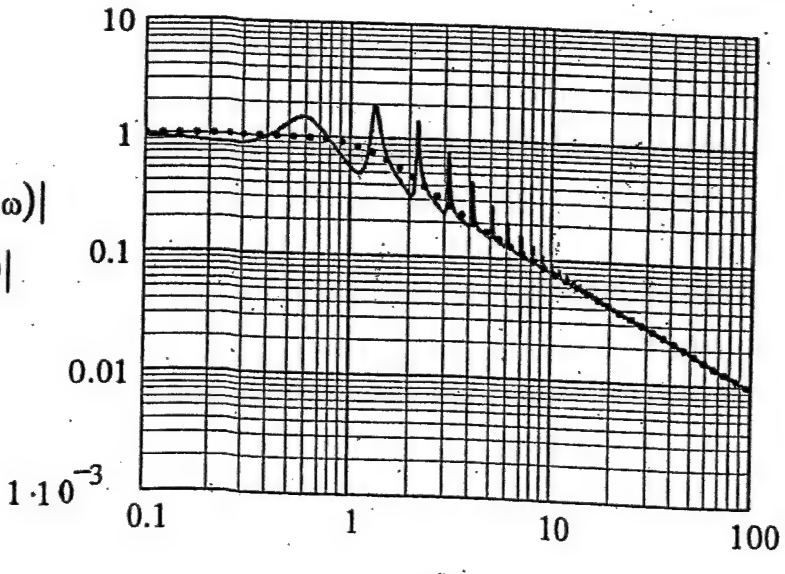

Figure II11d. Figure II4n is repeated except that the reflection coefficient (R) is changed from the standard value of $\exp(-10^{-7})$ to $\exp(-1)$. [cf. Table II1.]

$$\frac{|Tbc(k(\omega),\omega)|}{|Tc(k(\omega),\omega)|}$$

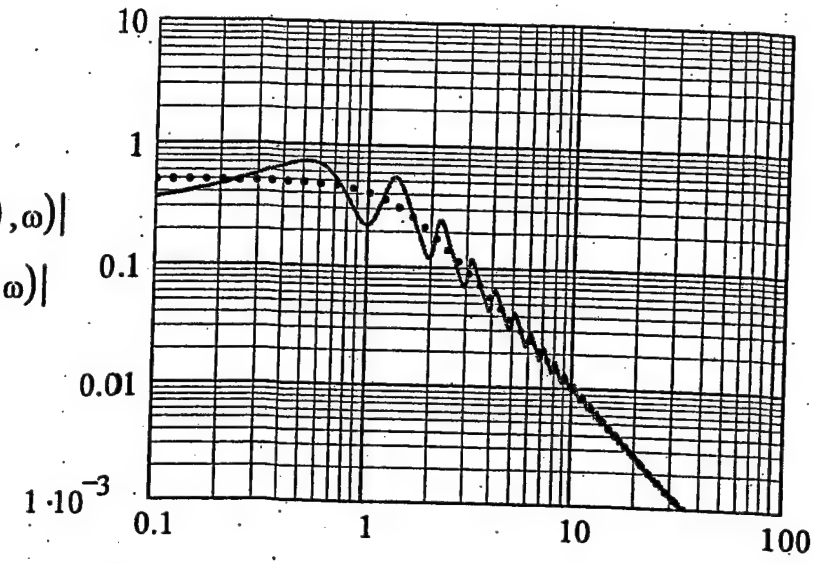

Figure II11e. Figure II4o is repeated except that the reflection coefficient (R) is changed from the standard value of $\exp(-10^{-7})$ to $\exp(-1)$. [cf. Table II1.]

$$\frac{|Tb(k(\omega),\omega)|}{|T(k(\omega),\omega)|}$$

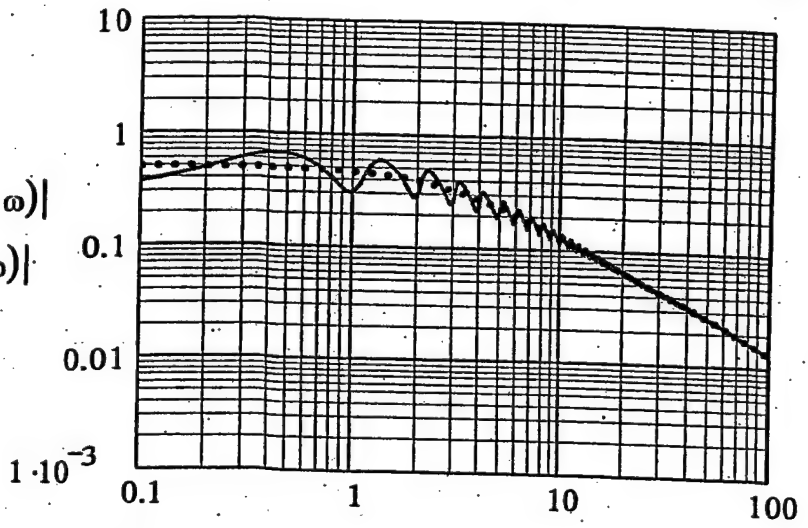

Figure II11f. Figure II4p is repeated except that the reflection coefficient (R) is changed from the standard value of $\exp(-10^{-7})$ to $\exp(-1)$. [cf. Table II1.]

$$\frac{|Tbc\_Tb(k(\omega),\omega)|}{|Tc\_T(k(\omega),\omega)|}$$

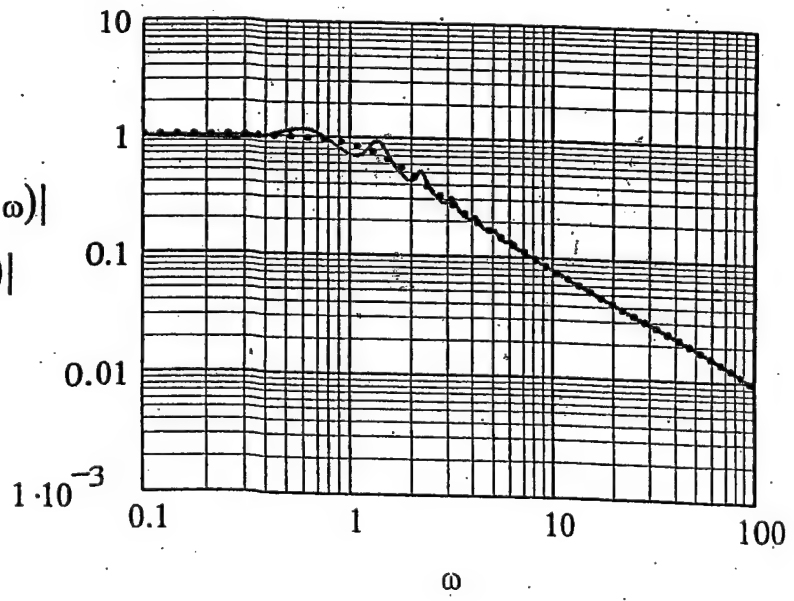

Figure II11g. Figure II6g is repeated except that the reflection coefficient (R) is changed from the standard value of $\exp(-10^{-7})$ to $\exp(-10^{-1})$. [cf. Table II1.]

$\frac{|Tbc(k(\omega),\omega)|}{|Tc(k(\omega),\omega)|}$ .....

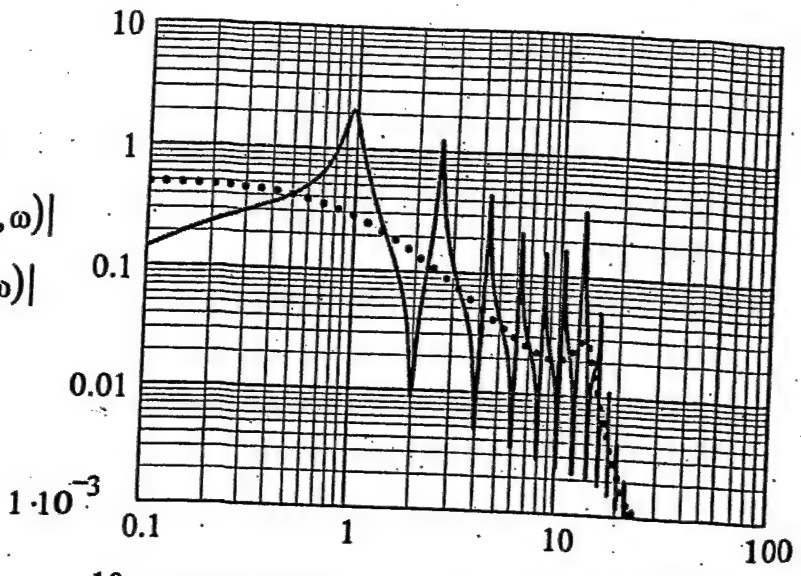

Figure II11h. Figure II6h is repeated except that is repeated except that the reflection coefficient (R) is changed from the standard value of $\exp(-10^{-7})$ to $\exp(-10^{-1})$. [cf. Table II1.]

$\frac{|Tb(k(\omega),\omega)|}{|T(k(\omega),\omega)|}$ .....

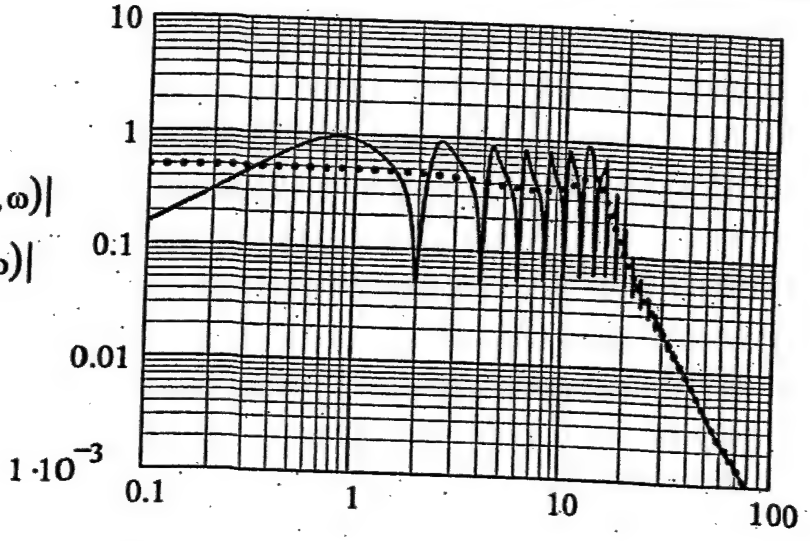

Figure II11i. Figure II6i is repeated except that the reflection coefficient (R) is changed from the standard value of $\exp(-10^{-7})$ to $\exp(-10^{-1})$. [cf. Table II1.]

$\frac{|Tbc\_Tb(k(\omega),\omega)|}{|Tc\_T(k(\omega),\omega)|}$ .....

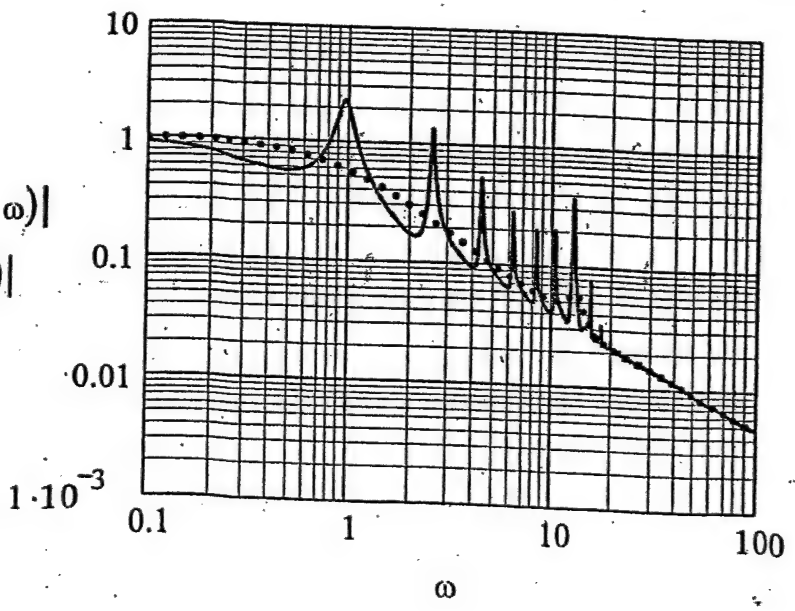

Figure II11j. Figure II6g is repeated except that the reflection coefficient (R) is changed from the standard value of $\exp(-10^{-7})$ to $\exp(-1)$. [cf. Table II1.]

$$\frac{|Tbc(k(\omega),\omega)|}{|Tc(k(\omega),\omega)|}$$

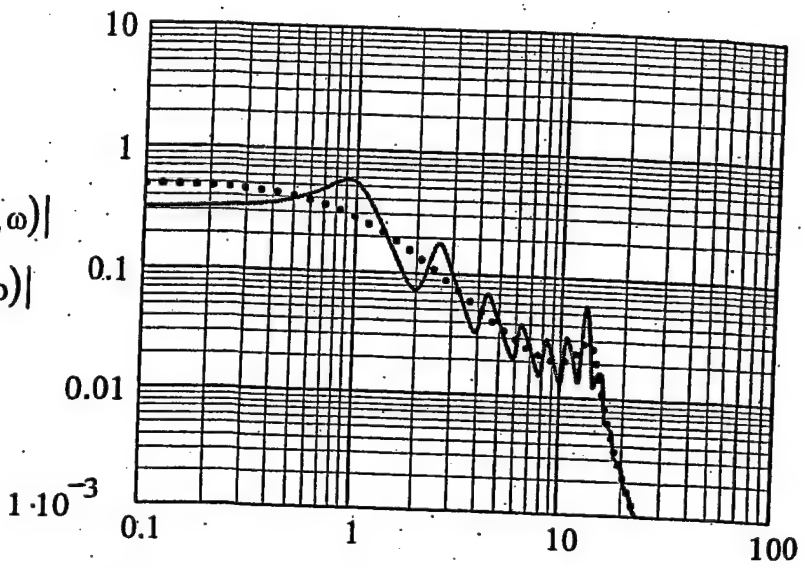

Figure II11k. Figure II6h is repeated except that the reflection coefficient (R) is changed from the standard value of $\exp(-10^{-7})$ to $\exp(-1)$. [cf. Table II1.]

$$\frac{|Tb(k(\omega),\omega)|}{|T(k(\omega),\omega)|}$$

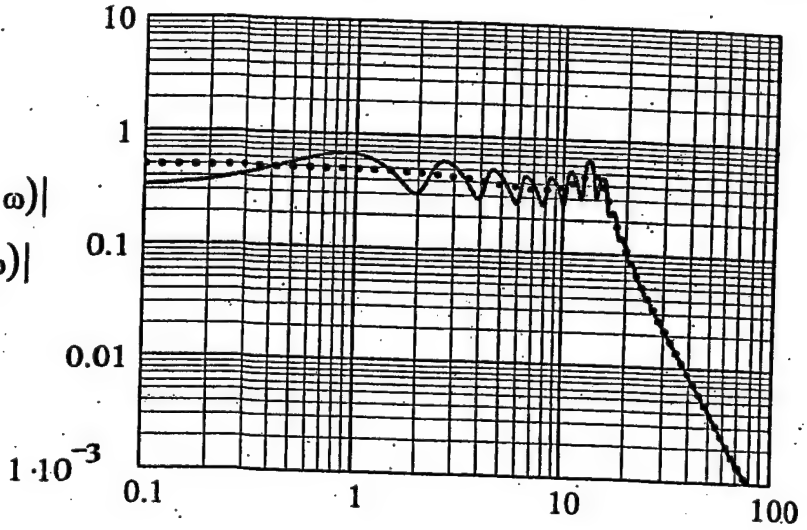

Figure II11l. Figure II6i is repeated except that the reflection coefficient (R) is changed from the standard value of $\exp(-10^{-7})$ to $\exp(-1)$. [cf. Table II1.]

$$\frac{|Tbc\_Tb(k(\omega),\omega)|}{|Tc\_T(k(\omega),\omega)|}$$

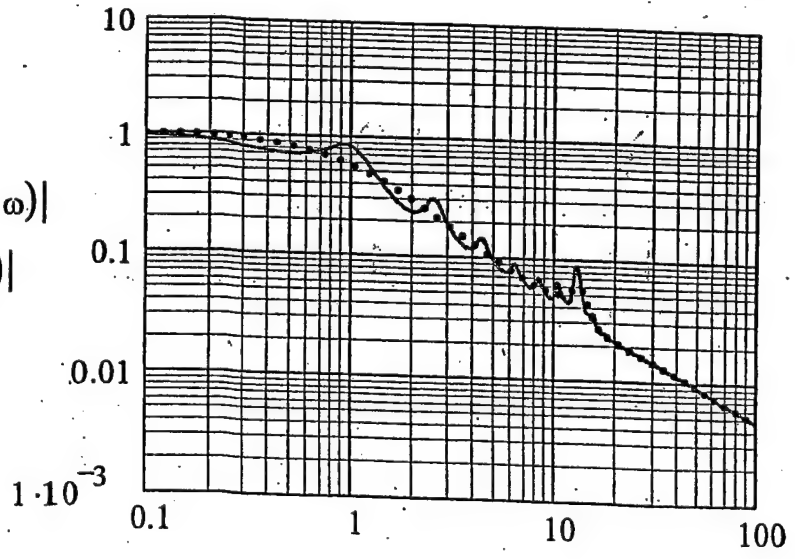

Figure II12a. Figure II4n is repeated except that the pole index (n) is changed from the standard value of (1) to (0).

$$\frac{|Tbc(k(\omega),\omega)|}{|Tc(k(\omega),\omega)|} \quad \cdots\cdots$$

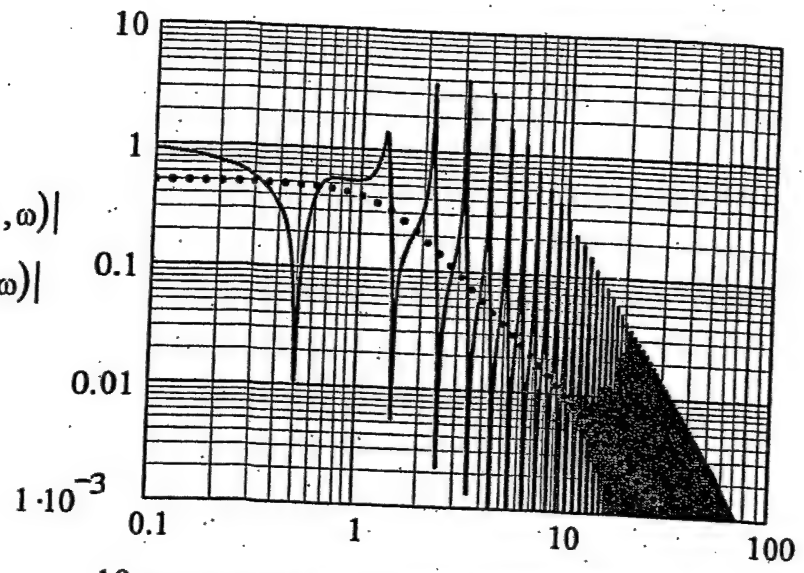

Figure II12b. Figure II4o is repeated except that the pole index (n) is changed from the standard value of (1) to (0).

$$\frac{|Tb(k(\omega),\omega)|}{|T(k(\omega),\omega)|} \quad \cdots\cdots$$

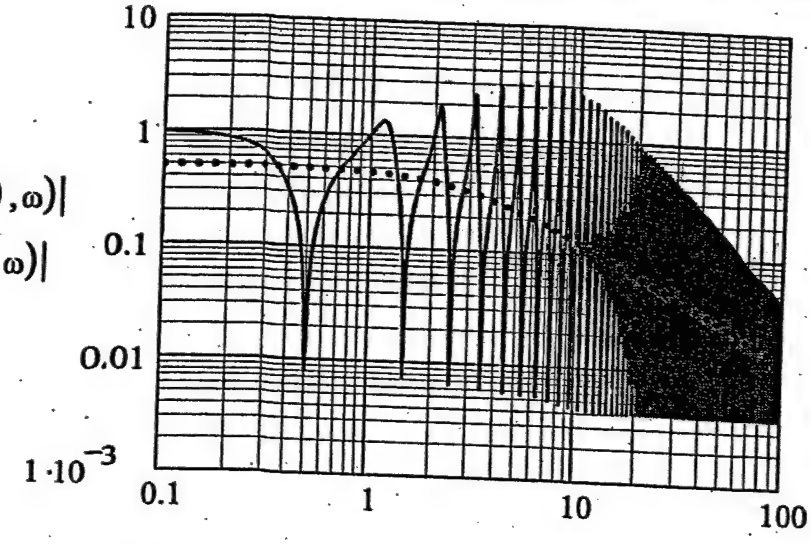

Figure II12c. Figure II4p is repeated except that the pole index (n) is changed from the standard value of (1) to (0).

$$\frac{|Tbc\_Tb(k(\omega),\omega)|}{|Tc\_T(k(\omega),\omega)|} \quad \cdots\cdots$$

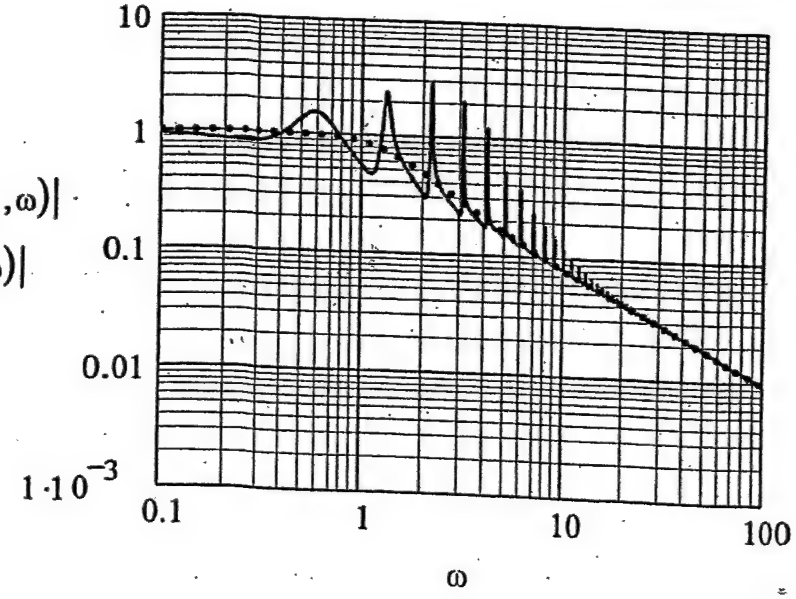

Figure II12d. Figure II6g is repeated except that the pole index (n) is changed from the standard value of (1) to (0).

$\frac{|Tbc(k(\omega),\omega)|}{|Tc(k(\omega),\omega)|}$

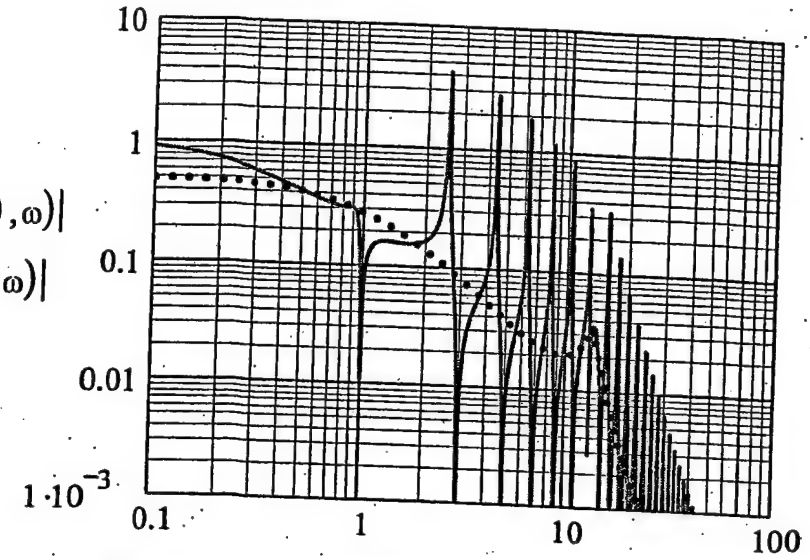

Figure II12e. Figure II6h is repeated except that the pole index (n) is changed from the standard value of (1) to (0).

$\frac{|Tb(k(\omega),\omega)|}{|T(k(\omega),\omega)|}$

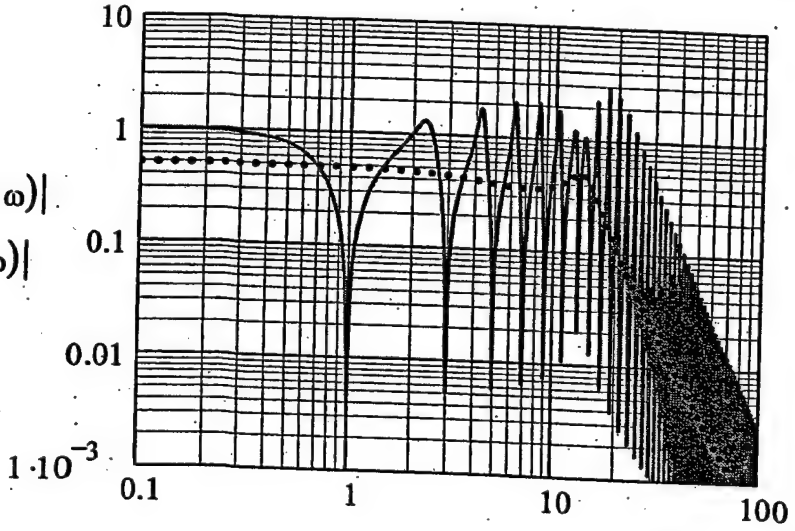

Figure II12f. Figure II6i is repeated except that the pole index (n) is changed from the standard value of (1) to (0).

$\frac{|Tbc\_Tb(k(\omega),\omega)|}{|Tc\_T(k(\omega),\omega)|}$

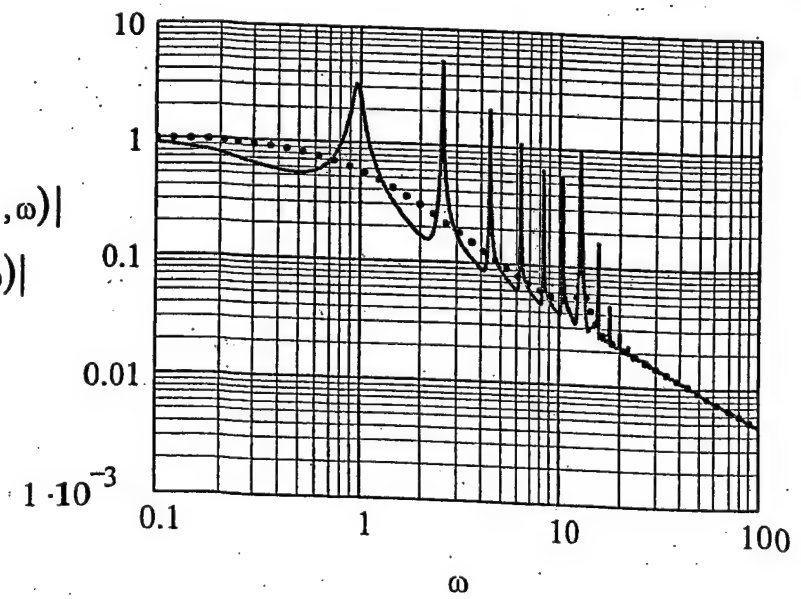

Figure II12g. Figure II6g is repeated except that the plane on which the external sources are placed is changed from the standard position of $b_2 = b$ to $b_2 = 0.8b$.

$\frac{|Tbc(k(\omega),\omega)|}{|Tc(k(\omega),\omega)|}$ .....

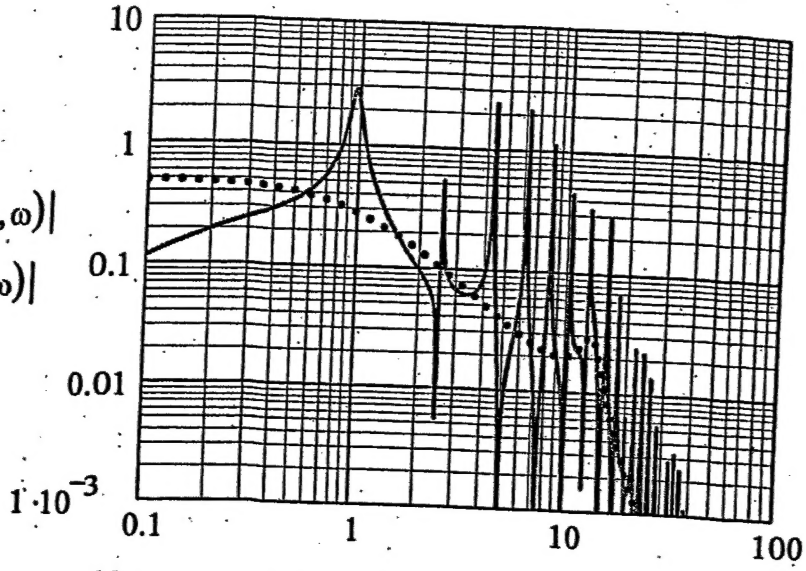

Figure II12h. Figure II6h is repeated except that the plane on which the external sources are placed is changed from the standard position of $b_2 = b$ to $b_2 = 0.8b$.

$\frac{|Tb(k(\omega),\omega)|}{|T(k(\omega),\omega)|}$ .....

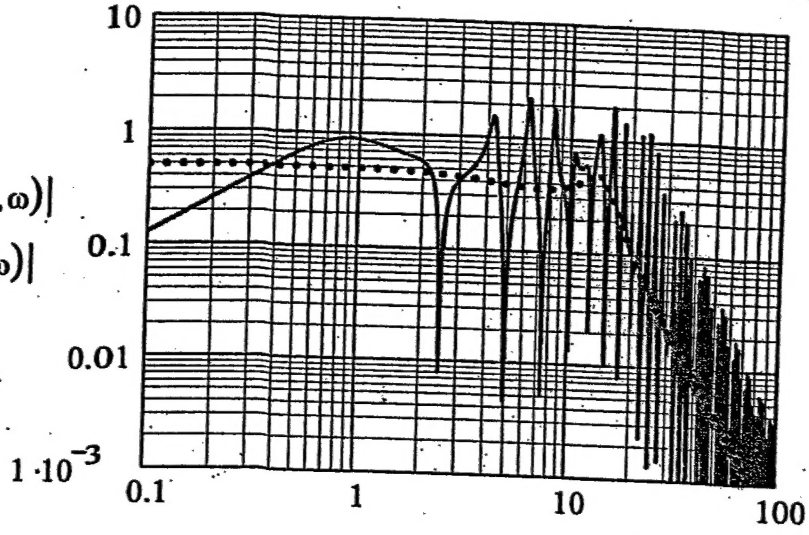

Figure II12i. Figure II6i is repeated except that the plane on which the external sources are placed is changed from the standard position of $b_2 = b$ to $b_2 = 0.8b$.

$\frac{|Tbc\_Tb(k(\omega),\omega)|}{|Tc\_T(k(\omega),\omega)|}$ .....

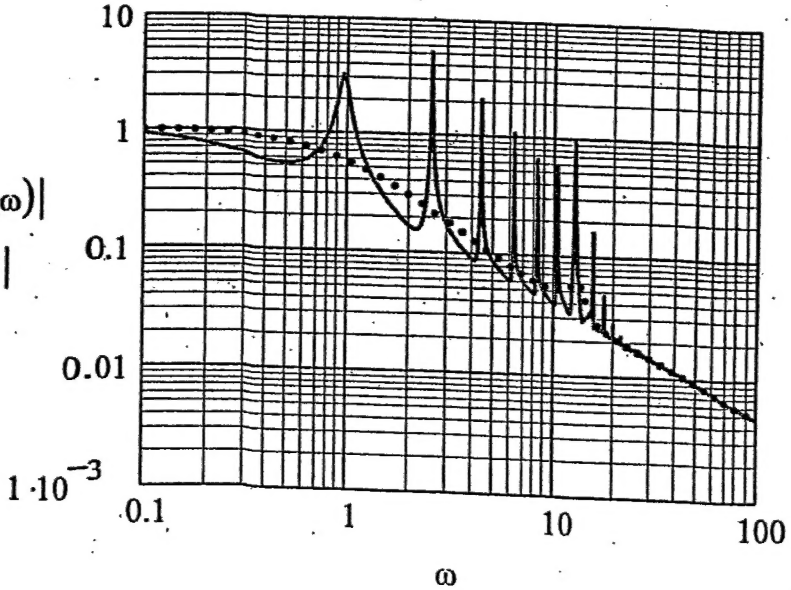

Figure II13a. Figure II4n is repeated except that the standard beam-directed radiation, for which $\theta = 0$, is changed to off beam-directed radiation, for which $\theta = (\pi/9.2)$.

$\frac{|Tbc(k(\omega),\omega)|}{|Tc(k(\omega),\omega)|}$ .....

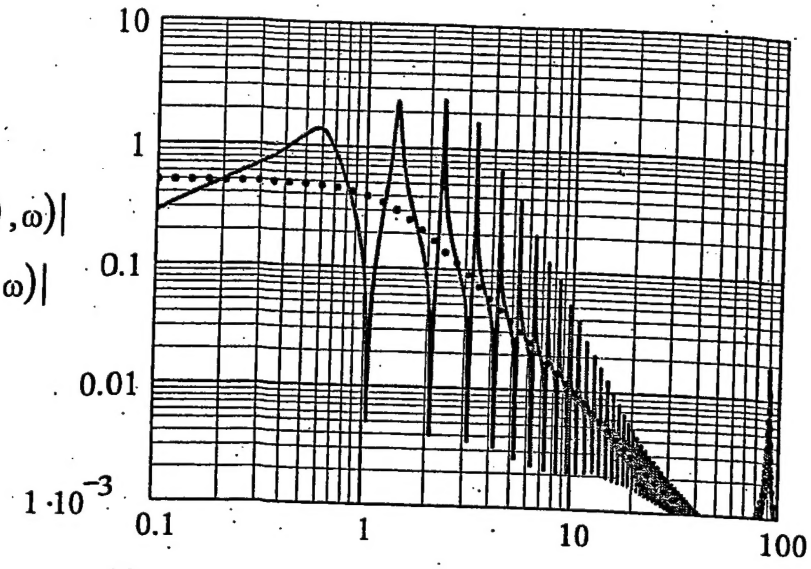

Figure II13b. Figure II4o is repeated except that the standard beam-directed radiation, for which $\theta = 0$, is changed to off beam-directed radiation, for which $\theta = (\pi/9.2)$.

$\frac{|Tb(k(\omega),\omega)|}{|T(k(\omega),\omega)|}$ .....

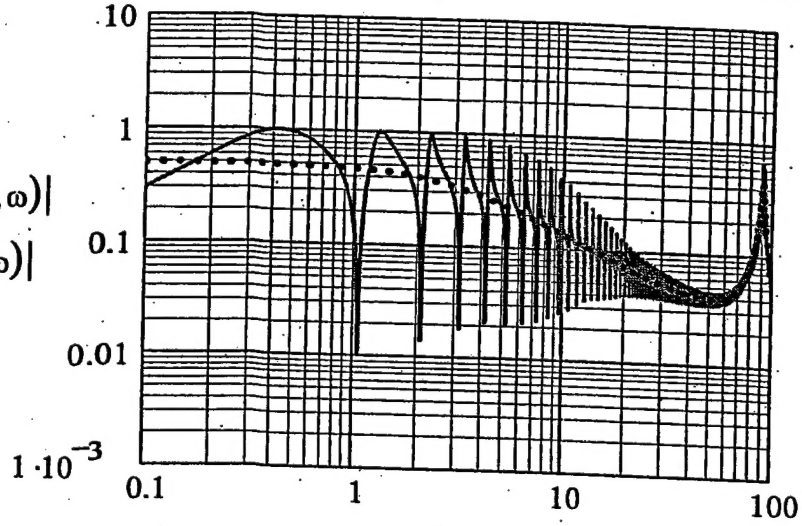

Figure II13c. Figure II4p is repeated except that the standard beam-directed radiation, for which $\theta = 0$, is changed to off beam-directed radiation, for which $\theta = (\pi/9.2)$.

$\frac{|Tbc\_Tb(k(\omega),\omega)|}{|Tc\_T(k(\omega),\omega)|}$ .....

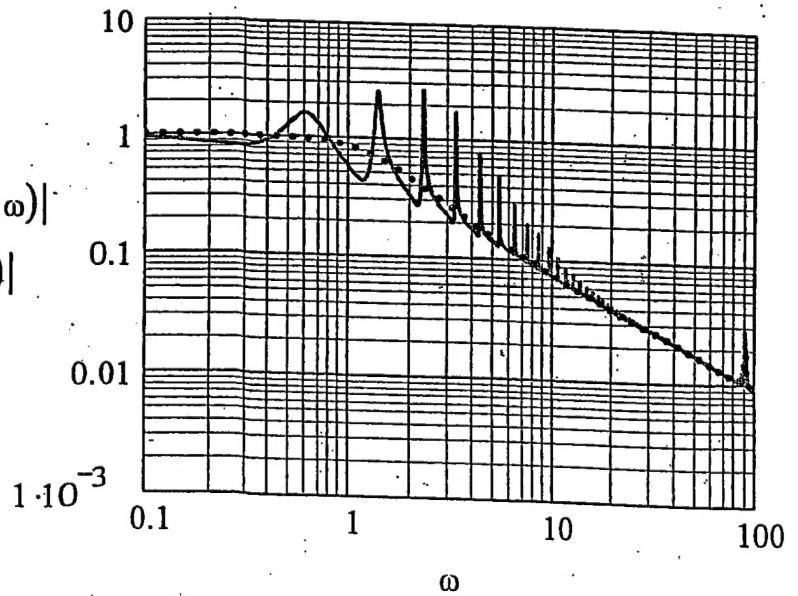

Figure II13d. Figure II4n is repeated except that the standard beam-directed radiation, for which $\theta = 0$, is changed to off beam-directed radiation, for which $\theta = (\pi/6)$. [cf. Figure II6g.]

$\frac{|Tbc(k(\omega),\omega)|}{|Tc(k(\omega),\omega)|}$ .....

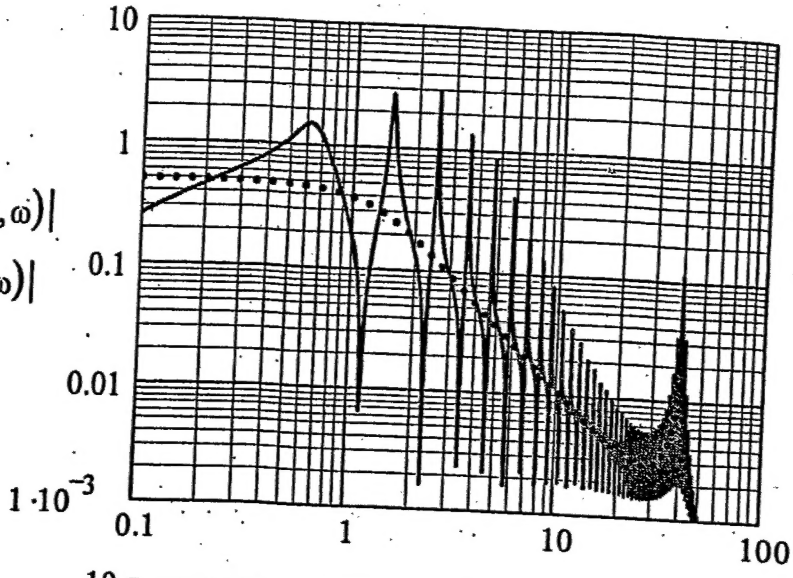

Figure II13e. Figure II4o is repeated except that the standard beam-directed radiation, for which $\theta = 0$, is changed to off beam-directed radiation, for which $\theta = (\pi/6)$. [cf. Figure II6h.]

$\frac{|Tb(k(\omega),\omega)|}{|T(k(\omega),\omega)|}$ .....

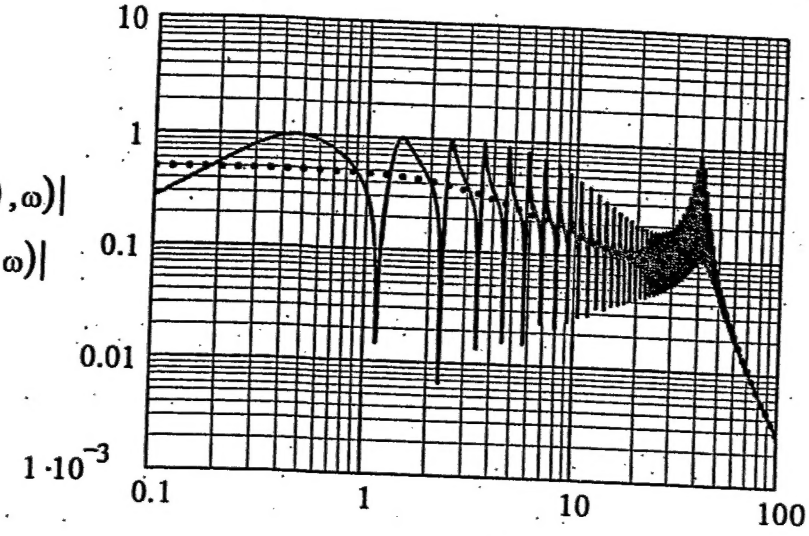

Figure II13f. Figure II4p is repeated except that the standard beam-directed radiation, for which $\theta = 0$, is changed to off beam-directed radiation, for which $\theta = (\pi/6)$. [cf. Figure II6i.]

$\frac{|Tbc\_Tb(k(\omega),\omega)|}{|Tc\_T(k(\omega),\omega)|}$ .....

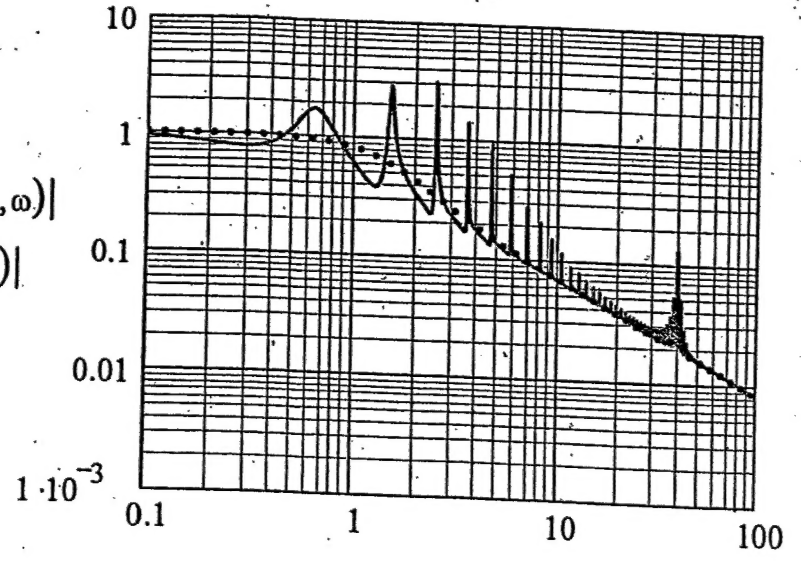

INITIAL DISTRIBUTION

Copies

3 NAVSEA 05T2
- 1 Taddeo
- 1 Biancardi
- 1 Shaw

3 ONR/ONT
- 1 334 Schreppler
- 1 334 Couchman
- 1 Library

2 DTIC

CENTER DISTRIBUTION

1 0112 Barkyoumb

1 7000 Jebsen

1 7020 Strasberg

1 7030 Maidanik

1 7200 Shang

1 7204 Niemiec

1 7205 Dlubac

3 7250 Noll
Maga
Diperna

1 3421 TIC-Carderock